

THE SOLID STATE POLYMERIZATION OF  
ALKALI METAL ACRYLATES

by

Pier Paolo Saviotti

A thesis submitted to the Faculty of Graduate  
Studies and Research in partial fulfilment of  
the requirements for the degree of  
Doctor of Philosophy

Department of Chemistry  
McGill University,  
Montreal, Quebec,  
Canada.

June 1975.



SOLID STATE POLYMERIZATION OF ALKALI METAL ACRYLATES

Pier Paolo Saviotti

To my wife Laura

for her patience,

understanding

and love.

## ABSTRACT

Ph.D.

Pier Paolo Saviotti

Chemistry

### THE SOLID STATE POLYMERIZATION OF ALKALI METAL ACRYLATES

The solid state polymerization of the acrylate salts of lithium, sodium, potassium and rubidium has been studied. The molecular mobility of the monomer plays an important role in the polymerization process and appears to exert different influences in different reaction stages.

Three different reaction periods A, B and C occur in the polymerization. Period A was not studied in detail. The rate constants for polymerization correlate with the properties of the initial crystal in reaction period B and of the modified matrix in period C. The modification of the reaction matrix occurring during the solid state polymerization leads to a slowing down of the reaction and finally to a limiting conversion.

The importance of the generation and annealing of strain in the monomer crystal lattice is discussed in relation to the mechanism of matrix modification.

## RESUME

Ph.D.

Pier Paolo Saviotti

Chimie

### LA POLYMERISATION A L'ETAT SOLIDE

### D'ACRYLATES DE METAUX ALCALINS

La polymérisation à l'état solide des acrylates de lithium, sodium, potassium et rubidium a été étudiée. La mobilité moléculaire du monomère joue un rôle important dans le processus de polymérisation, et semble exercer des influences différentes à différentes étapes de la réaction.

On peut distinguer trois périodes différentes A, B et C au cours de la polymérisation. La période A n'a pas été étudiée en détail. Il y a une corrélation des constantes de vitesse de polymérisation avec les propriétés du crystal initial pour la période B, et avec les propriétés de la matrice modifiée pour la période C. Les transformations de la matrice de la réaction, qui ont lieu au cours de la polymérisation à l'état solide, conduisent à un ralentissement de la réaction et finalement à une conversion limitée.

L'importance de la production et de la recuisson des tensions internes dans le réseau cristallin du monomère est discutée en rapport avec le mécanisme de modification de la matrice.

## ACKNOWLEDGEMENTS

The author wishes to express his sincere gratitude to Dr. D.F.R. Gilson for his encouragement and helpful criticism throughout this work.

Special thanks are due to Dr. T. Cyr for allowing the use of the ESR spectrometer of the Department of Chemistry of the Universite de Montreal.

Thanks are also due to:

The National Research Council of Canada for a scholarship from 1972 to 1975.

Ken Cole for creating a relaxed atmosphere in our laboratory and for continued friendship.

Patrice Grisard for stimulating discussions on solid state polymerization.

Renée Charron for her patience and efficiency in helping to prepare this manuscript.

## TABLE OF CONTENTS

	<u>CHAPTER I</u>	page
	INTRODUCTION	1
I-1	Effects of $\gamma$ rays on solids . . . . .	2
I-2	Solid state polymerization . . . . .	5
	a) Effect of crystal structure . . . . .	6
	b) Role of crystal lattice defects . . . . .	9
	c) Role of molecular motions . . . . .	14
	d) Reaction mechanism and kinetics . . . . .	16
I-3	Magnetic resonance . . . . .	26
	a) Applications of NMR to the study of molecular motions in solids . . . . .	27
	b) Applications of ESR to the study of molecular motions . . . . .	34
I-4	Previous studies on the salts of acrylic acid . .	42
I-5	Statement of the problem . . . . .	45

## CHAPTER II

	EXPERIMENTAL	
II-1	Preparation of the monomer . . . . .	47
II-2	Polymerization kinetics of K acrylate . . . . .	47
II-3	Wide-line NMR measurements . . . . .	49
II-4	DSC measurements . . . . .	50
II-5	ESR measurements . . . . .	50

CHAPTER III

page

RESULTS AND DISCUSSION

III-1	Polymerization kinetics . . . . .	52
III-2	Wide-line NMR measurements . . . . .	65
III-3	DSC measurements . . . . .	79
III-4	ESR measurements . . . . .	80
III-5	Discussion . . . . .	98

CHAPTER IV

CONTRIBUTIONS TO ORIGINAL KNOWLEDGE AND  
SUGGESTIONS FOR FURTHER WORK

IV-1	Contributions to original knowledge . . . . .	115
IV-2	Suggestions for further work . . . . .	116

	BIBLIOGRAPHY . . . . .	118
--	------------------------	-----

APPENDICES

A	Appendix A - Tables . . . . .	126
B	Appendix B - Wide-line NMR study of molecular motions in solid sulfolane . . . . .	151

LIST OF FIGURES

<u>Figure</u>		<u>page</u>
<u>CHAPTER I</u>		
I-1	Edge dislocation . . . . .	10
I-2	Screw dislocation . . . . .	11
I-3	Dependence of the free energy of the nucleus on its radius . . . . .	17
I-4	Time dependence of the polymer yield of a) nucleation, b) defect induced polymn, c) longitudinal fibril growth, d) transversal fibril growth, e) overall polymerization . . . .	25
I-5	Stepwise character of radical recombination . .	41
<u>CHAPTER III</u>		
III-1	Polymerization of K acrylate at 313 K (top) and 323 K (bottom) . . . . .	54
III-2	Polymerization of K acrylate at 333 K (top and 353 K (bottom) . . . . .	55
III-3	Temperature dependence of $dY/d\log t$ for K acrylic . . . . .	56
III-4	Polymerization of Li acrylate at 374 K (o) and 405 K (□) . . . . .	57
III-5	Polymerization of Na acrylate at 393 K (o) and 403 K (□) . . . . .	58
III-6	Polymerization of K acrylate at 273 K . . . . .	59
III-7	Polymerization of K acrylate at 323 K illus- trating the three reaction periods A, B and C .	61
III-8	Temperature dependence of $dY/dt$ for K acrylate .	63
III-9	Polymerization of K acrylate at 313 K: a) fresh sample (o) and b) sample prepolymerized at 353 K	64
III-10	Wide-line NMR lineshape of the alkali acrylates (top). Acrylate ion (bottom). . . . .	66

<u>Figure</u>	page
III-11 Temperature dependence of the linewidth (o) and second moment (●) of Li acrylate . . . .	67
III-12 Temperature dependence of the linewidth (o) and second moment (●) of Na acrylate . . . .	68
III-13 Temperature dependence of the linewidth (o) and second moment (●) of K acrylate . . . .	69
III-14 Temperature dependence of the linewidth (o) and second moment (●) of Rb acrylate . . . .	70
III-15 Molecular motions considered for the acrylate ion. Hydrogen atoms are not illustrated . . . .	75
III-16 Change of wide-line NMR lineshape with polymerization at 353 K - a) unirradiated sample, b) polymerizing sample . . . . .	78
III-17 ESR spectra of the alkali acrylate radicals recorded at low polymer yields or when no polymerization is occurring. The spectra were recorded under the following conditions: magnetic field = 3205-3215 G; mod. ampl. = 4 G; sweep range = 200 G; sweep time = 200 s; time constant = 0.5 s; klystron power = 0.5-2.0 mw . . . . .	81
III-18 ESR spectra of the alkali acrylate radicals at high polymer yields . . . . .	83
III-19 Decay of Li acrylate radicals at 353 K . . . . .	85
III-20 Decay of Li acrylate radicals at 423 K . . . . .	86
III-21 Decay of Na acrylate radicals at 353 K . . . . .	87
III-22 Decay of Na acrylate radicals at 423 K . . . . .	88
III-23 Decay of K acrylate radicals at 313 K (●), 323 K (■) and 353 K (▲) . . . . .	89
III-24 Decay of Rb acrylate radicals at 303 K (■), 313 K (▲) and 353 K (●) . . . . .	90
III-25 Second order decay of Li acrylate radicals at 353 K . . . . .	91
III-26 Second order decay of Na acrylate radicals at 423 K . . . . .	92

<u>Figure</u>	page
III-27 Second order decay of Na acrylate radicals at 423 K . . . . .	93
III-28 Second order decay of K acrylate radicals at 313 K ( $\Delta$ ), 323 K ( $\square$ ), 353 K (o) and 373 K ( $\blacksquare$ ) . . . . .	94
III-29 Second order decay of Rb acrylate radicals at 303 K ( $\square$ ), 313 K ( $\Delta$ ) and 353 K (o) . . . . .	95
III-30 Temperature dependence of the second order radical recombination rate constants of K acrylate . . . . .	97
III-31 Temperature dependence of $dY/dt$ (o) and of the second moment ( $\bullet$ ) of K acrylate . . . . .	107
III-32 Temperature dependence of the radical recombina- tion rate constant ( $\square$ ), $dY/d\log t$ (o) and of the average degree of polymerization ( $\Delta$ ) of K acrylate . . . . .	108

APPENDIX B

B-1 Temperature dependence of the linewidth of solid sulfolane . . . . .	153
B-2 Temperature dependence of the second moment of solid sulfolane . . . . .	154

LIST OF TABLES

<u>Table</u>		<u>page</u>
<u>CHAPTER II</u>		
II-1	Results of the elemental analysis of the acrylates of Li, Na, K and Rb . . . . .	48
<u>CHAPTER III</u>		
III-1	Correlation of polymer yields $Y$ with $t$ and with $\log t$ at short polymerization times . . . . .	53
III-2	Experimental and calculated second moments for alkali acrylates . . . . .	73
III-3	Temperature dependence of the radical recombination rate constants of the alkali acrylate radicals . . . . .	96
III-4	$dY/dt$ and $dY/d\log t$ for the polymerization of some vinyl monomers . . . . .	103
III-5	$dY/dt$ for Li, Na and K acrylates . . . . .	105
<u>APPENDIX A</u>		
A-1	Polymerization of K acrylate at 313 K - Data for Fig. (III-1) - . . . . .	126
A-2	Polymerization of K acrylate at 323 K - Data for Fig. (III-1) - . . . . .	126
A-3	Polymerization of K acrylate at 333 K - Data for Fig. (III-2) - . . . . .	126
A-4	Polymerization of K acrylate at 353 K - Data for Fig. (III-2) - . . . . .	126
A-5	Temperature dependence of $dY/d\log t$ for K acrylate - Data for Fig. (III-3) - . . . . .	127
A-6	Polymerization of Li acrylate at 374 K - Data for Fig. (III-4) - . . . . .	128
A-7	Polymerization of Li acrylate at 405 K - Data for Fig. (III-4) - . . . . .	128

<u>Table</u>	page
A-8	Polymerization of Na acrylate at 393 K - Data for Fig. (III-5) - . . . . . 128
A-9	Polymerization of Na acrylate at 403 K - Data for Fig. (III-5) - . . . . . 128
A-10	Polymerization of K acrylate at 273 K - Data for Fig. (III-6) - . . . . . 129
A-11	Polymerization of K acrylate at 323 K - Data for Fig. (III-7) - . . . . . 129
A-12	Temperature dependence of $dY/dt$ for K acrylate - Data for Fig. (III-8) - . . . . . 130
A-13	Effect of one hour of prepolymerization at 353 K on the polymerization of K acrylate at 313 K - Data for Fig. (III-9) - . . . . . 130
A-14	Temperature dependence of the linewidth and second moment of Li acrylate - Data for Fig. (III-11) - . . . . . 131
A-15	Temperature dependence of the linewidth and second moment of Na acrylate - Data for Fig. (III-12) - . . . . . 131
A-16	Temperature dependence of the linewidth and second moment of K acrylate - Data for Fig. (III-13) - . . . . . 132
A-17	Temperature dependence of the linewidth and second moment of Rb acrylate - Data for Fig. (III-14) - . . . . . 134
A-18	Decay of Li acrylate radicals at 353 K - Data for Fig. (III-19) - . . . . . 135
A-19	Decay of Li acrylate radicals at 423 K - Data for Fig. (III-20) - . . . . . 136
A-20	Decay of Na acrylate radicals at 353 K - Data for Fig. (III-21) - . . . . . 137
A-21	Decay of Na acrylate radicals at 423 K - Data for Fig. (III-22) - . . . . . 138
A-22	Decay of K acrylate radicals at 313 K - Data for Fig. (III-23) - . . . . . 139

<u>Table</u>	page
A-23 Decay of K acrylate radicals at 323 K - Data for Fig. (III-23) - . . . . .	140
A-24 Decay of K acrylate radicals at 353 K - Data for Fig. (III-23) - . . . . .	141
A-25 Decay of Rb acrylate radicals at 303 K - Data for Fig. (III-24) - . . . . .	142
A-26 Decay of Rb acrylate radicals at 313 K - Data for Fig. (III-24) - . . . . .	143
A-27 Decay of Rb acrylate radicals at 353 K - Data for Fig. (III-24) - . . . . .	144
A-28 Second order decay of Li acrylate radicals at 353 K - Data for Fig. (III-25) - . . . . .	145
A-29 Second order decay of Na acrylate radicals at 353 K - Data for Fig. (III-26) - . . . . .	145
A-30 Second order decay of Na acrylate radicals at 423 K - Data for Fig. (III-27) - . . . . .	146
A-31 Second order decay of K acrylate radicals at 313 K - Data for Fig. (III-28) - . . . . .	147
A-32 Second order decay of K acrylate radicals at 323 K - Data for Fig. (III-28) - . . . . .	147
A-33 Second order decay of K acrylate radicals at 353 K - Data for Fig. (III-28) - . . . . .	148
A-34 Second order decay of K acrylate radicals at 373 K - Data for Fig. (III-28) - . . . . .	148
A-35 Second order decay of Rb acrylate radicals at 303 K - Data for Fig. (III-29) - . . . . .	149
A-36 Second order decay of Rb acrylate radicals at 313 K - Data for Fig. (III-29) - . . . . .	149
A-37 Second order decay of Rb acrylate radicals at 353 K - Data for Fig. (III-29) - . . . . .	150

APPENDIX B

B-1 Temperature dependence of the linewidth of solid sulfolane - Data for Fig. (B-1) - . . . .	162
B-2 Temperature dependence of the second moment of solid sulfolane - Data for Fig. (B-2) - . .	163

3

CHAPTER I  
INTRODUCTION

## INTRODUCTION

The study of solid state polymerization started in a systematic way in 1954 when Mesrobian et al. [Mesrobian (1954)] described the radiation induced polymerization of acrylamide. A few examples of solid state polymerization had been reported previously [Eastmond (1970)] but these had not attracted widespread attention. The recent upsurge of interest in this topic can be attributed to the possibility of obtaining crystalline stereoregular polymers through the control of the host monomer lattice. Further studies in solid state polymerization showed that there are very few monomers in which the crystal lattice strictly controls the structure of the polymer obtained. In general one cannot expect any direct geometrical correspondence between the monomer and polymer structures. Furthermore later studies showed that variables other than crystal structure, mainly crystal lattice defects and monomer mobility, were important in determining the rate and the mechanism of polymerization.

It was also hoped that studies in solid state polymerization could contribute to fundamental understanding of solid state organic chemistry: the product polymer molecule was hoped to be a photograph of the successive reaction steps. This situation is possible only when the monomer crystal structure controls polymer formation and again is to be considered exceptional.

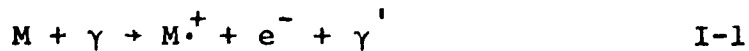
Most studies in solid state polymerization have so far consisted of empirical correlations of other variables with the rate of polymerization and a comprehensive theory has not yet been developed. The lack of very general ideas accounts for the fact that usually conclusions reached for certain monomers tend to be applicable only to very similar monomers. In particular this thesis deals with the polymerization of the lithium, sodium, potassium and rubidium salts of acrylic acid. These salts are vinyl monomers, ionic crystals with a high melting point and their polymerization occurs without a geometrical correspondence between the monomer and polymer structures. The main parameter investigated in this thesis is the mobility of the monomer. Solid state polymerization will from now on be indicated by SSP.

#### I-1 EFFECT OF $\gamma$ RAYS ON SOLIDS

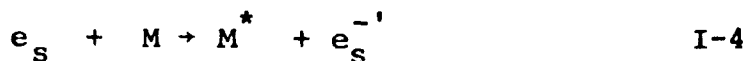
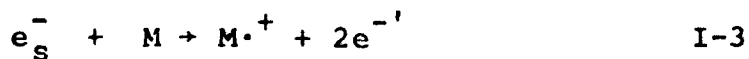
Many types of high energy radiation can cause ionization and the formation of excited species during their passage through matter [O'Donnell (1970), Swallow (1973)]. Such radiations, either particles ( $\alpha, \beta$ , neutrons etc.) or waves (X,  $\gamma$  rays etc.) differ in their penetration through matter, the spatial distribution of the species generated and the mechanism of ionization. Waves and uncharged particles have much higher penetration than charged particles. In particular,  $\gamma$  rays have such a penetration that their ef-

fect, can be considered as distributed throughout an irradiated crystal. Energy loss occurs by means of Compton scattering whereby incident photons cause ionization and the ejected electron has considerable kinetic energy.

The immediate effect of the interaction of  $\gamma$  rays with matter is the formation of radical-ions and of excited species:

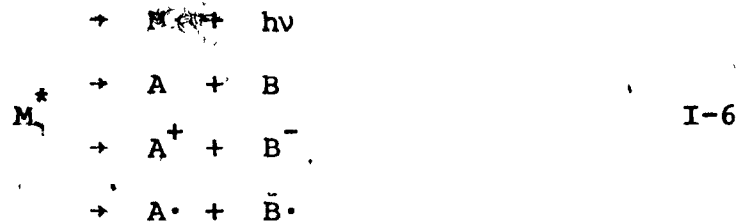


The electrons ejected in the formation of ions, called secondary electrons, often have enough energy to ionize or excite other molecules:



All these species are not homogeneously distributed in the crystal. They can either be formed in isolated spurs, widely separated along the main or branch tracks of the radiation, or in larger regions formed by the overlapping of isolated species as short tracks, cylinder-shaped regions, or blobs, pear shaped regions. Blobs have a higher density of active species than short tracks.

All the species formed can either undergo intra site reactions:



or escape from the sites where they were generated. The species that escape are called primary species. Primary species can react with the substrate to form primary products:



Under some conditions primary products can become so abundant that they compete with the substrate for primary species. The reaction between primary species and primary products gives secondary products:

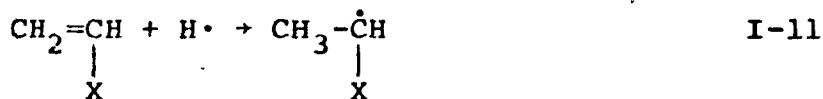


High radiation doses can favour secondary products over primary products.

The preceding features of the interaction of  $\gamma$  rays

with matter are relative to all condensed phases. They are indeed all chemical effects. In the case of solids another possible effect of  $\gamma$  rays is the creation of defects the concentration of which depends on the energy deposited by the radiation for unit path length (Linear energy transfer).

Given the extremely high energy of  $\gamma$  rays the formation of a wide variety of products might be expected. However in general very few species are formed. For example the low temperature  $\gamma$  ray irradiations of vinyl monomers studied to date, have given mainly one type of radical derived via the addition of a hydrogen atom to a double bond [Adler (1965), Marx (1963)]:



## I-2 SOLID STATE POLYMERIZATION

As already stated in the introduction, most investigations in SSP have so far consisted of empirical correlations of the rate of polymerization with other variables. The effect of the main parameters found to play a role in SSP, crystal structure, defects and molecular motions, will now be described. A discussion of the theoretical ideas proposed and of the problems that a theory of SSP should solve will follow.

I-2,a Effect of crystal structure

The hope that the size and shape of a polymer chain formed in a solid state polymerization was controlled by the crystal lattice of the monomer, which gave initially stimulus to SSP studies, was later shown to be a rather naive view. In the polymerization of vinyl monomers, for example, the hybridization of C atoms changes from  $sp^2$  to  $sp^3$  and some intermolecular distances become bond lengths. Therefore both the geometry of the monomer units and their total length change during the formation of the polymer chain. It is then apparent that one cannot expect in general a true topotaxy or tridimensional correspondence between the structure of the polymer product and its host monomer beyond the first few addition steps [Bamford (1969)]. In fact in most of the SSP reactions investigated the polymers are amorphous. Furthermore electron microscopy and X-ray observations [Adler (1960), Sella (1962), Kargin (1967), Wegner (1973b)] show that the polymer tends to form a second phase within the reacting monomer crystals.

It is to be noticed here that the production of a crystalline polymer is not a proof of topotaxy. For example, it is not yet clear whether there is lattice control of the polymerization of trioxane and tetraoxane type monomer crystals. The crystallinity of the polymer [Okamura (1960)] was later on attributed to the geometry of the polymer fiber crystallites, to annealing processes or

to solvent induced recrystallization [Adler (1966), Wegner (1973a), (1973b)]. On the other hand the most recent study reported shows that the polymerization is easier in the perfect crystal than in the defects [Voigt-Martin (1974)]. In general it must be remembered that there are artifacts which can simulate a topotactic polymerization.

There are however few solid monomers which do undergo a true topotactic polymerization, sometimes even leading to polymer single crystals [Morawetz (1964), (1965), Nakanishi (1972), Baughmann (1974)]. These monomers are in general longer molecules and their crystal structure is such that they can join to form a polymer chain with a minimum displacement [Wegner (1972), Baughmann (1974)]. The formation of polymer single crystals requires also the isomorphism of the polymer product and the host monomer with consequent solid solubility.

Although true topotaxy cannot be expected the crystal structure can exert other types of influence on the SSP reaction. It is known for example that the initial radical is oriented in the monomer lattice [Onishi (1963), O'Donnell (1964), Adler (1965), Chapiro (1972)]. Then the geometry of the crystal must be such to allow a monomer molecule to join the initiating radical. In fact a crystallographic study of monomers polymerizing in the solid state showed that in general the distance between the reacting centres should be  $4 \text{ \AA}^{(*)}$  or less in order that polymerization

(\*)  $1 \text{ \AA} = 10^{-10} \text{ m}$

can occur [Schmidt (1964)]. Although there is at least one exception to this rule [Laing (1968)] the control over the first addition steps is probably the most general effect of the crystal structure in SSP. Possibly related to this effect are the large variations in polymerizability found among different polymorphic modifications of the same compound [Grabar (1964), Werner (1971), Thomas (1971)]. These observations show that although SSP is not a topotactic reaction it is very often a topochemical reaction, or a reaction that occurs because of the particular crystal structure of the host lattice.

The crystal structure can also influence the polymerization through the interphase between monomer and polymer. The interphase between reactant and product can be coherent or incoherent [Young (1966)]. In the first case the natural position of atom  $i$  in the reactant is either precisely the same as in the product, or at least one plane in the reactant is identical with one plane in the product; in the second case there is no special crystallographic relationship between the atoms of the product and of the reactant molecules. The most general type of interphase is probably the semi-coherent, consisting of small regions of coherent interphase separated by an array of intersecting line dislocations. For a coherent or semi-coherent interphase the crystal structure can still control the polymer product. Also, the degree of coherence of the interphase

could change with the extent of reaction producing polymers of different properties. This could explain the change in polymer tacticity with the extent of polymerization found for methacrylic acid [Lando (1972), Chachaty (1975)].

The crystal structure of the monomer can therefore influence the polymerization mechanism in many ways, topotaxy being only one of the possible results of this influence.

Further progress in this field has been delayed by the lack of information concerning the crystal structures of the monomer materials. There are experimental difficulties in determining these structures since polymerization can occur during an X-ray or a neutron diffraction study.

#### I-2,b Role of crystal lattice defects

Defects in a crystalline solid are the deviations from the perfect tridimensional order and the chemical purity of a perfect crystal lattice. Many investigations, mainly on inorganic solids, have shown that defects can radically modify the reactivity of solids [Garner (1955), Farad (1959), Hedvall (1966), Galwey (1967), Schwab (1965)].

Defects can be classified as point, line and plane defects. Point defects, such as interstitials and vacancies, are not considered to have an important effect at the temperatures at which SSP is usually studied [Bamford (1969)].

Line defects are of two types: edge and screw

dislocations [Kittel (1966), Hannay (1967)]. An edge dislocation can be thought of as being produced by the insertion of an extra half plane of atoms in a perfect crystal lattice.

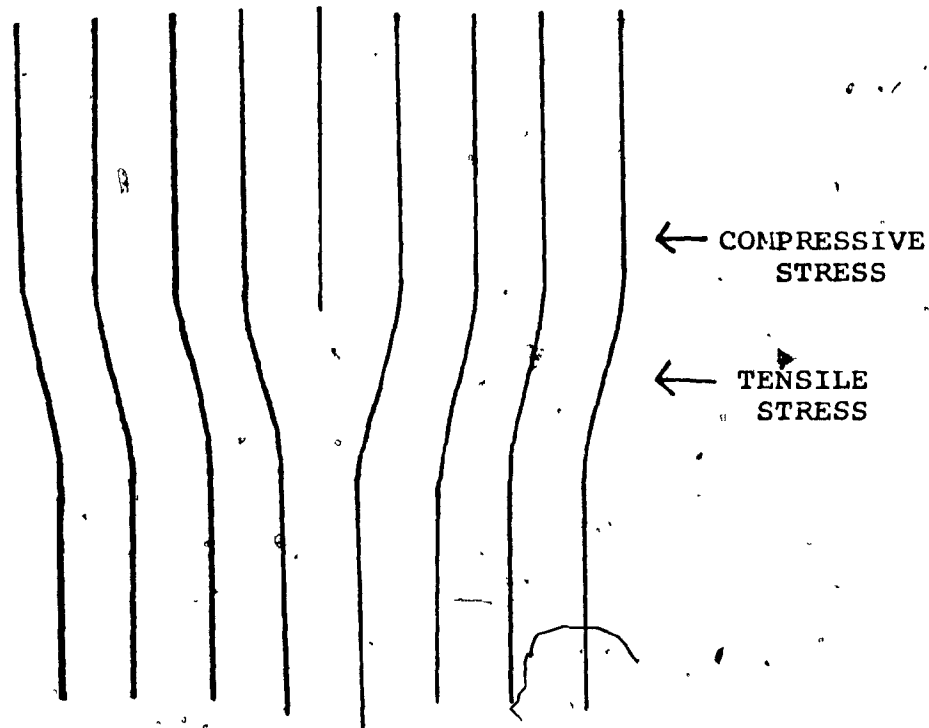


Fig. (I-1): Edge dislocation

A screw dislocation can be thought of as produced by cutting the crystal partway through with a knife and shearing it parallel to the edge of the cut by one lattice spacing. A screw dislocation transforms successive atom planes into

the surface of an helix,

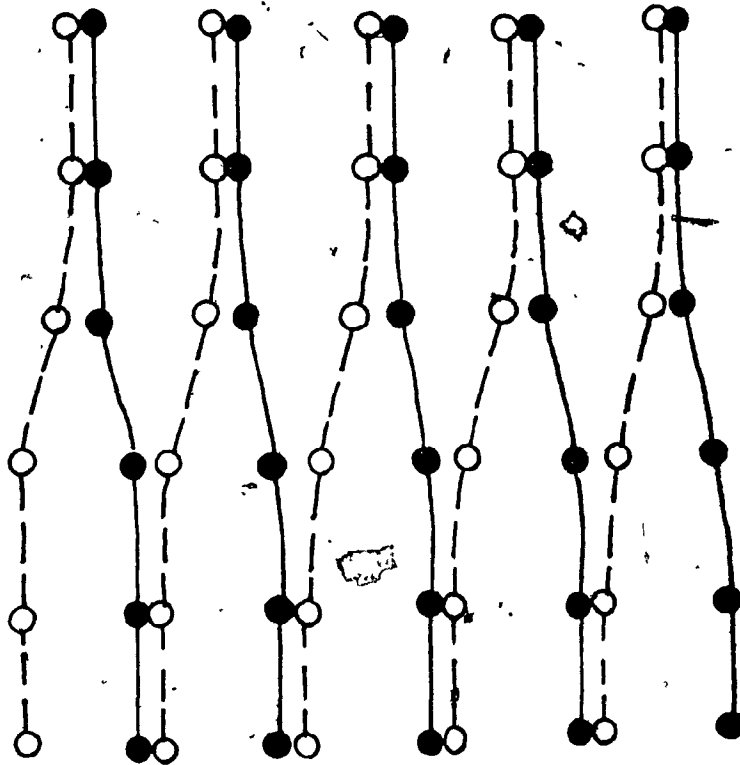


Fig. (I-2): Screw dislocation

Near the core of a dislocation there are both regions of compressive stress and of tensile stress. Reaction at these sites should minimize the buildup of additional strains. Dislocations should therefore favour the nucleation of a new phase. Dislocations reduce three to four orders of magnitude relative to a perfect crystal the critical shear stress or minimum stress needed to plastically deform a solid. The plastic deformation is brought about by the

movement of dislocations inside the crystal. The simple presence of dislocations in a crystal does not explain the plastic flow. As dislocations are annihilated when they meet the surface of a crystal new dislocations must continuously be generated by the applied stress if the process of plastic flow is to continue. In a solid state reaction the product does not fit perfectly in the crystal lattice of the reagent and therefore the reaction generates strains in the crystal. It is likely that this strain can be accommodated by the lattice through the movement of dislocations and generation of new ones. Dislocations are also known to provide regions of higher diffusion coefficient in a crystal thus facilitating the collision of reactants. Indeed observations on organic crystals undergoing various reactions, including SSP, seem to indicate that dislocations are a preferred site for nucleation. Thomas and Williams [Thomas (1969)] showed, by a chemical etching study, that the regions of preferred dimerization in anthracene coincide with etch pits. Thomas and Williams [Thomas (1967)] suggest that the protuberances found on the surfaces of partially decomposed sucrose crystals correspond to the emergence of dislocations at the crystal surface. Furthermore they explain the satellites surrounding the protuberances by the introduction of further dislocations during decomposition. Similar protuberances have been observed after the polymerization of p-benzamidostyrene to low conversions [Morawetz (1964)]. In the polymerization of

acrylamide Sella et al. [Sella (1961), (1962)] observed by electron microscopy the development of polymer globules along lines oriented in crystallographic directions. They concluded that the polymerization starts in dislocations. Bamford et al. [Bamford (1963)] inferred from the pressure dependence of the rate of photopolymerization of acrylic and methacrylic acids that the polymerization occurs preferentially in dislocations. Eastmond [Eastmond (1973)] showed that the directions in which dislocation lines can be formed more easily coincide with the directions of known polymer growth, in trioxane.

All the experimental results and ideas reported so far are relative only to the properties of individual dislocations. Dislocations interact also with one another and for very high dislocation concentrations their interaction becomes responsible for such properties of solids as work hardening [Kittel (1966), Martin (1972)]. It would be interesting to investigate if the interaction of dislocations plays any role in SSP.

The properties of dislocations described above must be possessed also by low angle grain boundaries since they are an array of dislocations. The effect of low angle grain boundaries on SSP is then expected to be qualitatively the same as of dislocations.

Large angle grain boundaries and phase boundaries are characterized by a higher degree of disorder than dis-

locations. On the basis of the previous arguments they are expected to favour the polymerization even more. However their influence on SSP has not been sufficiently investigated.

I-2,c      Role of molecular motions

Several experimental observations indicate that monomer mobility is an important parameter in SSP. Wide-line NMR has shown that trioxane [Komaki (1963)], acrylonitrile [Chachaty (1973)], acrylic and methacrylic acids [Eastmond (1971)], methyl methacrylate [Marx (1965)] and sodium methacrylate [Odajima (1961)] polymerize only at temperatures at which the monomer undergoes a considerable molecular reorientation. Wide-line NMR however detects only molecular motions occurring over the whole crystal [see (I-3,a)]. If polymerization starts mainly in dislocations it is the monomer mobility in dislocations that should be investigated. This was done by ESR in the case of methacrylic acid [Bamford (1968)]. The polymerization was shown to start only above a temperature at which there are enough molecular motions in the defects where the reaction occurs. General molecular reorientation could then be important only because it implies a higher defect mobility.

Self diffusion is known to be the rate determining step in many solid state reactions [Wintle (1972)] including radical recombination. Rate constants for radical diffusion can then be determined by ESR. If a radical and the corresponding monomer

are not very different their diffusion rate constants are very similar [see (I-3,b)]. By ESR it was shown that the frequencies of self diffusion and polymerization of acrylonitrile at low temperatures are very similar [Gol'danskii (1971a)]. On the other hand the same method gave for acrylic acid a frequency of polymerization much smaller than the frequency of self diffusion [Gol'danskii (1971c)]. Probably self diffusion is a rate determining step only in certain ranges of temperature or at some polymerization times [Gol'danskii (1971b)]. Both for acrylonitrile and acrylic acid the frequency of polymerization is much smaller than the frequency of molecular reorientation measured by wide-line NMR. It is also to be remarked that the frequency of monomer addition changes during the growth of the polymer chain [Adler (1969)] and it is its "instantaneous" value that should be compared with the frequency of molecular motion. Evidence for the importance of impurity diffusion in the polymerization of trioxane was found in a study of its dielectric relaxation [Reneker (1974)].

The empirical evidence of the importance of molecular reorientation in SSP is rationalized by the assumption that it supplies the correct geometry for the monomer and the radical to join whereas their equilibrium positions might be unsuitable [Adler (1969)]. This can be true in general only for the first few addition steps preceding phase separation. Self-diffusion is necessary to supply monomer molecules to the

growing chain end. Other roles have been postulated for monomer mobility: to assist the change from  $sp^2$  to  $sp^3$  hybridization of a vinyl monomer by allowing the necessary displacement of the surrounding molecules [Gol'danskii (1972)]; to help anneal stresses set up in the lattice by the polymerization and to allow recrystallization of the polymer. Lattice control of the polymerization was considered to be possible only in presence of molecular motions which would allow the reaction to take place in the perfect crystal while in a rigid crystal polymerization could only occur in defects [Kargin (1967)].

In conclusion there is empirical evidence that molecular mobility is in general a prerequisite for SSP but the exact mechanism by which this occurs is not known.

#### I-2,d Reaction mechanism and kinetics

In order to understand the problems that a theory of SSP should try to solve it must be considered that SSP is both a solid state reaction, in most of the cases occurring through a two-phase mechanism, and a polymerization reaction.

A solid state reaction leading to the formation of a new phase is considered to occur through the steps of nucleation and growth [Hannay (1967), Garner (1955)]. A nucleus is a point in the crystal where the reaction starts. Although the free energy for the formation of the new phase is negative the nucleus can initially be unstable because it creates positive interphase and elastic strain free energies. The net change in free energy is:

$$\Delta G = \Delta G_v + \Delta G_s + \Delta G_e \quad (I-12)$$

where  $v$ ,  $s$  and  $e$  represent respectively the volume or chemical, surface and elastic free energy changes. Neglecting  $\Delta G_e$ , as can be done for most of the cases<sup>(\*)</sup>,  $\Delta G_v$  and  $\Delta G_s$  can be written as:

$$\Delta G = \frac{4}{3} \pi r^3 \Delta g_v + 4 \pi r^2 \Delta g_s \quad (\text{I-13})$$

where  $\Delta g_v$  and  $\Delta g_s$  are the unit volume and unit surface free energy. For very small radii the surface free energy is the dominant term and the nucleus is unstable, but above a certain critical radius the volume free energy becomes more important because of its  $r^3$  dependence and the nucleus growth becomes a favoured process:

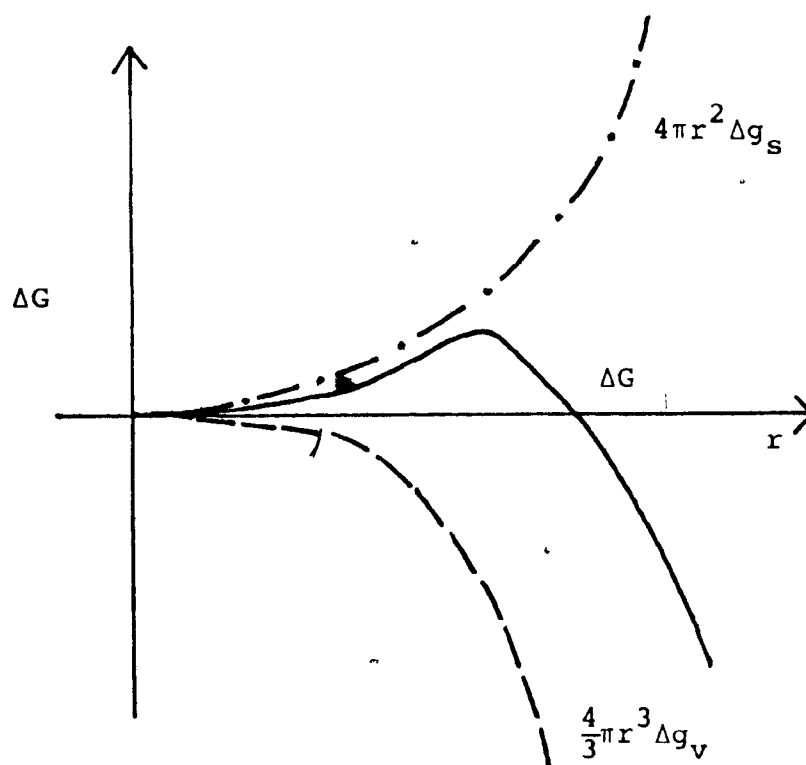


Fig. (I-3): Dependence of the free energy of the nucleus on its radius

(\*)

The limits of this approximation will be discussed later.

The critical radius is the value of  $r$  for which the derivative of  $\Delta G$  with respect to  $r$  is zero.

The kinetic law describing a solid state reaction will contain in general both the rates of nucleation and of nucleus growth.

This model has been successfully applied to a large number of solid state inorganic reactions.

In the specific case of SSP, apart from describing the variation of polymer yield with time, this model should also answer the following questions:

- a) For what chain length does the nucleus reach its critical size?
- b) Under what conditions will the initial radical grow to form a stable nucleus rather than undergo recombination?
- c) How many polymer chains will be contained in the critical nucleus? What will be their size and shape?
- d) Does the growth of the nucleus occur by increase of length of the chains?
- e) What is the structure of the interphase between the nucleus and the monomer crystal?
- f) In what regions of the crystal will nucleation be facilitated?

So far few attempts have been made to answer these questions. Kargin et al. [Kargin (1965), (1966)] assumed that the nucleus is a cylinder formed by parallel growing chains. They found that the number of chains forming the critical

nucleus is directly proportional to the interphase free energy and inversely proportional to the volume free energy. By this model they also derive kinetic curves qualitatively similar to those obtained in many solid state polymerizations. The value of this and of similar treatments is limited by the many unconfirmed assumptions.

The vast majority of SSP investigations do not explicitly consider the steps of nucleation and growth. Instead the behaviour of some parameters likely to affect SSP has been tested and the reaction has been subdivided into initiation, propagation and termination, as in liquid-phase polymerization. Research in SSP seems to be still at the stage of the collection of data from which a theory will eventually be built.

The steps of propagation and termination deserve some comment because they show some differences from solution polymerization.

Propagation in SSP differs from solution polymerization since it can be further subdivided into two steps: the addition of the first monomer units to the initiating species, which occurs in the lattice, and the subsequent addition of the monomer to a long polymer chain, occurring at the monomer-polymer interphase [Chapiro (1972)]. The very first addition steps can also occur at a temperature at which polymerization itself does not take place<sup>(\*)</sup>.

In SSP initiation and propagation can be made to

(\*)

This is true only for radical polymerizations.

occur simultaneously (in source-polymerization) or separately (post-polymerization). The latter method has the advantage that the polymer is not damaged by the radiation.

Termination in SSP is again different from solution polymerization since for most of the monomers investigated in the solid state termination does not involve chemical destruction of the active species, e.g. recombination, but some physical changes occur in the reacting system. Active species remain after the reaction has stopped and the polymerization can usually be started again at a higher temperature<sup>(\*)</sup> (reanimation effect). The mechanism of termination is far from being well understood but its elucidation is of considerable importance to the understanding of SSP. Further discussion of this point will be done in Chapter III.

As the mechanism of SSP is not well known kinetic treatments cannot lead to true reaction theories. They are mainly empirical correlations of variables. Two kinetic schemes that can be applied to the SSP of the alkali acrylates will be illustrated here. The first, due to Morawetz [Morawetz (1960)], deals with SSP in terms similar to solution polymerization. The second, introduced by Chachaty twelve years later [Chachaty (1972b)], considers variables more typical of a solid state reaction. Both illustrate

(\*)

Except at temperatures where there is a minimum in the rate of reaction.

some problems characteristic of SSP in general.

In Morawetz's kinetic scheme a bimolecular decay of the active chain ends is assumed.

$$-\frac{d[R\cdot]}{dt} = k_t [R\cdot]^2 \quad (I-14)$$

$$[R\cdot] = [R\cdot]_0 / (1 + k_t [R\cdot]_0 t) \quad (I-15)$$

The change in monomer concentration is given by:

$$-\frac{d[M\cdot]}{dt} = k_p [M] [R] \quad (I-16)$$

leading to a time dependence of  $Y$ , the fractional polymer yield

$$Y \approx -\ln(1-Y) = (k_p/k_t) \ln(1 + k_t [R\cdot]_0 t) \quad (I-17)$$

This treatment gives a kinetic curve of the correct form but it has a number of shortcomings, some of which were recognized by its authors. For example a bimolecular termination of the polymer chains is incompatible both with a radical and an ionic mechanism as discussed by Morawetz in the case of acrylamide. The radical concentration decays at a rate different from the rate of polymerization. On the other hand an ionic bimolecular termination is inconsistent with the radiation dose dependence of the polymer molecular weight. The recombination of active species cannot then be a cause for termination.

The monomer concentration also is rather difficult to define. For instance, if the reaction occurs by a two-phase mechanism the monomer concentration encountered by the advancing interphase is constant. Concentrations and orders of reaction are used with the same meaning as in solution polymerization but in the solid state the reactivity of a species depends also on its position in the crystal (e.g. perfect crystal, near defects, at the surface etc.). A distribution function for the reactivity of the active species should thus be introduced.

In Chachaty's kinetic treatment the fall in the rate of post-polymerization is attributed to the gradual immobilization of the groups carrying the free valency and to a modification of the matrix structure consisting of a linear increase of the average energy of activation with the polymer chain length  $L$ . The rate constant for either polymerization or radical recombination is given by:

$$K = (kT/h) \exp[-(\Delta F_0/RT)(1 + \lambda L)] \quad (\text{I-18})$$

where  $k$  is the Boltzmann constant,  $h$  is Planck's constant,  $\Delta F_0$  is the initial activation energy,  $R$  is the gas constant and  $\lambda$  is a constant. The rate of propagation of a chain is given by:

$$\frac{dL}{dt} = A \exp[-\alpha L] \quad (\text{I-19})$$

$$A = (RT/h) \exp[-\Delta F_0/RT] \quad (\text{I-20})$$

$$\alpha = (\Delta F_0/RT) \lambda \quad (I-21)$$

A is the rate constant of the polymerization in the initial crystal and  $\alpha$  the rate of increase of the free energy of activation with increasing chain length or in other words the increasing difficulty of polymerization. Similar equations apply to radical recombination:

$$-\frac{dC}{dt} = B \exp(-\beta L) C^2 \quad (I-22)$$

$$B = (RT/h) \exp[-\Delta F_0/RT] \quad (I-23)$$

$$\beta = (\Delta F_0/RT) \lambda \quad (I-24)$$

where C is the local radical concentration and  $\beta$  is a measure of the increasing difficulty of recombination with polymer chain length. Combination of equations (I-19)-(I-24) gives the variation of the local radical concentration deriving from both polymerization and recombination. When recombination is highly favoured with respect to polymerization ( $\beta/\alpha \ll 1$ ) the decay of radical concentration becomes a normal second-order process. Average radical concentrations  $[R\cdot]$  measured by ESR are obtained from local concentrations by a distribution function  $f(\alpha)$  for the reactivity of the radicals:

$$[R\cdot] = N_0 \int_0^\infty f(\alpha) C \, d\alpha \quad (I-25)$$

where  $N_0$  is the number of radical packets per unit volume,

$v$  is the volume of a packet and  $C$  is the local radical concentration. The resultant general equation for SSP:

$$Y = \frac{[R\cdot]_{\infty}}{\bar{\alpha}M_0} \ln \left[ \frac{A}{A_0} - \left( \frac{A}{A_0} - 1 \right) \exp[-\bar{\alpha}A_0 t] \right] \quad (I-26)$$

where  $[R\cdot]_{\infty}$  is the stable radical concentration at long times,  $\bar{\alpha}$  is the average value of  $\alpha$  with respect to the whole crystal,  $M_0$  is the initial monomer concentration,  $A_0$  is a constant introduced to account for limiting conversion. In particular cases equation (I-26) can be approximated to give a linear time dependence of the polymer yield  $Y$ :

$$Y = ([R\cdot]_{\infty}/M_0) (A - A_0) t \quad (I-27)$$

an exponential time dependence:

$$Y = ([R\cdot]_{\infty}/\bar{\alpha}M_0) \left[ \left( \frac{A}{A_0} - 1 \right) (1 - \exp[-\bar{\alpha}A_0 t]) \right] \quad (I-28)$$

or a logarithmic time dependence:

$$Y = ([R\cdot]_{\infty}/\bar{\alpha}M_0) \ln [1 + \bar{\alpha}(A - A_0) t] \quad (I-29)$$

All these types of kinetic behaviour are found experimentally.

Chachaty's kinetic treatment is based on assumptions physically more realistic than the Morawetz treatment. It is also a very general kinetic treatment. Unfortunately it contains many parameters that at the moment cannot be measured and it is therefore difficult to test experimentally

the validity of this treatment. In this aspect it illustrates a problem that is characteristic of many kinetic treatments of SSP: with a proper choice of parameters it is possible to obtain any kinetic curve.

At the moment the most fruitful approach seems to be the investigation of the individual reaction steps and reaction variables rather than the derivation of overall kinetic schemes. Without this information not only are many assumptions necessarily arbitrary but kinetic equations, even if formally correct, might be without physical meaning. For instance in an investigation of the reaction steps of the SSP of trioxane [Voigt-Martin (1974)] the overall kinetics of polymerization was found to be the resultant of the four subsequent or parallel processes nucleation, longitudinal fibril growth, fibril thickening, grain boundary and defect induced growth [Fig. (I-4)].

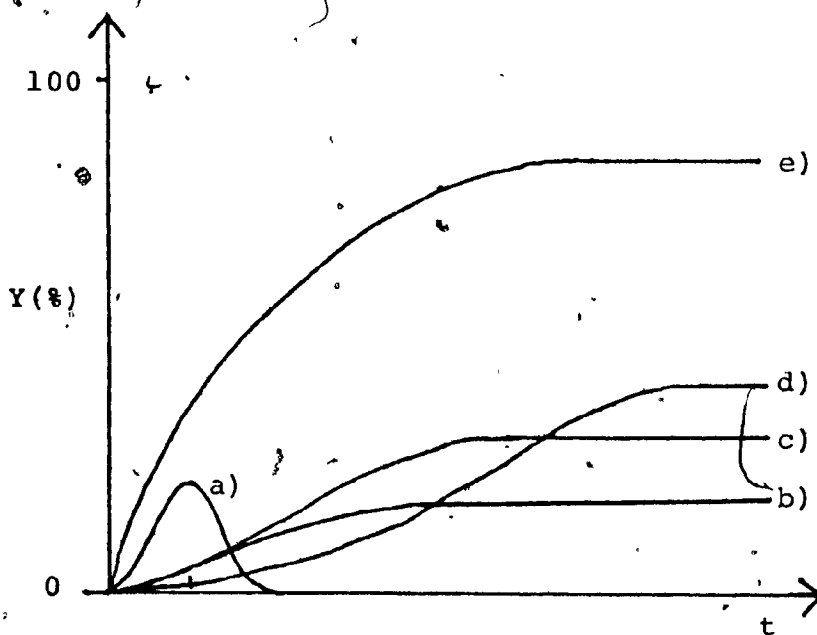


Fig. (I-4): Time dependence of the polymer yield of a) nucleation, b) defect induced polymerization, c) longitudinal fibril growth, d) transversal fibril growth, e) overall polymerization

Any attempt to derive a kinetic equation from the overall kinetics of polymerization only would have been without physical meaning.

I-3

MAGNETIC RESONANCE

A charged particle possessing a spin has also a magnetic moment which orients itself with respect to an external magnetic field. The number of allowed orientations is restricted by quantization and it is possible to induce transitions between the states having different orientations and therefore different energies. Radiowaves and microwaves are used respectively in nuclear magnetic resonance (NMR) and electron spin resonance (ESR). The usefulness of these techniques for chemistry lies in the fact that transition frequencies, linewidths and lineshapes are probes of inter- and intra-molecular environment. Other information about the environment surrounding the spins can be obtained from studies of the relaxation behaviour of the spin system. An excited spin system tends to return to the ground state by transferring energy to degrees of freedom out of the spin system (spin-lattice relaxation) or within the spin system (spin-spin relaxation). The characteristic times  $T_1$  (spin-lattice relaxation time) and  $T_2$  (spin-spin relaxation time) with which these processes occur are also determined by the environment surrounding the spins.

The general ideas so far outlined are common to NMR and ESR but both the experimental techniques and the information that one can obtain are different. Their applications to solid state problems will thus be described separately.

I-3,a Applications of NMR to the study of molecular motions in solids

Nuclei in a solid placed in a magnetic field interact with the external magnetic field and through dipole-dipole interaction with other magnetic nuclei. Interactions within other nuclei lead to considerable differences in local environments which broaden the NMR line. The NMR of solids is then called wide-line NMR. Calculation of the lineshape, i.e. of all possible transition frequencies and of the relative probabilities, requires the solution of the Schrodinger equation:

$$\mathcal{H}\psi = E\psi \quad (\text{I-30})$$

where  $\mathcal{H}$  is the following hamiltonian:

$$\begin{aligned} \mathcal{H} &= g_N \beta_N H \sum_i I_{zi} + \\ &+ g_N^2 \beta_N^2 \sum_{i,j} \frac{I_i \cdot I_j}{r^3} - \frac{(I_i \cdot r_{ij})(I_j \cdot r_{ij})}{r^5} = \\ &= Z + D \end{aligned}$$

where  $g_N$  is the nuclear g factor,  $\beta_N$  is the nuclear magneton,  $I_i$  and  $I_j$  are the nuclear spin vectors of nuclei i and j,  $I_{z_i}$  is the z component of the nuclear spin,  $r_{ij}$  is the distance between nuclei i and j, Z represents the Zeeman interaction of the nuclei with the field and D the dipolar interaction. Equation (I-31) can be solved only for very simple spin

systems (two, three or four nuclei) and for more complex cases the method of moments is customarily used. The  $n$ th moment of a normalized resonance curve  $f(H)$  is defined as:

$$M_n = \int_{-\infty}^{+\infty} (H-H_0)^n f(H) dH \quad (I-32)$$

where  $H_0$  is the field at the centre of the resonance curve. Van Vleck [Van Vleck (1948)] showed that the second moment can be calculated in terms of internuclear distances and angles. For a single crystal:

$$M_2 = \frac{3}{4} I(I+1) g_N^2 \beta_N^2 N^{-1} \sum_{i,j} (3\cos^2\theta_{ij}-1)^2 R_{ij}^{-6} + \frac{1}{3} \beta_N^2 N^{-1} \sum_{i,f} I_f(I_f+1) g_f^2 (3\cos^2\theta_{if}-1)^2 R_{if}^{-6} \quad (I-33)$$

where  $I$  is the nuclear spin number,  $N$  the number of nuclei at resonance,  $\theta_{ij}$  the angle between the field and the distance between nuclei  $i$  and  $j$   $R_{ij}$ , all the symbols with the subscript  $f$  have analogous meaning but referred to nuclei not at resonance.

To compute  $M_2$  by (I-33) one should calculate  $R_{ij}$  for all the possible pairs of nuclei in the lattice but in practice  $R_{ij}^{-6}$  vanishes beyond one or two unit cell distances and many terms can be neglected.

$M_2$  for a polycrystalline sample is found by averaging equation (I-33) over all the possible  $\theta$  values:

$$M_2 = \frac{3}{5} g_N^2 \beta_N^2 I(I+1) N^{-1} \sum_{i,j} R_{ij}^{-6} + \frac{4}{15} \beta_N^2 N^{-1} \sum_{i,f} I_f(I_f+1) g_f^2 R_{if}^{-6} \quad (I-34)$$

The exact computation of  $M_2$  requires the knowledge of the crystal structure. When the crystal structure is not known approximate methods can be used. This is usually done by dividing  $M_2$  into an intramolecular part  $S_1$  and an intermolecular part  $S_2$ . The intramolecular second moment is calculated by assuming reasonable bond lengths and angles while the intermolecular part is estimated from a comparison with known similar structures. Molecular motions of high enough frequency will decrease the dipolar interactions by averaging them over other possible orientations. The corresponding decrease in the second moment is obtained by averaging the term  $(3\cos^2\theta_{ij}-1)$  over all the possible orientations assumed during the motion [Gutowsky (1950)]. The intramolecular second moment for a single crystal in presence of molecular rotation is then given by:

$$S_{1,rot} = (3\cos^2\theta'-1)^2 \left[ \frac{3}{4} I(I+1) g_N^2 \beta_N^2 N^{-1} \sum_{i,j} F(\beta_{ij}) R_{ij}^{-6} + \frac{1}{3} \beta_N^2 N^{-1} \sum_{i,f} I_f(I_f+1) g_f^2 F(\beta_{if}) R_{if}^{-6} \right] \quad (I-35)$$

$$F(\beta_{ij}) = \frac{1}{4} (3\cos^2\beta_{ij}-1)^2 \quad (I-36)$$

where  $\theta'$  is the angle between the field and the axis of

rotation,  $\beta_{ij}$  is the angle between the axis of rotation and  $R_{ij}$ . In the case of polycrystalline material the term  $(3\cos^2\theta - 1)$  is replaced by its average over all possible  $\theta$  values  $\frac{4}{5}$ :

$$S_{1,rot} = \frac{3}{5} I(I+1)g_N^2 \beta_N^{2N-1} \sum_{i,j} F(\beta_{ij}) R_{ij}^{-6} + \frac{4}{15} \beta_N^{2N-1} \sum_{i,f} I_f(I_f+1)g_f^2 F(\beta_{if}) R_{if}^{-6} \quad (I-37)$$

Each term is reduced with respect to the rigid lattice value by the factor  $F(\beta)$ .  $S_{1,rot}$  can then be calculated for any type of molecular reorientation.

A method for the calculation of the intermolecular and intergroup contribution was developed by Andrew and Eades [Andrew (1953)]. This is more complicated than the calculation of the corresponding intramolecular contribution because of the simultaneous variation of angles and distances during the motion.

Rotational oscillation causes a reduction of the second moment dependent on the oscillation amplitude. In this case the reduction factor for the intramolecular second moment is given by [Andrew (1950)]:

$$\rho = 1 - \frac{3}{4} [(1 - J_0^2(\alpha)) \sin^2 2\gamma + (1 - J_0^2(2\alpha)) \sin^4 \gamma] \quad (I-38)$$

where  $\gamma$  is the angle between the interproton vector  $R_{ij}$  and the axis of rotational oscillation,  $\alpha$  is the oscillation amplitude and  $J_0(\alpha)$  is a zero order Bessel function.

Isotropic molecular reorientation cancels the intramolecular second moment [McCall (1960), Dmitrieva (1964)] while leaving a finite intermolecular contribution that can be calculated considering all the protons concentrated at their molecular centres. This leads to the formula:

$$M_{2, \text{reor}} = 358.1 N_0 \sum_{i=1}^{\infty} N_i R_i^{-6} \quad (\text{I-39})$$

where  $N_0$  is the number of protons per molecule,  $N_i$  is the number of  $i$ th nearest neighbours and  $R_i$  is the centre-centre distance (in  $\text{\AA}$ ) between a molecule and its  $i$ th nearest neighbour.

The intermolecular second moment vanishes only when the centre of mass of the molecule moves, for instance if self diffusion occurs.

In an experimental curve of second moments vs. temperature  $M_2$  may decrease with increasing temperature only over certain temperature ranges and remain constant over others. If the frequencies of molecular reorientation increase continuously with temperature it means that only certain frequencies are effective in reducing the second moment. The reason for this phenomenon can be understood with reference to the relaxation behaviour of a spin system. A nuclear spin precesses about the magnetic field  $H = H_0 \pm H_{\text{loc}}$  where  $H_0$  is the external field and  $H_{\text{loc}}$  is the local field determined by the nuclear dipolar interaction, with a frequency  $\omega = \gamma H = \gamma H_0 \pm \gamma H_{\text{loc}} = \omega_0 \pm \Delta\omega$ . If all the nuclei

precessed in phase, with the same frequency  $\omega$ , at a certain instant, they would lose phase after a time  $T_2 = 1/\gamma H_{loc} = 1/\Delta\omega$ . If a molecular motion is to affect the relaxation behaviour and the linewidth it must occur at a minimum frequency  $\omega = 1/T_2$ .

The comparison of calculated and experimental second moments allows the determination of the molecular motion occurring in a solid, but information obtained from the second moment within a transition region is of doubtful significance due to the theoretical invariance of the second moment with molecular motions. Andrew and Newing [Andrew (1958)] showed that molecular motions can only split an absorption curve into a central part and sidebands. These are separated by the frequency of molecular motion and therefore the sidebands move outward with increasing temperature above the transition. The total second moment remains constant but its distribution between central and sidebands varies. The second moment of the central part, given by the modified Van Vleck expression, cannot be accurately determined near a transition temperature because of the overlapping with the sidebands.

Information from the transition region itself can be obtained from the linewidths. An equation initially formulated by Purcell and Pound [Purcell (1948)] and modified by Gutowsky and Pake [Gutowsky (1950)]:

$$(\delta H)^2 = (A^2 - B^2) (2/\pi) \text{TAN}^{-1} [\alpha (\gamma \delta H / 2\pi \nu_c)] + B^2 \quad (\text{I-40})$$

where  $\delta H$  is the linewidth,  $\gamma$  is the magnetogyric ratio,  $\nu_C$  is the reorientation frequency,  $A$  and  $B$  are respectively the linewidth below and above the transition, allows the determination of reorientation frequencies from the linewidth values:

$$\nu_C = (\alpha\gamma\delta H/2\pi) [\text{TAN}(\pi/2) ((\delta H^2 - B^2)/(A^2 - B^2))]^{-1} \quad (\text{I-41})$$

By the usual assumption that molecular reorientation is an activated process:

$$\nu_C = \nu_0 \exp(-E_a/RT) \quad (\text{I-42})$$

activation energies for molecular motions can be determined.

Some assumptions made in the derivation of equation (I-40), like the existence of a constant lineshape all through the transition, limit considerably its usefulness. When absurd results are obtained by means of equation (I-40) an alternative treatment developed by Waugh and Fedin [Waugh (1963)] can be used. The results of this treatment are expressed by the equations:

$$E_a = 1.8 RT_C \ln [(n/\Delta) (kT_C/2I)^{1/2}] \quad (\text{I-43})$$

$$E_a = 37 T_C \text{ (kcal mol}^{-1}\text{)} \quad (\text{I-44})$$

where  $T_C$  is the temperature at which the line starts narrowing,  $n$  is the symmetry number of the axis of reorientation,  $\Delta$  is the difference between the linewidths below and above the

transition,  $I$  is the moment of inertia of the molecule. Equation (I-44) is an approximate version of equation (I-43) which in most of the cases gives results accurate within  $\pm 10\%$ .

The wide-line NMR method illustrated so far has some limitations. For example it is sensitive only to molecular motions occurring over the whole crystal and it does not detect motions taking place in defects only. Also frequencies of molecular reorientation can be determined only over very limited ranges, and simultaneous motions taking place in the same solid cannot be unambiguously separated. Both an extension of the range of measurable frequencies and a better identification of simultaneous motional processes can be achieved by NMR pulse methods [McBrierty (1974)]. It is therefore to be hoped that pulse methods will be applied also to the study of SSP.

### I-3,b Application of ESR to the study of molecular motions

The interactions of the electron spin of an organic radical in a magnetic field are expressed by the following hamiltonian:

$$\mathcal{H}_S = \beta \cdot \underline{H} \cdot \underline{g} \cdot \underline{S} + \underline{S} \cdot \underline{T} \cdot \underline{I} - g_N \beta_N \underline{H} \cdot \underline{I} \quad (\text{I-45})$$

where  $\beta$  is the Bohr magneton,  $\underline{H}$  is the external field,  $\underline{S}$  and  $\underline{I}$  are the electron and nuclear spin,  $\underline{g}$  and  $\underline{T}$  are tensors. The energy of the unpaired spin of an organic radical is thus

determined by its interaction with the field and with nuclear spins and by the interaction of the nuclear spins with the field. The last term gives only a second order contribution and can be neglected in the present discussion (\*). The hyperfine interaction term  $\underline{S} \cdot \underline{T} \cdot \underline{I}$  can be considered equivalent to a local field. To each value of  $M_S$  in the main field correspond  $(2S+1)$  orientations of  $S$  in the local field. The local "hyperfine" field then splits each ESR line. The hyperfine interaction term can be subdivided into an isotropic or contact interaction and an anisotropic or dipolar interaction:

$$\mathcal{H}_S = \beta \cdot \underline{H} \cdot \underline{g} \cdot \underline{S} + a \cdot \underline{S} \cdot \underline{I} + \underline{S} \cdot \underline{T} \cdot \underline{I} \quad (\text{I-46})$$

where  $a$  is the hyperfine coupling constant,  $a \cdot \underline{S} \cdot \underline{I}$  the isotropic term and  $\underline{S} \cdot \underline{T} \cdot \underline{I}$  the anisotropic term. The nuclear spins contributing to the hyperfine interaction are the nuclear spin of the atom containing the unpaired electron and of the atom in position  $\alpha$  with respect to it. Nuclear spins in the  $\beta$  position with respect to the unpaired electron contribute substantially only to the isotropic hyperfine term. The  $\beta$  hyperfine coupling constant is given by the expression:

$$a_\beta = B_0 + B_1 \cos^2 \theta \quad (\text{I-47})$$

(\*) The possible effect of the nuclear Zeeman energy is to allow certain transitions that would be forbidden by the selection rule  $\Delta M_S = 0$ .

where  $B_0$  and  $B_1$  are constants and  $\theta$  is the angle between the directions of the  $\alpha$ - $\beta$  bond and of the orbital containing the unpaired electron. Hyperfine coupling constants with a nucleus on the same atom or with a nucleus in  $\alpha$  position do thus depend mainly on the electronic structure of the radical while the  $\beta$  hyperfine coupling constant depends mainly on the radical conformation. The ESR spectrum of an organic radical will then depend on the radical conformation and on the orientation of the radical with respect to the applied field  $H$ . ESR can then be used to detect radical motions [Marx (1966)]. The shape of the spectrum changes primarily due to intramolecular motions.

The effect of the  $g$  factor anisotropy on the shape of the ESR spectrum will be mainly evident when the hyperfine interaction term is negligible, as for example for the radicals  $ROO\cdot$  and  $RS\cdot$ . In these cases the absorption maximum of the spectrum of a single crystal is displaced by changing the orientation of the crystal in the field. The spectrum of a polycrystalline material shows instead three maxima corresponding to the three main values of  $g$  when the radical is fixed in the lattice. The occurrence of rapid molecular motion destroys the structure of the spectrum. The reorientation frequency of the radical can be determined by the change with temperature of the distances between the absorption maxima [Moriuchi (1970)]. For most organic radicals  $g$  is almost symmetric and the main cause of

( ) anisotropy is the hyperfine coupling. The orientation of a radical contained in a single crystal with respect to the external magnetic field can be varied by rotating the crystal in the field. A different spectrum corresponds to each orientation of the radical. Analysis of these spectra allows determination of the principal axes of the hyperfine tensor of the radical with respect to the external magnetic field [Carrington (1967)]. If the crystal structure of the solid is known then the orientation of the radical in the crystal can be determined and compared with the orientation of the original molecule. If the radical starts reorienting with respect to the crystal lattice the same ESR spectrum will be obtained whatever the position of the crystal with respect to the field. The loss of anisotropy of the ESR spectrum of a radical is therefore a qualitative indication that the radical is reorienting with respect to the lattice. The effect of radical reorientation on the spectra of polycrystalline material is less direct: it can only be detected by comparison of the spectra calculated for the rigid and reorienting radical with the experimental spectrum.

Interconformational conversion of a high enough frequency would change each  $\beta$  hyperfine coupling constant to its average over the oscillations:

$$a_{\beta} = B_0 + B_1 \langle \cos^2 \theta \rangle \quad (\text{I-48})$$

where  $\langle \cos^2 \theta \rangle$  indicates the average of the  $\cos^2 \theta$  function

over the oscillations undergone during the conformational change.  $a_\beta$  can be calculated at different temperatures as a function of the activation energy for the conformational change if the rotational wave function for the group C-H $_\beta$  is known. Comparison of the experimental with the calculated curves  $a_\beta$  vs T allows a determination of  $E_a$  for the conformational change.

Intermolecular motions of radicals do not modify the ESR spectrum. The detection of these motions is based on the detection of radical reactions. Radicals can either recombine or react with the substrate: in the first case there is a decrease in intensity of the spectra, in the second an irreversible change in their shape. Radical recombination will be mainly discussed here because it is more related to the content of this thesis.

According to the theories of solid state reaction, which also apply to radical recombination, radicals react with one another only if they meet in a single cage, usually but not necessarily the unit cell of the solid. The total reaction rate constant  $k_t$  will then be determined by the rate constant of self diffusion  $k_d$  of the radicals to this reaction cage and by the rate of reaction  $k_r$  within the cage [Waite (1957), (1958), Lebedev (1967), Butiagyn (1972)]. The theory has been developed to allow for all the possible ratios between the rate constant of self diffusion  $k_d$  and the rate constant of reaction  $k_r$ . When  $k_d$  and  $k_r$  are

( ) comparable radical recombination does not follow a second order equation but at short reaction times the measured rate constant is time dependent. In the extreme cases in which either  $k_d \gg k_r$  or  $k_d \ll k_r$  the measured rate constant  $k_t$  will be equal to the smaller of the two. Almost always  $k_d \ll k_r$  because the activation energy for radical recombination is usually much smaller than the activation energy for radical diffusion [Shepp (1956), Ayscough (1956)], and then  $k_t \sim k_d$ . Both in this case and when the diffusion constant is time dependent ESR measurements of radical concentration as a function of time allow determination of the diffusion constant.

Mobilities of radicals in irradiated crystals can be used to determine the mobility of the surrounding molecules if the relationship between these two quantities is known [Marx (1966)]. The differences between a radical and its parent molecule are due to intra- and inter-molecular interactions and to the presence of defects created by the radiation used to produce the radicals. The different hybridization of one C atom in the radical with respect to the molecule will cause a difference in intramolecular forces. This difference will affect only the part of the radical one or two bonds distant from the unpaired electron and its importance will decrease with the increasing size of the radical. Intermolecular forces do not seem to change substantially from the molecule to the radical. Calculations

by Szwarc [Szwarc (1965)] for the cyclohexyl radical in cyclohexane matrix showed that the intermolecular forces acting on the radical and on the molecule differ by only a small amount. This result can probably be extended to all the organic radicals that do not have a large difference in polarity from the molecules. Several radicals have been found to have the same orientation with respect to the crystal lattice as the parent molecule, which is a further proof of the near equality of intermolecular forces between radicals and molecules. However radicals deriving from very small molecules will show larger differences in intra- and inter-molecular forces from the respective molecules. Another difference between the mobility of a radical and of the parent molecule in the unirradiated crystal is due to the defects caused by the high energy radiation. It is therefore important to use a radiation dose as low as possible to produce radicals.

Radical recombination has been shown to have a "stepwise" character for a large number of organic solids [Lebedev (1964)]. The recombination starts considerably below the melting point and at any temperature only a definite fraction of the radicals disappears. The remaining stable concentration of free radicals decreases with increasing temperature until all the radicals disappear at a phase transition [Fig. (I-5)]. However only phase transitions having an entropy larger than 4.6 e.u. lead to

a complete disappearance of radicals [Claes (1973)]. In all known cases the recombination rate constant increases dramatically near a phase transition [Marx (1966)]. This could be expected since at a phase transition there are very large fluctuations in density and consequently enhanced molecular motions [Bensasson (1963)].

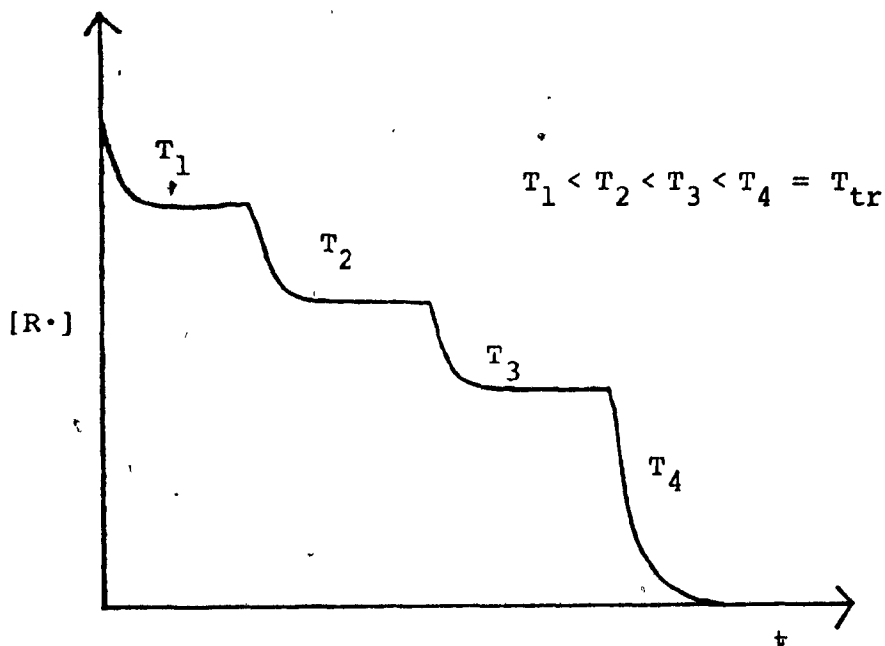


Fig. (I-5): Stepwise character of radical recombination

These data show that there is a very wide distribution of activation energies for radical diffusion. As radical recombination implies radical mobility the starting

temperature for the recombination could be expected to coincide with the temperature at which molecules start moving in the solid. Dielectric measurements have been compared with ESR results for phenol, aniline, O-nitro N-methylaniline and N-ethylaniline showing that radical recombination starts at a much lower temperature than molecular motions. [Tolkachev (1970a), (1970b), (1971)]. Dielectric measurements are not sensitive enough to detect molecular motions in defects, but show an increase of the dielectric constant only when there are very extensive motions in the solid. It was then concluded that radical migration occurs in defects. This would also explain the large temperature range over which radical recombination occurs. Given the heterogeneous nature of defects it would be much more likely to have a broader spectrum of activation energies than in the perfect lattice.

In conclusion, ESR allows the determination of rate constants of radical diffusion, which occurs mainly in crystal lattice defects. Rate constants of self-diffusion of the parent molecule are considered to be in general only slightly lower.

#### I-4 PREVIOUS STUDIES ON THE SALTS OF ACRYLIC ACID

Morawetz and Rubin [Morawetz (1962)] investigated the solid state polymerization of the acrylates of Li, Na, K and Rb. They observed wide differences in reactivity

among these samples: K acrylate was found to polymerize at 273 K as fast as Li and Na acrylates around 400 K. Preliminary measurements on Rb acrylate showed that at 303 K it polymerizes slightly less fast than K acrylate. These results will be described in some detail because of their close relationship to this thesis. In particular the nature of the reaction kinetics and some measurements of molecular weight of the polyacrylates will be illustrated.

a) Nature of the reaction kinetics. The polymer yield  $Y$  was found to be linear when plotted versus the logarithm of time for long enough reaction times. At short reaction times  $Y$  vs.  $\log t$  showed a different behaviour that was not explained. The minimum reaction time after which  $Y$  became linear with respect to  $\log t$  decreased with increasing temperature. The slope of the linear part was found to be parallel at different temperatures and the yield after a fixed time increased with increasing temperature. An activation energy of  $69.9 \text{ kJ mol}^{-1}$  was found for the polymerization of K acrylate at 19% conversion.

b) Measurements of molecular weight of the polymer products. Average molecular weights were determined for Li, Na and K acrylate polymers by light scattering in aqueous solutions of the corresponding alkali chlorides. The molecular weight of K acrylate polymers was found to be independent of the extent of conversion to polymer at all the temperatures studied except at 273 K where the molecular weight increased

with the extent of conversion. The molecular weight of K acrylate polymers showed a minimum at about 333 K. The molecular weight of potassium acrylate polymers decreased with increasing radiation dose. Molecular weights of Li and Na acrylate polymers are one order of magnitude smaller than those of K acrylate polymers.

The large differences in the polymerizability of the four acrylates were attributed to a crystal lattice effect but no direct evidence was given. The reaction was considered to have a radical mechanism although no definitive proof of it was given. A comparison of molecular weight and radical concentration, measured by ESR, for K acrylate showed the occurrence of some chain transfer for K acrylate.

The few other studies on the SSP of salts of acrylic acid are not very directly related to this case. Some Russian workers observed a rapid polymerization in the system Na acrylate - Li chloride moistened with aqueous ethanol [Kargin (1960)]. The high polymerizability was attributed to the increase in defect concentration following the heterogeneous exchange reaction producing Na chloride. The same workers also observed a fast polymerization in sodium and potassium acrylates mechanically treated in a vibrating ball mill in the presence of small quantities of water [Kargin (1962)]. Again the increased rate of polymerization was attributed to defects created by the mechanical treatment. It is very doubtful whether these

observations are comparable to those of Morawetz et al. because the presence of water could cause considerable changes in the reaction mechanism.

Numerous studies have been devoted to the polymerization of Ca acrylate hydrates with various degrees of hydration [Costaschuck (1970) and bibliography therein] but again these observations could partly depend upon the chemical role of water which is obviously absent for the alkali acrylate salts.

#### I-5        STATEMENT OF THE PROBLEM

The acrylates of Li, Na, K and Rb appeared to constitute a good case-study in solid state polymerization because the different cations are not supposed to take part in the reaction but only to cause differences in the physical parameters that are likely to affect the polymerization. These acrylates have melting points much higher than the temperatures at which the polymerization was investigated and thus avoid any premelting phenomenon. Preliminary wide-line NMR measurements on Na and K acrylates [Costaschuck (1969)] suggested that there was a difference in the degree of molecular motion in Na and K acrylate over the temperature range at which polymerization occurs. This observation showed promise as an alternative explanation for the different polymerizability of the four acrylates with respect to the effect of the crystal lattice postulated by Morawetz et al.

Measurements intending to obtain a quantitative estimate of the molecular motions of the four acrylates have been carried out in this thesis. The objectives of this study were:

a) To compare the relative rates of polymerization of the four acrylates with the molecular motions of the respective monomers.

b) To see if any of the acrylates have a phase transition over the range of temperature investigated and if so to compare the rates of polymerization below and above the transition.

CHAPTER II  
EXPERIMENTAL

## II-1 PREPARATION OF THE MONOMERS

Li, Na and K acrylates were prepared by addition of acrylic acid to a methanolic solution of the alkali hydroxide. The salts were precipitated by addition of ethyl ether, washed with ether, dried, dissolved in methanol and slowly reprecipitated by further addition of ethyl ether. The reprecipitation procedure was repeated three times. The final reprecipitation was made over a period of twelve hours.

To prepare Rb acrylate the carbonate was added to a 20% solution of acrylic acid in methanol. The rest of the procedure was as described above.

The acrylic acid used was not distilled because the stabilizer commonly used (p-methoxy phenol) is soluble both in methanol and in ether.

The salts were characterized by elemental analysis of C and H. The results are reported in Table (II-1).

## II-2 POLYMERIZATION KINETICS OF K ACRYLATE

Samples of about 1.5 g of the monomer were placed into 25 ml glass ampoules which were evacuated, flushed with dry nitrogen, reevacuated and sealed under a pressure of about  $5 \times 10^{-2}$  Torr. The flasks were then placed into a Dewar filled with dry ice and irradiated with 0.2 Mrads<sup>(\*)</sup> in a Gammacell 220. The dose rate used was 0.22 Mrads/hour. The dose rate was measured by Fricke dosimetry [Weiss (1956)].

(\*) 1 Rad = 100 erg/gr =  $10^{-2}$  J/kg

TABLE (II-1): Results of the elemental analysis of the acrylates of Li, Na, K and Rb

		<u>Exp %</u>	<u>Calc %</u>
Li	H	3.87	3.88
	C	46.33	46.20
Na	H	3.31	3.22
	C	38.38	38.32
K	H	2.72	2.75
	C	32.86	32.72
Rb	H	1.92	1.93
	C	22.84	23.02

The post-polymerization was then started by placing the samples in a thermostatic bath at the desired reaction temperature. The progress of the polymerization was followed by extracting the residual monomer from a flask with anhydrous methanol containing a small amount of hydroquinone inhibitor and filtering off the polymer into a sintered glass filter. The polymer was then washed with methanol, dried to constant weight under vacuum and weighed.

The polymerizations were studied at 313 K, 323 K, 333 K and 353 K.

### II-3 WIDE-LINE NMR MEASUREMENTS

Samples for wide-line NMR measurements were prepared by the same vacuum treatment of samples used for polymerization kinetics and sealed in  $9 \times 10^{-3}$  m.O.D. sample tubes. Wide-line NMR spectra were recorded at 60 MHz using a spectrometer built essentially from Varian components. The sample temperature was varied by passing a heated or cooled nitrogen stream around the sample and monitored by copper-Constantan thermocouples placed up- and down-stream from the sample. The temperature variation during the recording of a spectrum was estimated to be  $\pm 0.5$  K. The experimental second moments were calculated from the first derivative traces with the aid of a computer program containing a correction for finite modulation broadening.

II-4 DSC MEASUREMENTS

Samples of Li, Na, K and Rb acrylate were placed in aluminum sample pans and studied between 173 K and 600 K with a Perkin Elmer DSC-1B, differential scanning calorimeter. Special sample pans that could be sealed were used to study irradiated acrylates. The sealed pans were placed into glass ampoules and given the same vacuum treatment as the samples used for the kinetics of polymerization. The samples were then irradiated with 0.2 Mrads at a dose rate of 0.22 Mrads per hour. Repeated scans with raising and decreasing temperature were done for each acrylate sample between 173 K and 600 K.

II-5 ESR MEASUREMENTS

Li, Na, K and Rb acrylates were irradiated in quartz tubes having a bulb on one end. The monomer was placed into the bulb and the tube was sealed under a vacuum of about  $5 \times 10^{-2}$  Torr. The samples were irradiated at 195 K at a dose rate of 0.22 Mrads per hour with a total dose of 0.2 Mrads. After irradiation the narrow end of the tube was annealed with a blow torch to remove F centres from the quartz while the bulb with the sample was kept immersed in dry ice. The tube was then turned upside down transferring the sample into the narrow end and warmed up to the reaction temperature.

For each acrylate sample spectra were recorded as a function of time at several temperatures. Measurements were

taken for reaction times up to 12 days. The ESR instrument used was based upon a Bruker spectrometer with 100 KMz modulation and operating in the X band. Spectra were recorded in such conditions as to avoid signal saturation and broadening. The temperature was varied by means of a gas flow thermostat system, including a temperature control system that kept the temperature within  $\pm 0.5$  K from a preset value.

The ESR spectrometer was calibrated with a pitch sample of known radical concentration. The spectra of the acrylates and of the pitch sample were recorded simultaneously with an internal reference placed in the ESR cavity to take into account the change in the adjustable parameters in different spectra.

CHAPTER III  
RESULTS AND DISCUSSION

III-1 POLYMERIZATION KINETICS

Some additional measurements on the polymerization kinetics of K acrylate were made to extend the data obtained by Morawetz and Rubin [Morawetz (1962)]. Plots of polymer yield  $Y$  versus  $\log t$  are straight lines at long reaction times at 313, 323, 333 and 353 K. The data obtained are shown in Figs. (III-1) and (III-2). The slopes of the straight lines, however, are not constant with temperature as found earlier [Morawetz (1962)] but show a minimum at 323 K, as in Fig. (III-3), which includes also data from Morawetz and Rubin. At all the temperatures studied the polymer yield  $Y$  is linear with respect to  $\log t$  only at relatively long polymerization times. To see what is the kinetic behaviour at short polymerization times data from Morawetz for Li, Na and K acrylate were plotted both versus time and versus  $\log t$  [Figs. (III-4), (III-5) and (III-6)]. These plots and a correlation analysis [Table (III-1)] show that a constant rate of polymerization fits the experimental results better than a logarithmic rate law at short polymerization times. The period in which this occurs becomes shorter with increasing polymerization rate. Another interesting feature shown by Figs. (III-4)-(III-6) is the nonzero intercept of the curves ( $Y, t$ ). This could either imply that there is some in-source polymerization at the temperature of irradiation or that a different rate law is followed at extremely short polymerization times. A test of

5

TABLE (III-1): Correlation of polymer yields Y with t and with logt at short polymerization times

<u>Cation</u>	<u>Temp/K</u>	(Y, t) <u>Corr. (%)</u>	(Y, logt) <u>Corr. (%)</u>
Li	374	95.2	82.0
Li	405	98.6	88.0
Na	393	98.8	96.7
Na	403	99.9	97.8
K	273	99.8	93.8
K	323	96.3	90.9



Fig. (III-1): Polymerization of K acrylate at 313 K  
(top) and 323 K (bottom)

( )

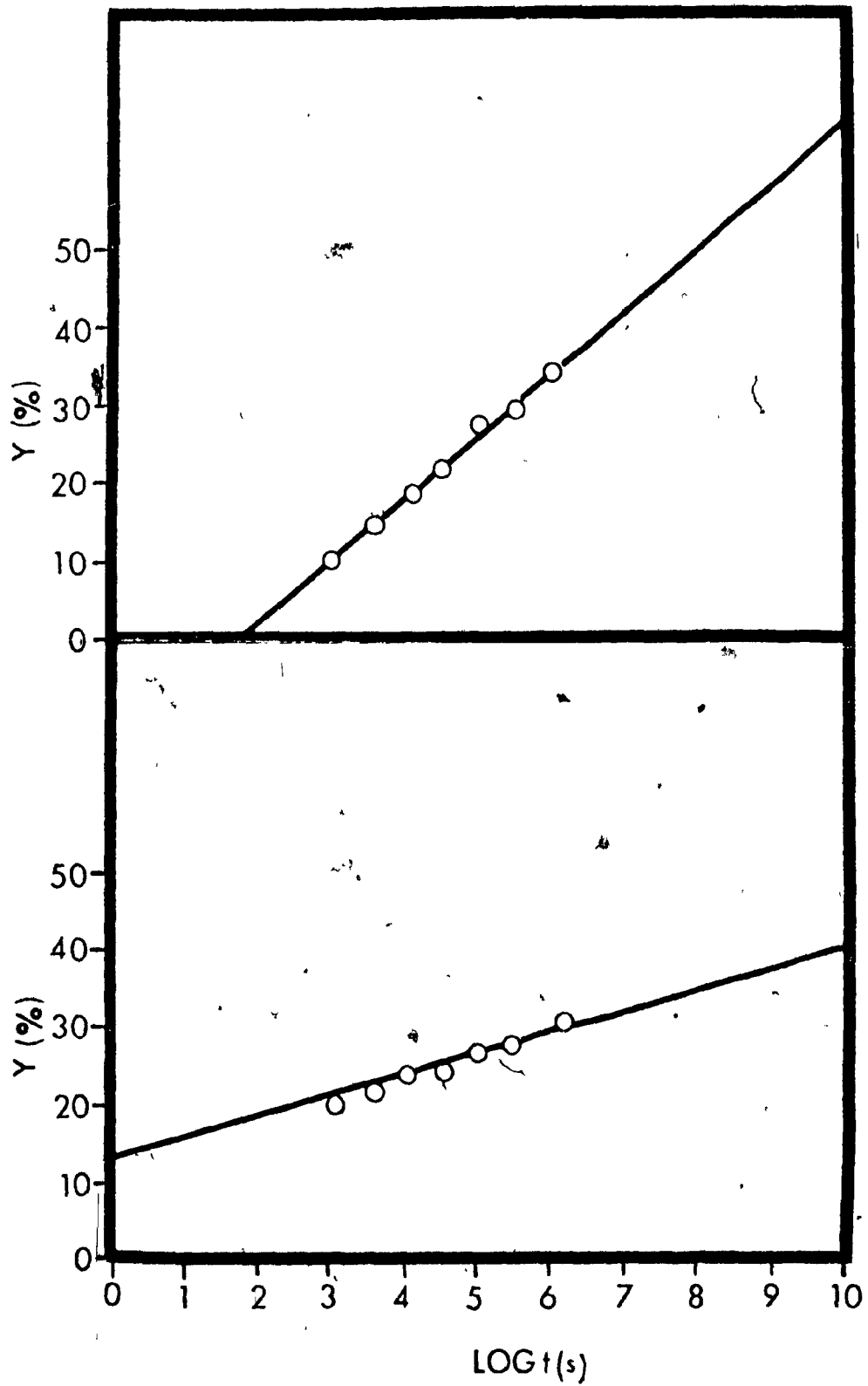


Fig. (III-2): Polymerization of K acrylate at 333 K  
(top) and 353 K (bottom)

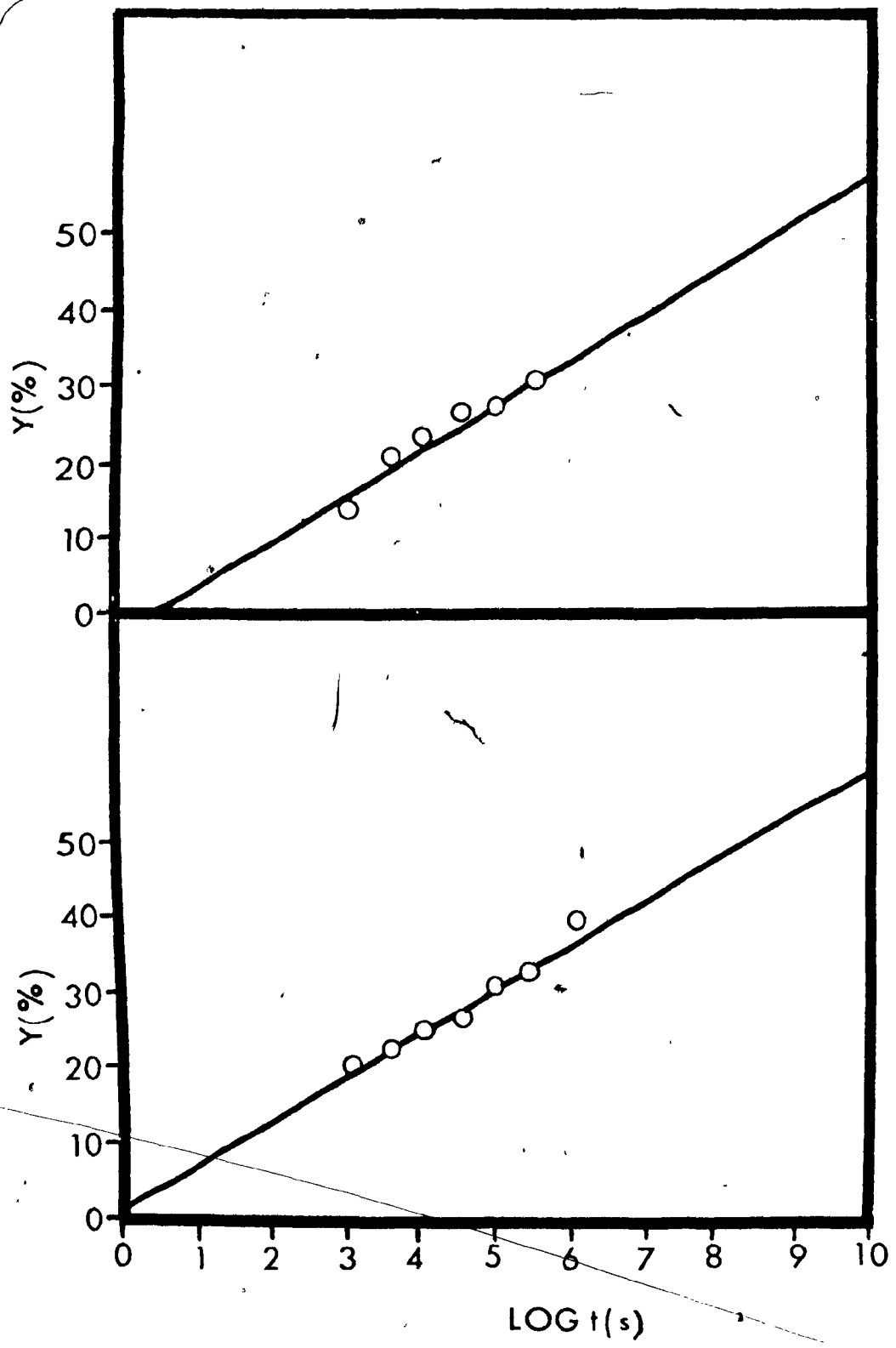


Fig. (III-3): Temperature dependence of  $dY/d\log t$  for  
K acrylate

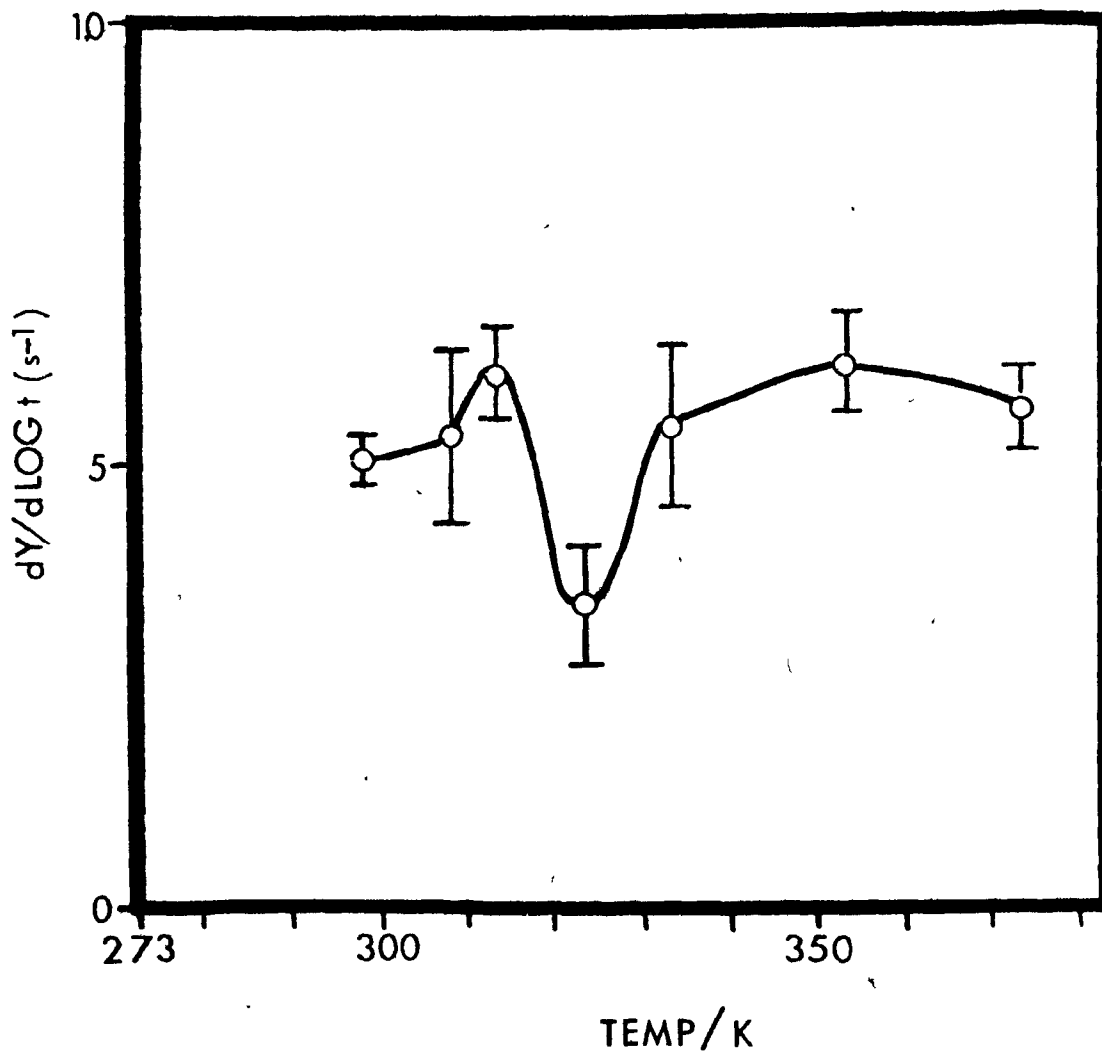


Fig. (III-4): Polymerization of Li acrylate at 374 K (o)  
and 405 K (□)

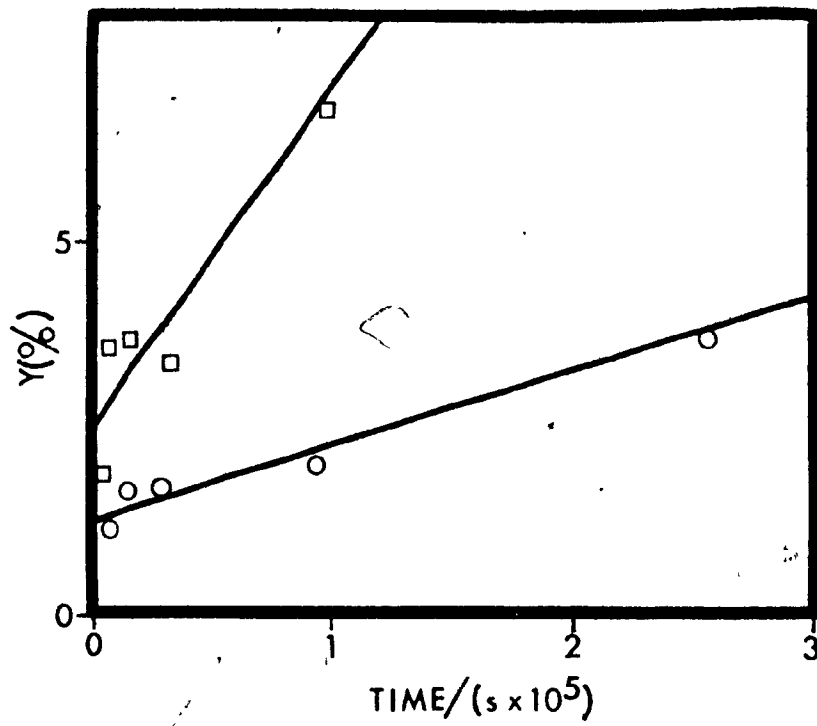
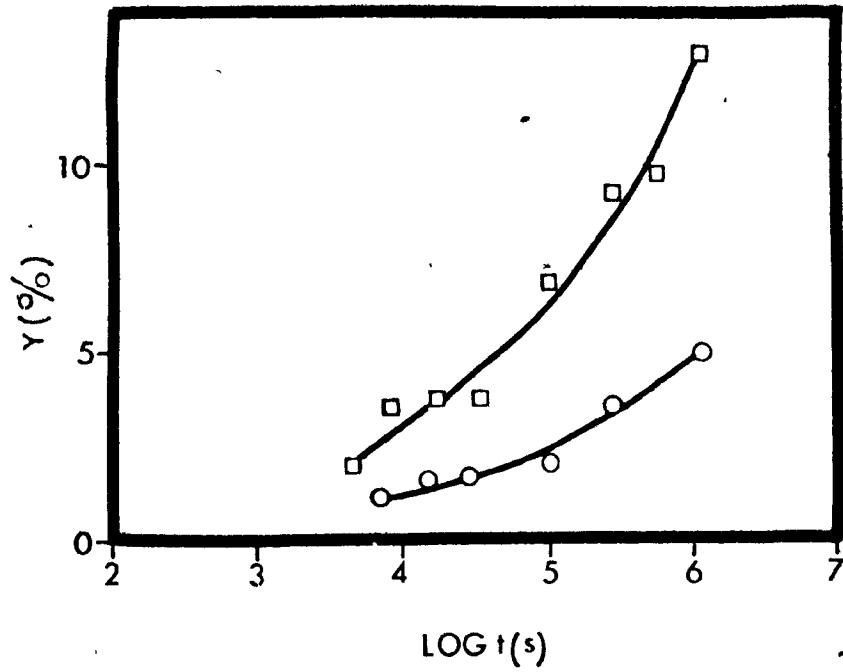


Fig. (III-5): Polymerization of Na acrylate at 393 K (o)  
and 403 K (□)

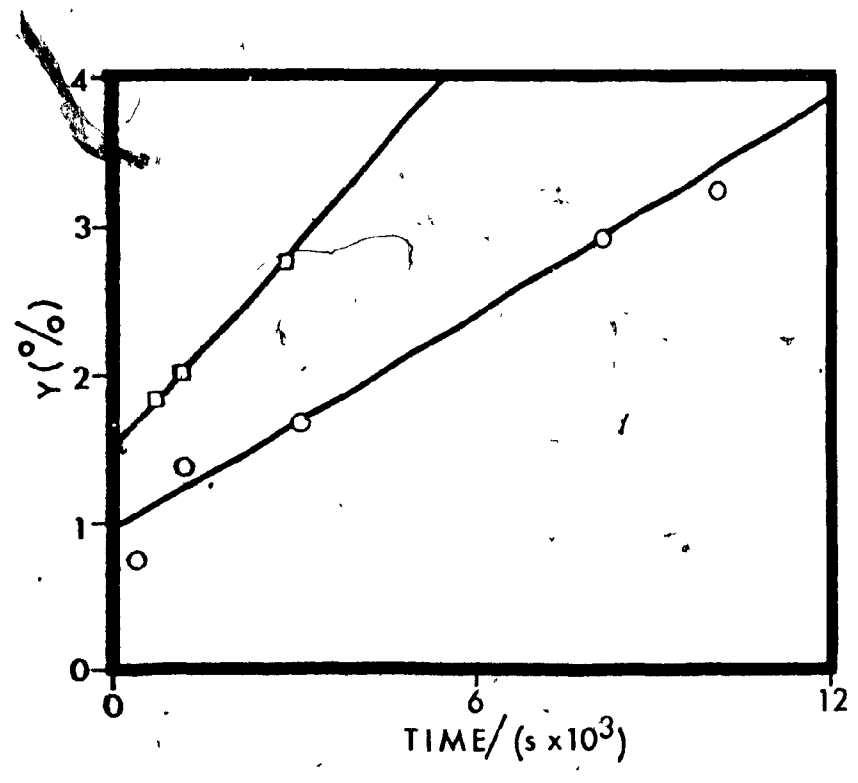
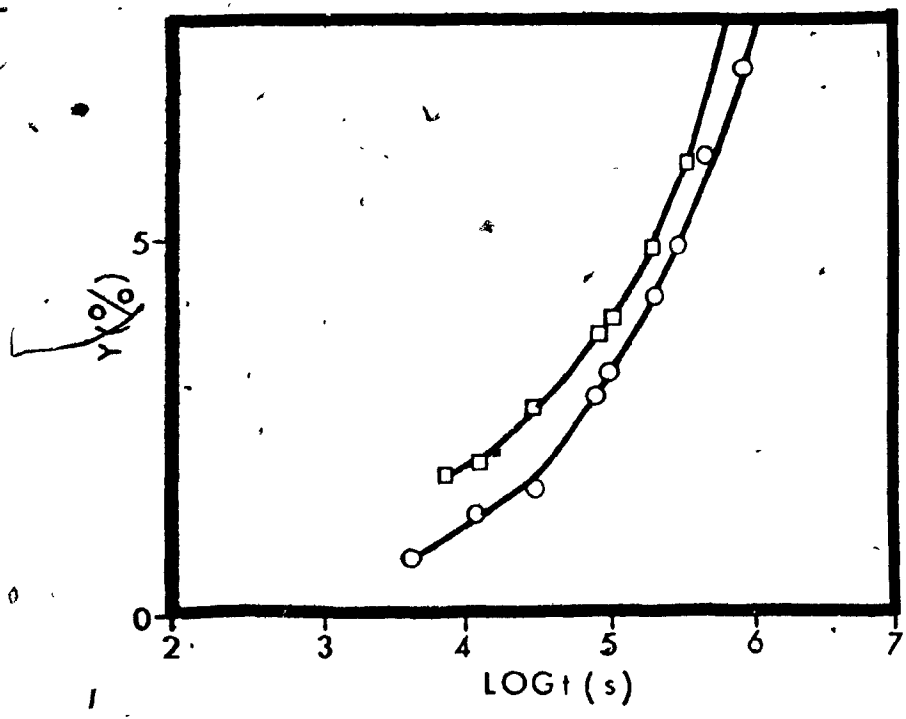
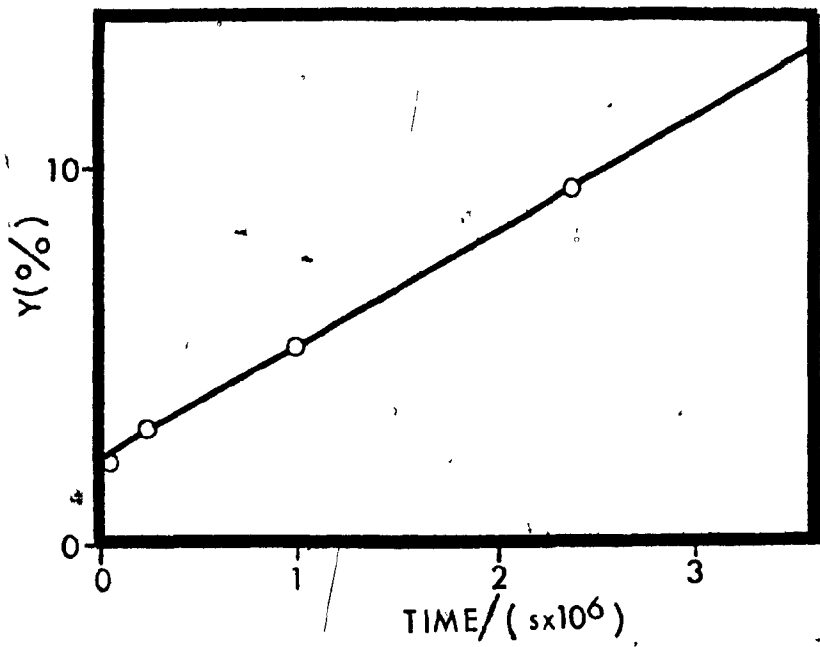
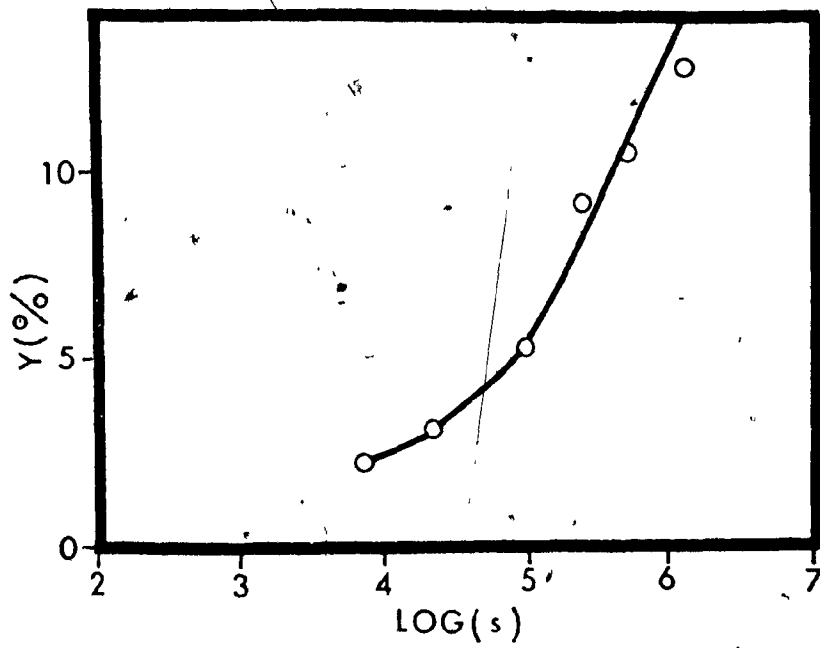


Fig. (III-6): Polymerization of K acrylate at 273 K



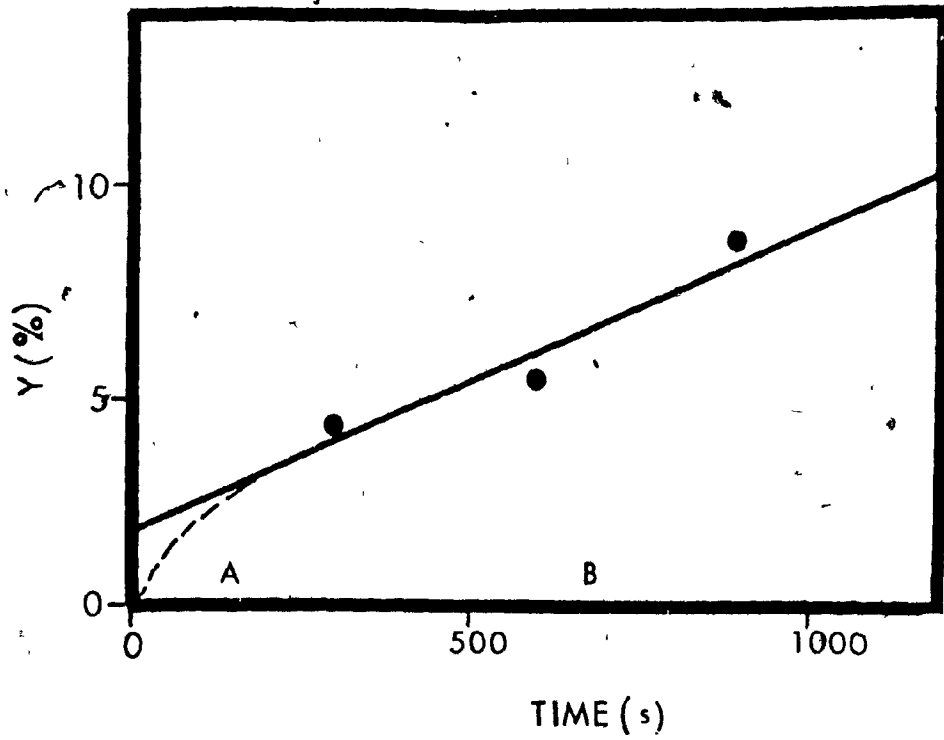
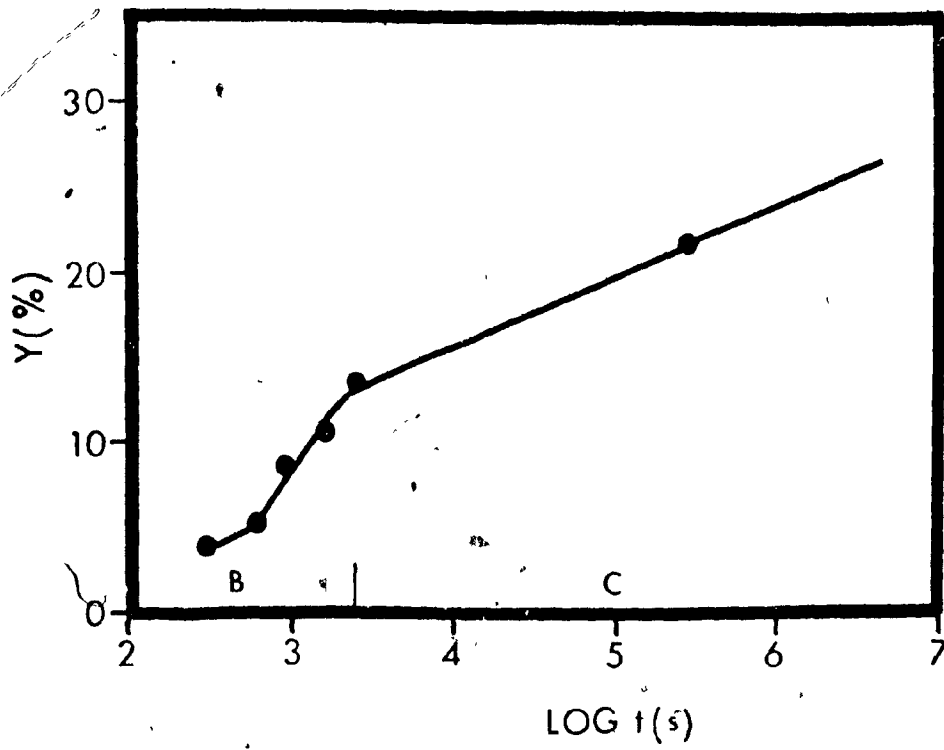
in-source polymerization performed on K acrylate did not show the formation of any polymer. It looks therefore unlikely that Li and Na acrylates, which do not polymerize even at 353 K, can polymerize at 195 K. A different rate law followed at very low conversions seems a more probable explanation for the nonzero intercept of the linear period.

There seem thus to be three stages in the polymerization of the alkali acrylates:

- (1) an initial period A extremely fast, for which at the moment there are not enough data to be able to define a rate law
  - (2) a successive reaction period B in which the rate of polymerization is constant with time
  - (3) a final reaction period C in which the rate of polymerization slows down continuously until the polymer yield reaches a limiting conversion
- The three stages are illustrated in Fig. (III-7).

It is then interesting to see if the same three reaction periods occur at all the temperatures studied, in particular at 323 K, and if so to compare the relative reaction rates at different temperatures in the periods of constant and decreasing polymerization rate. The results of kinetic measurements performed with this purpose on K acrylate at 323 K are shown in Fig. (III-7). Also at this temperature  $Y$  is not linear with respect to  $\log t$  at short

Fig. (III-7): Polymerization of K acrylate at 323 K, illustrating the three reaction periods A, B and C



reaction times and in the first fifteen minutes of reaction Y shows a better correlation with  $t$  than with  $\log t$ . Again also the intercept of the  $(Y, t)$  straight line is different from zero. A plot of polymerization rates in period B at different temperatures [Fig. (III-8)] does not show the minimum found at 323 K in period C. Instead, the rate increases continuously from 273 K to 353 K with a maximum rate of increase between 298 K and 333 K.

An energy of activation of  $69.9 \text{ kJ mol}^{-1}$  was determined [Morawetz (1962)] for potassium acrylate at 19% conversion. The meaning of such an activation energy is not particularly clear. Both the existence of regions with different rate laws in the polymerization of alkali acrylates and the kinetic schemes that will be later illustrated show that, at least at long reaction times, a complex reaction occurs depending on several variables at the same time. The energy of activation is then probably the resultant of energies of activation for individual phenomena. Furthermore in region C calculated energies of activation will depend on the particular extent of conversion chosen.

A kinetic experiment was performed on potassium acrylate to test if the decreasing rate of reaction could be related to a modification of the matrix structure. Samples prepolymerized for one hour at 353 K and fresh samples were both polymerized at 313 K. While the fresh samples reacted normally the prepolymerized samples did not undergo any

Fig. (III-8): Temperature dependence of  $dY/dt$  for K acrylate

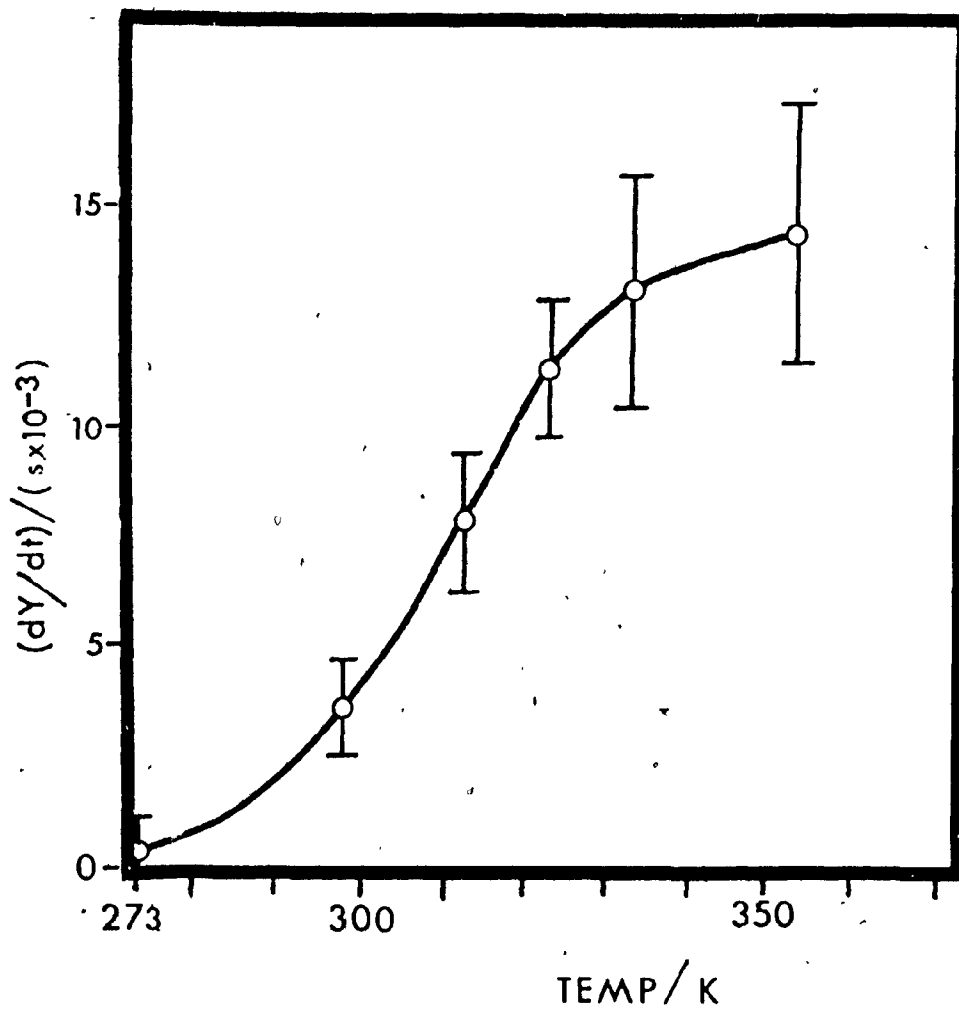
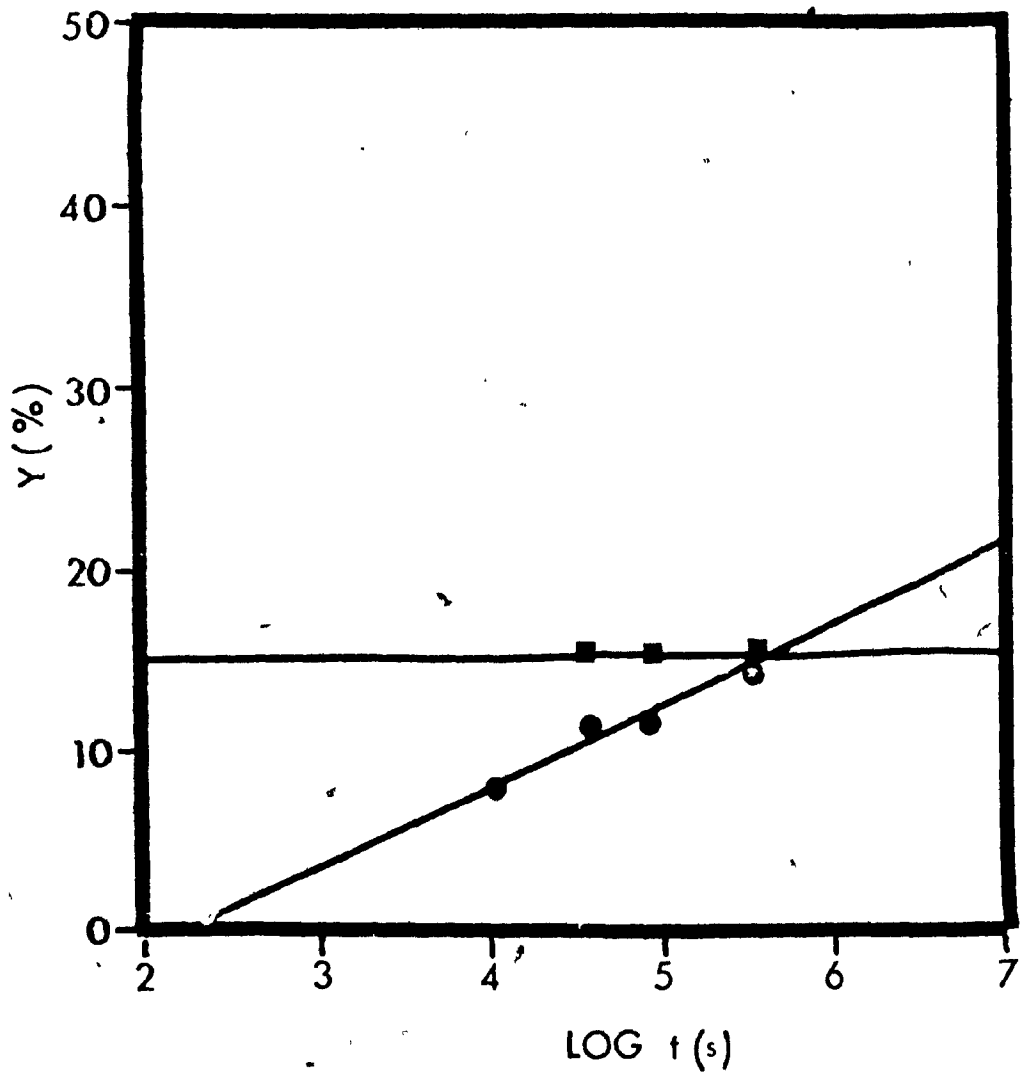


Fig. (III-9): Polymerization of K acrylate at 313 K:  
a) fresh sample (●) and b) sample pre-  
polymerized at 353 K (■)



further polymerization [Fig. (III-9)].

### III-2 WIDE-LINE NMR MEASUREMENTS

Wide-line NMR measurements were made on the acrylates of Li, Na, K and Rb in the range of temperature 77 K - 430 K, thus covering the temperature region in which the rates of polymerization were studied. The lineshape found for all four acrylates [Fig. (III-10)] apparently shows a narrow line superimposed on a broader peak. The relative intensity of the central narrow line with respect to the outer peak can change slightly but there is no sharp change in lineshape with temperature. The permanence of the central narrow line in spectra of carefully dried samples shows that it is not due to water present as an impurity. On the other hand a reduction in the modulation amplitude decreased with the components by the same amount showing that the true lineshape of the acrylates is observed. Such a lineshape can be understood with reference to Fig. (III-10): as the interaction H<sub>2</sub>-H<sub>3</sub> is going to be stronger than the interactions H<sub>1</sub>-H<sub>2</sub> and H<sub>1</sub>-H<sub>3</sub> then the spectrum will be a superposition of a doublet due to the two-protons system (H<sub>2</sub>,H<sub>3</sub>) and a singlet due to the H<sub>1</sub> proton with some additional broadening from H<sub>1</sub>-H<sub>2</sub>, H<sub>1</sub>-H<sub>3</sub> and intermolecular interactions.

Measured linewidths and second moments are shown in Figs. (III-11)-(III-14). On the basis of these results

Fig. (III-10): Derivative of the wide-line NMR lineshape of  
the alkali acrylates (top).<sup>o</sup> Acrylate ion  
(bottom).

C

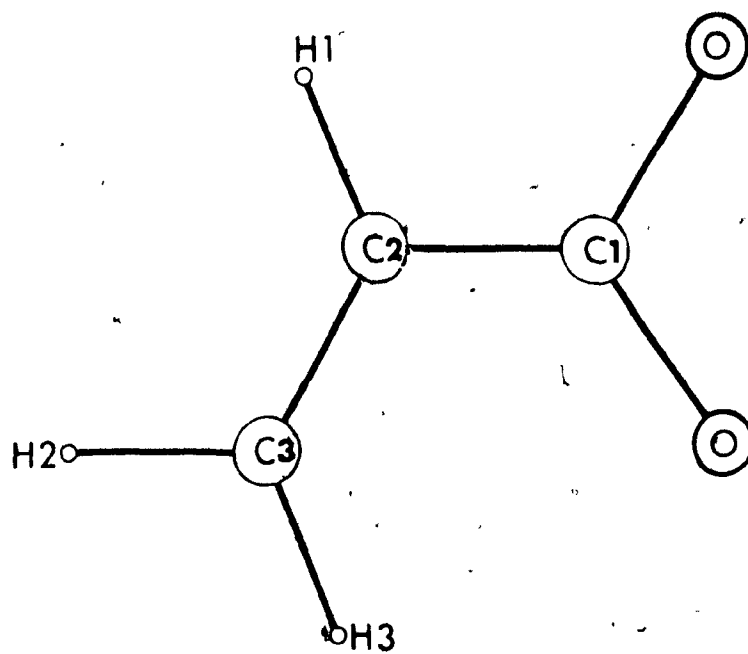
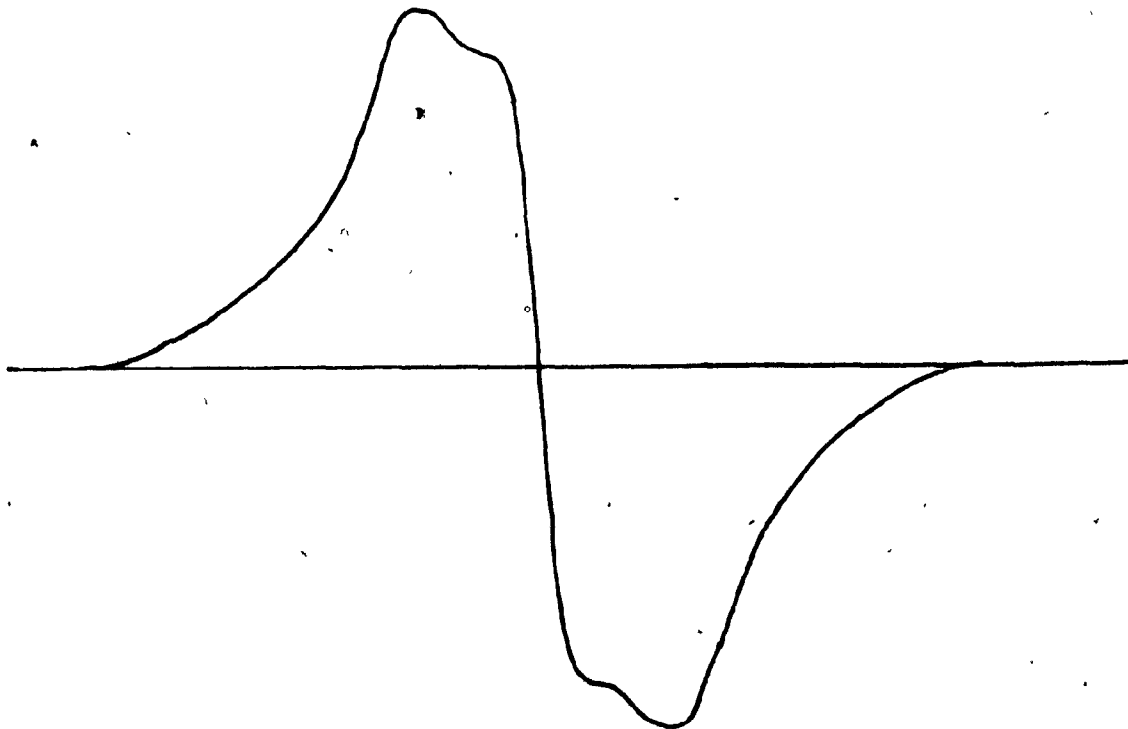


Fig. (III-11): Temperature dependence of the linewidth (o) and second moment (●) of Li acrylate

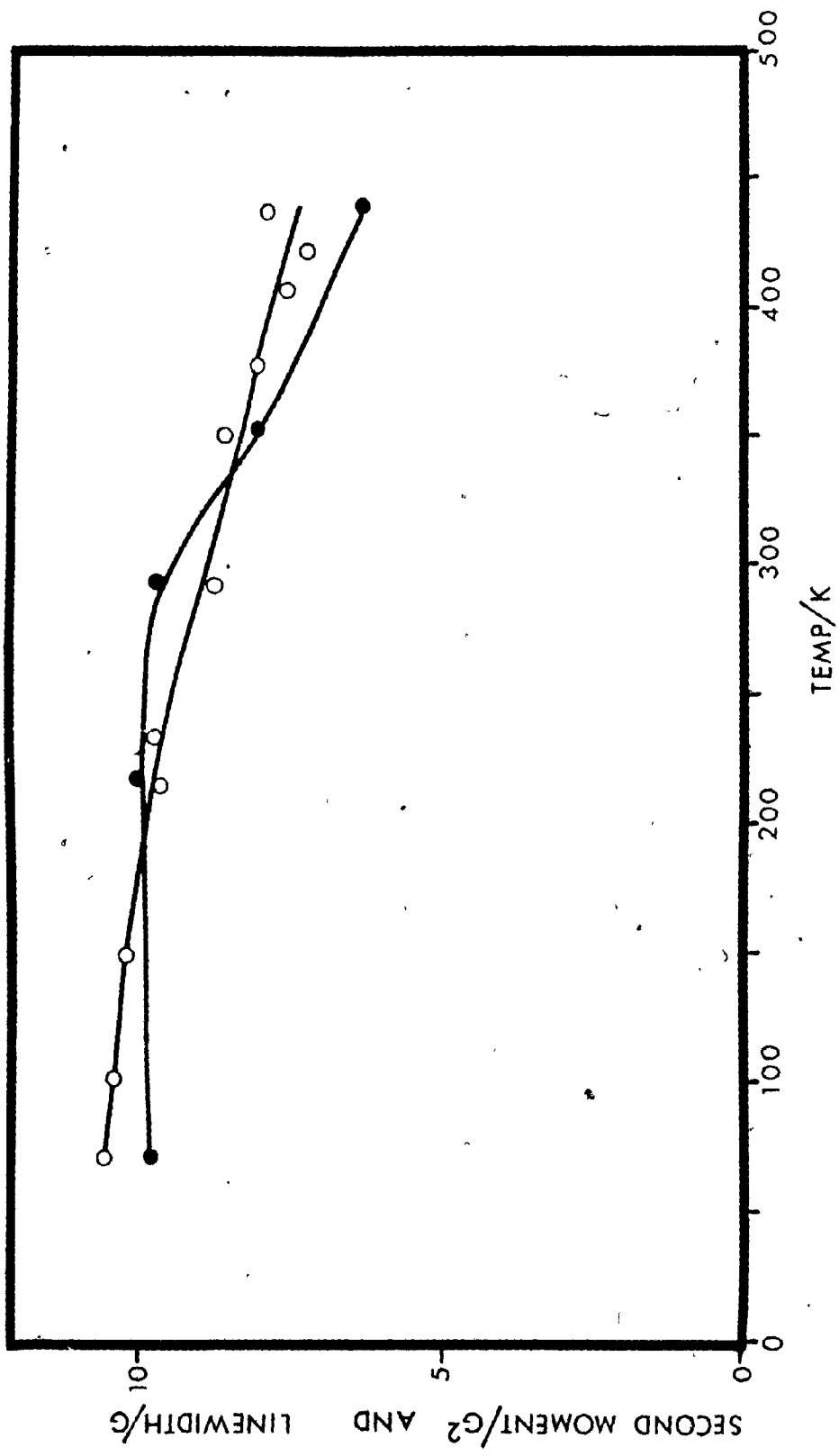


Fig. (III-12): Temperature dependence of the linewidth (o) and second moment (●)  
of Na acrylate

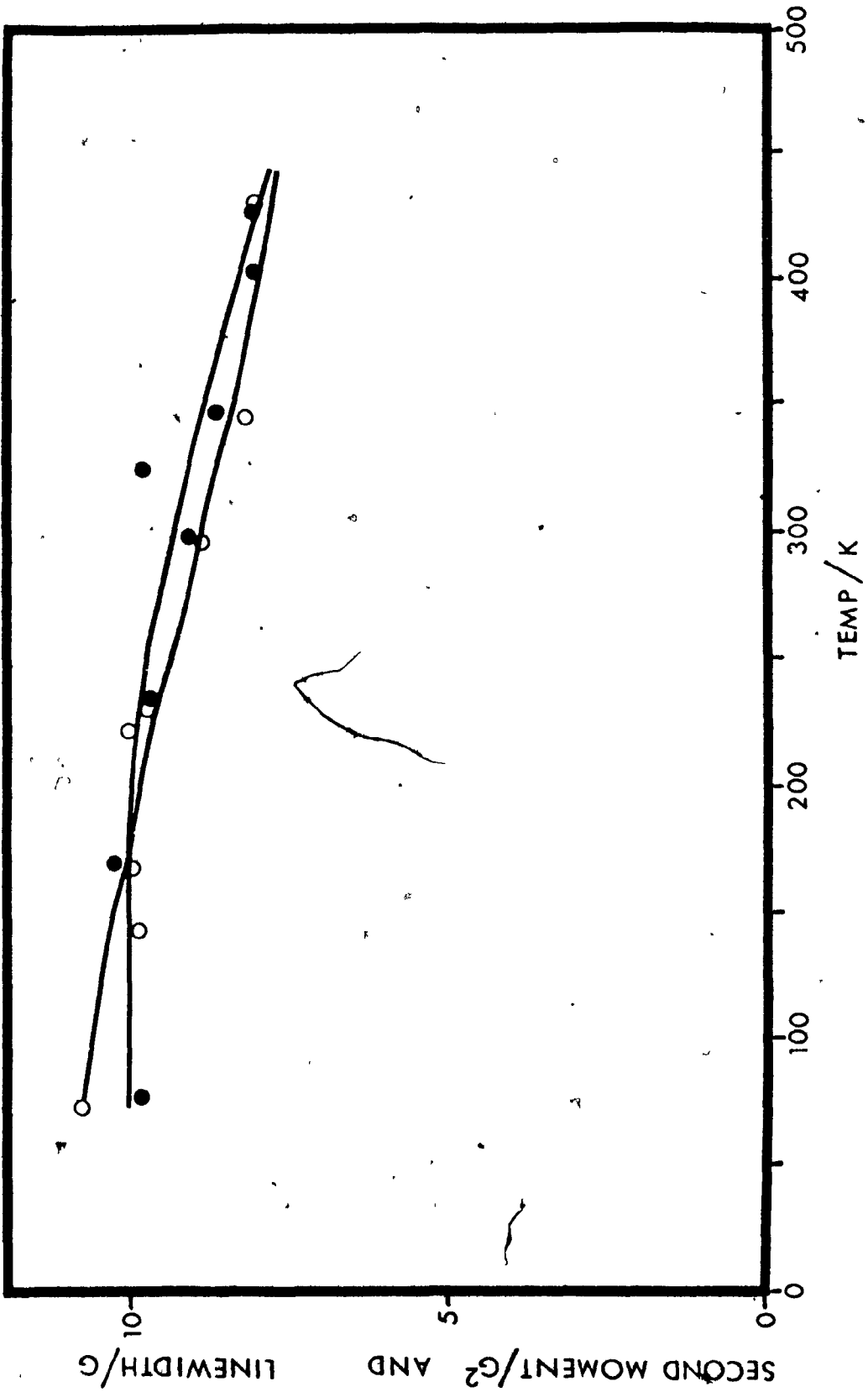


Fig. (III-13): Temperature dependence of the linewidth (o) and second moment (●) of K acrylate

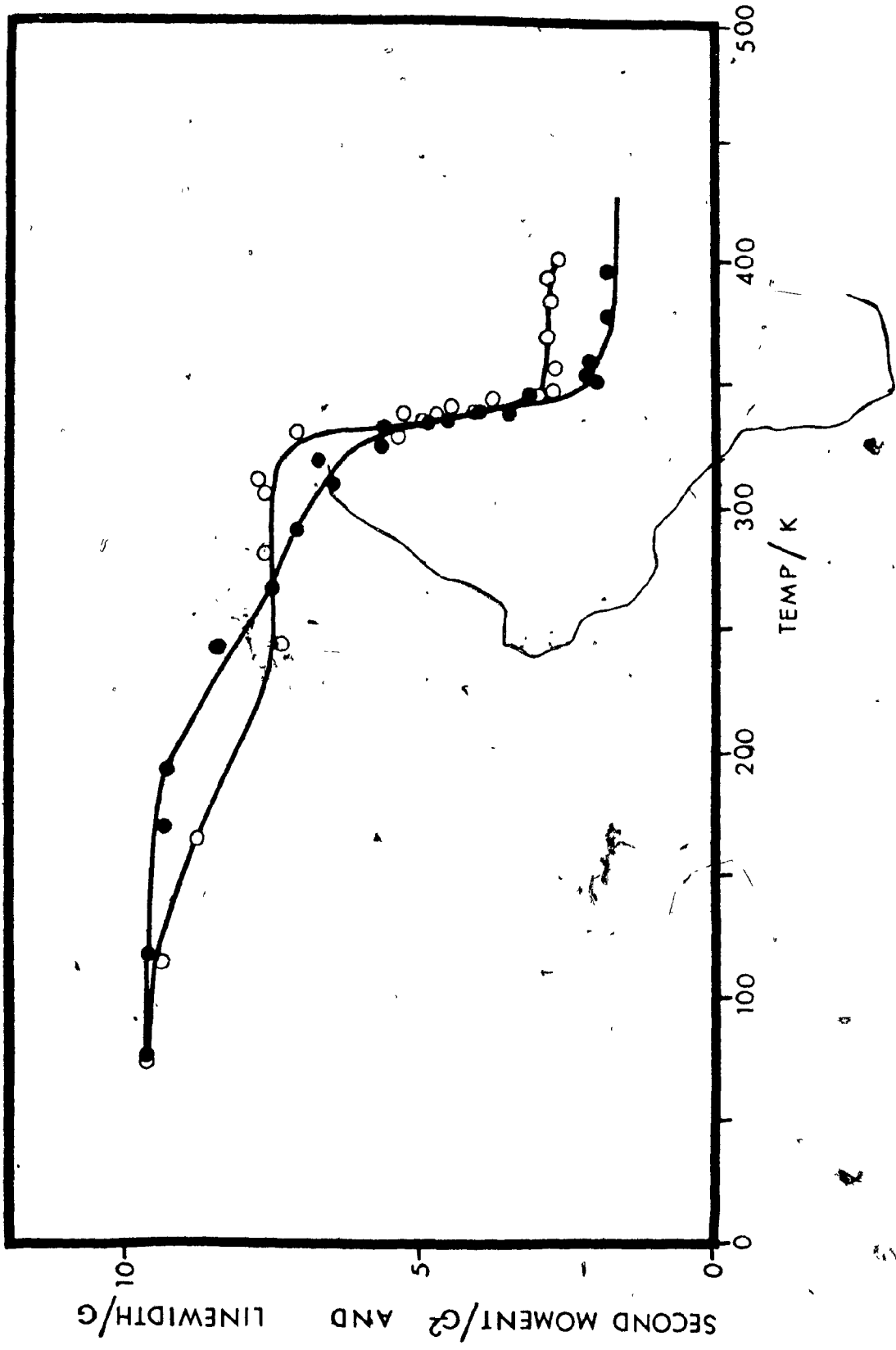
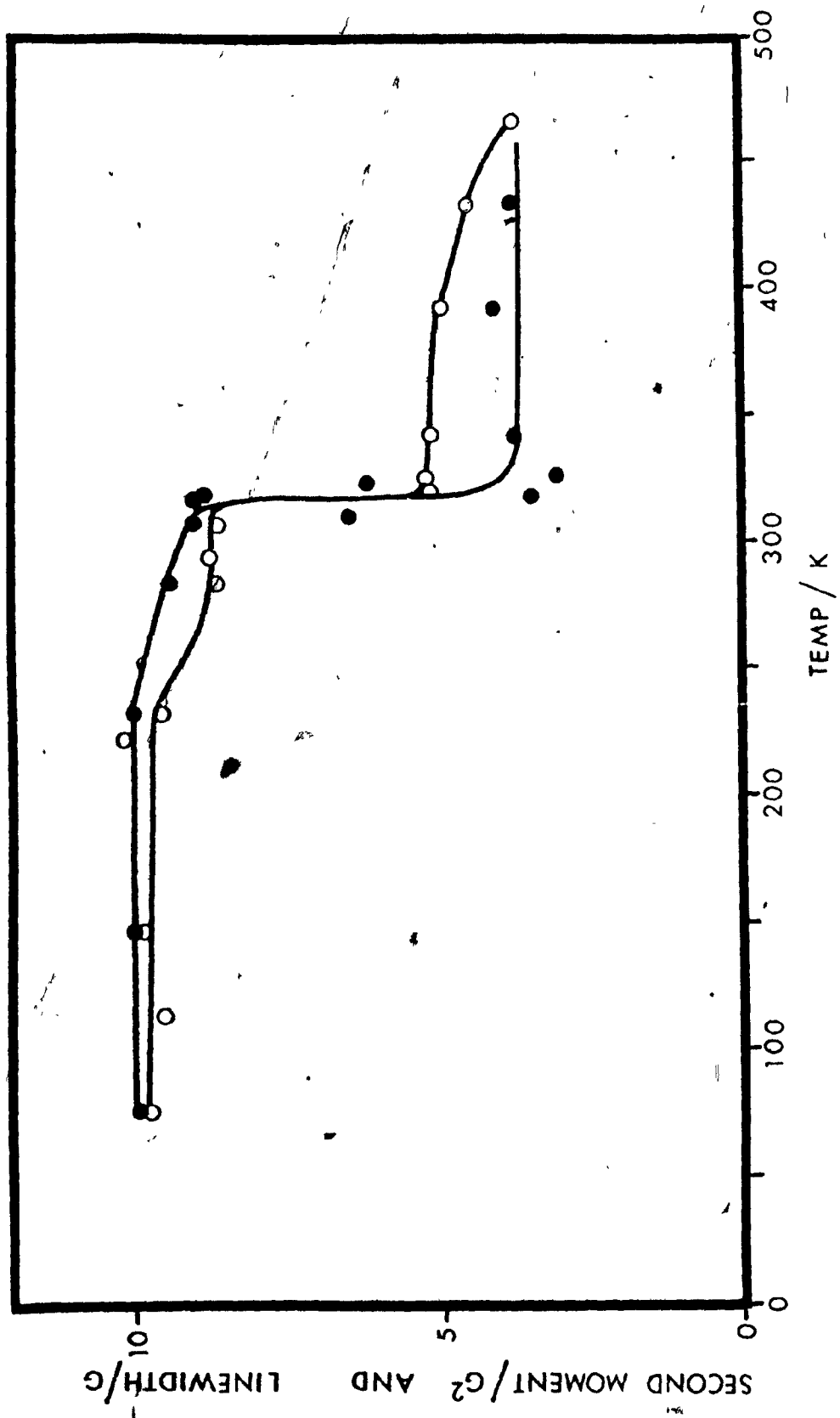


Fig. (III-14): Temperature dependence of the linewidth ( $\sigma$ ) and second moment ( $\bullet$ ) of Rb acrylate



acrylates can be subdivided into two classes: a) Li and Na acrylates which show only a gradual decrease of linewidth and second moment and at temperatures above 400 K still retain high values of both these quantities; b) K and Rb acrylates which show a sharp motional transition slightly above room temperature and have final values of linewidths and second moments above the transition considerably lower than those of Li and Na acrylates at the same temperatures. Within each of the classes a) and b) more subtle differences can be observed: Li acrylate shows a decrease of second moment larger than that of Na acrylate; K acrylate has a second moment lower than Rb acrylate above the transition temperature; both K and Rb acrylates show a gradual decrease of linewidth and second moment below the transition temperature.

From these observations it can be seen that K and Rb acrylates at temperatures above  $\sim 200$  K have a higher monomer mobility than Li and Na acrylates, that at temperatures around 400 K Li acrylate has a slightly higher monomer mobility than Na acrylate, that above their motional transition K acrylate has more monomer mobility than Rb acrylate.

Theoretical second moments were calculated to determine the types of molecular motions existing in these acrylates. The crystal structure is not known for any of the alkali acrylates. The intramolecular second moment was

thus calculated from bond angles and distances deduced from the crystallographic [Higgs (1963), Chatany (1963)] and electron diffraction [Ukaji (1959)] data for acrylic acid and by data obtained for similar molecules. C-C bond lengths and angles were assumed not to change from acrylic acid to the acrylates. C-O bond lengths could change but they have a negligible effect on the calculation of the second moment. A C-H bond length of 0.91 Å and an H-C-H bond angle of 112° reported in one of the crystallographic determinations [Higgs (1963)] were considered unreliable. C-H bond lengths of 1.08 or 1.09 Å and H-C-H bond angles of 120° were thus assumed giving the following set of molecular parameters for the acrylate ion:

$$\begin{aligned} C1-C2 &= 1.45 \text{ \AA}; C2-C3 = 1.34 \text{ \AA}; C_2-H_1 = C_3-H_2 = C_3-H_3 = \\ &= 1.09 \text{ \AA}; C1-C2-C3 = 120.3^\circ; C1-C2-H1 = C2-C3-H2 = \\ &= C2-C3-H3 = H2-C3-H3 = 120^\circ; C1-O1 = C1-O2 = 1.29 \text{ \AA}; \\ O1-C1-O2 &= 123.5^\circ; C2-C1-O1 = 116.3^\circ \end{aligned}$$

where the numbering of the atoms is the same as in Fig. (III-10). The molecule is considered to be planar and the proton coordinates calculated by this set of molecular parameters were used to compute [(I-34)] an intramolecular second moment of  $6.9 \pm 0.3 \text{ G}^2$  for the rigid molecule. The uncertainty of  $0.3 \text{ G}^2$  is due to the variation of the C-H bond length from 1.08 to 1.09 Å. The intermolecular second moment for the

TABLE (III-2): Experimental and calculated second moments for alkali acrylates

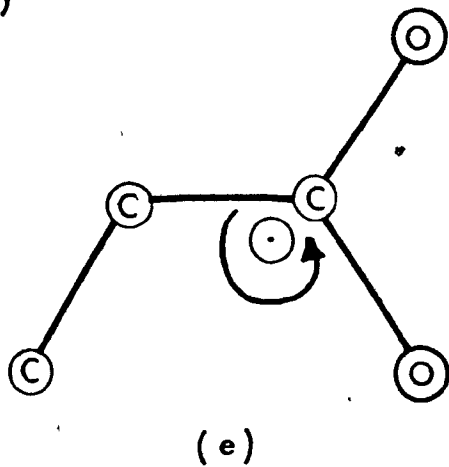
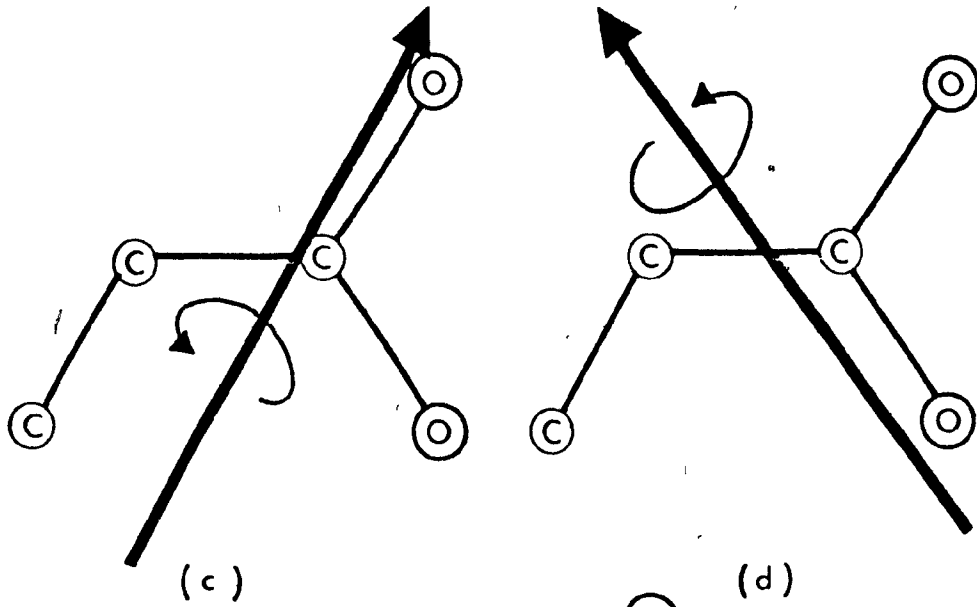
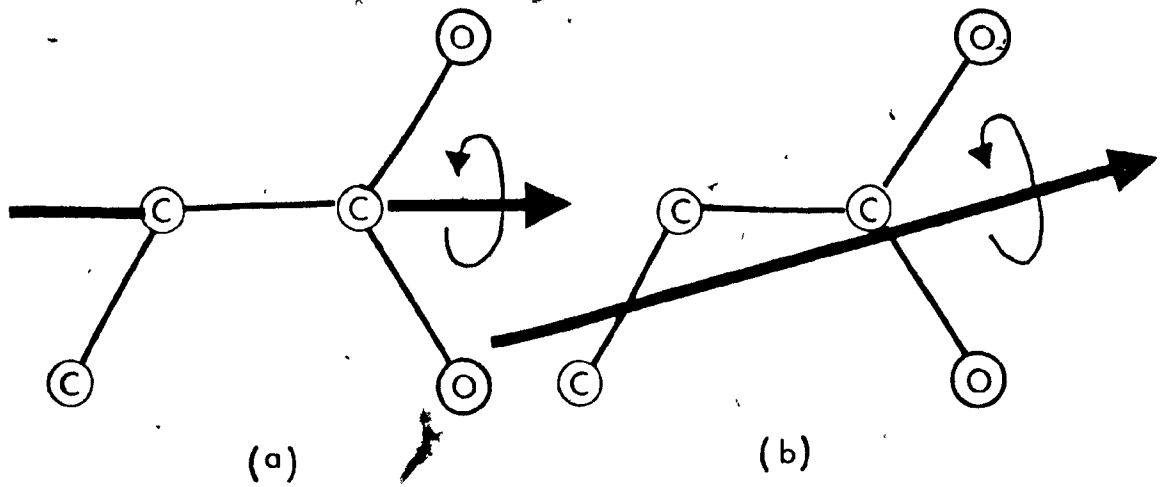
<u>Cation</u>	<u>Exp.</u> <u>(G<sup>2</sup>)</u>	<u>Motion</u>	<u>Calc. Intra</u> <u>(G<sup>2</sup>)</u>	<u>Calc. Inter</u> <u>(G<sup>2</sup>)</u>	<u>Calc. Total</u> <u>(G<sup>2</sup>)</u>
Li <sup>+</sup>	9.7 ± 0.1	Rigid	6.9 ± 0.3	3.1	10.0 ± 0.3
Na <sup>+</sup>	9.8 ± 0.1				
K <sup>+</sup>	9.7 ± 0.2				
Rb <sup>+</sup>	9.9 ± 0.7				
		Rotation about one axis	2.2 ± 0.1	0.9 ± 0.2	3.1 ± 0.3
		a)	2.2 ± 0.1	0.9 ± 0.2	2.5 ± 0.3
K <sup>+</sup>	2.0 ± 0.4	b)	3.8 ± 0.5	0.9 ± 0.2	4.7 ± 0.7
Rb <sup>+</sup>	3.7 ± 0.4	c)	1.6 ± 0.1	0.9 ± 0.2	2.5 ± 0.3
		d)	1.6 ± 0.1	0.9 ± 0.2	2.5 ± 0.3
		e)	1.7 ± 0.1	0.9 ± 0.2	2.6 ± 0.3

rigid crystal was obtained by correcting the value of  $4.2 \text{ G}^2$  of acrylic acid [Eastmond (1971)] for the different number of protons. It is possible to use the value of the acrylic acid because its second moment was calculated considering the hydrogen-bonded dimer as the basic unit of the crystal and the hydrogen bond contribution does not affect the intermolecular second moment. Another potential contribution to the second moment comes from the alkali ions, all of which have at least one isotope with nonzero spin. Again the calculation of this contribution would require a knowledge of the crystal structures of the acrylates but this term is expected to be small and the fact that the measured second moments for the acrylates are equal within the experimental error [Table (III-2)] and coincide reasonably with the total calculated proton second moment for the rigid crystal indicates that the alkali ion contribution to the second moment is negligible. It can then be concluded that at 77 K all the acrylates are rigid.

The acrylate ion has no symmetry axis and therefore no apparent axis about which a preferred motion would occur. It is to be expected that ionic interactions would tend to maintain the carboxylic acid group in a fixed position in the lattice while any motion that does occur should do so with the lowest moment of inertia. Thus to account for the observed decrease in second moment of K and Rb acrylate five types of molecular motion can be considered [Fig. (III-15)].



Fig. (III-15): Molecular motions considered for the acrylate ion. Hydrogen atoms are not illustrated



( ) Motion a) does not change the distance between the  $\text{-CO}_2$  group and the alkali cation and it has a low moment of inertia, motion b) has the minimum moment of inertia and a small change in the distance between  $\text{-CO}_2$  and the alkali cation, motions c), d) and e) have both large moments of inertia and large distances between  $\text{-CO}_2$  and the alkali cation.

Intramolecular second moments have been calculated for these motions by the Gutowsky-Pake formula [eq. (I-35)]. Without knowing the crystal structure of the acrylates only a range of possible values can be calculated for the intermolecular second moment using typical values of reduction factors due to molecular reorientation given by G.W. Smith [Smith (1965)]. A comparison of total calculated and experimental second moments [Table (III-2)] shows that the range of the calculated values includes the experimental second moments for K and Rb acrylates. Typical values of second moment for isotropic molecular reorientation are  $\sim 1\text{G}^2$  [Andrew (1953), McCall (1960), Smith (1965), Fried (1973)]. Values of 0.18 and  $0.37\text{G}^2$  were calculated respectively for f.c.c. and b.c.c. structures. The experimental second moments of K and Rb acrylates seem thus too high to allow for isotropic reorientation. For none of the acrylates self-diffusion seems to occur so extensively or at a high enough rate to cause line narrowing.

( ) The most likely molecular motion for K and Rb

acrylate is a reorientation about one axis, the axis being different for K and Rb.

A comparison of the experimental second moments of Li and Na acrylates with calculated values shows also that, even at the highest temperatures studied, these acrylates cannot undergo complete molecular reorientation but only limited oscillations.

As the purpose of the wide line NMR measurements was to see if there is any correlation between monomer mobility and polymerization some spectra of irradiated acrylates were recorded to ascertain if radiation damage modifies the monomer mobility in comparison with the unirradiated crystals. Additional information on the change of molecular mobility in the reacting matrix could be obtained by performing these experiments at temperatures at which polymerization occurs. In some other systems, as for example acrylic acid and acrylamide [Chachaty (1972a) and (1972b)], the appearance of a narrow line of increasing intensity with the progress of polymerization was reported. This line was interpreted as arising from increased monomer mobility around the growing chain or from mobile regions of the product polymer. Wide line NMR spectra were recorded at 353 K for Li, Na, K and Rb acrylates irradiated with the same dose used for kinetic measurements. At this temperature Li and Na acrylates do not polymerize while K and Rb acrylates polymerize. Spectra of Li and Na acrylates recorded at

several times after the samples had been warmed up to 353 K did not change with respect to those of unirradiated samples. Spectra of K and Rb acrylates recorded at the irradiation temperature showed no change with respect to those of unirradiated acrylates; when irradiated samples were warmed up to 353 K the linewidth and second moment progressively increased as the polymerization proceeded. In the meantime there was a change of lineshape: the relative intensity of the wings increased with respect to the central part of the spectrum.

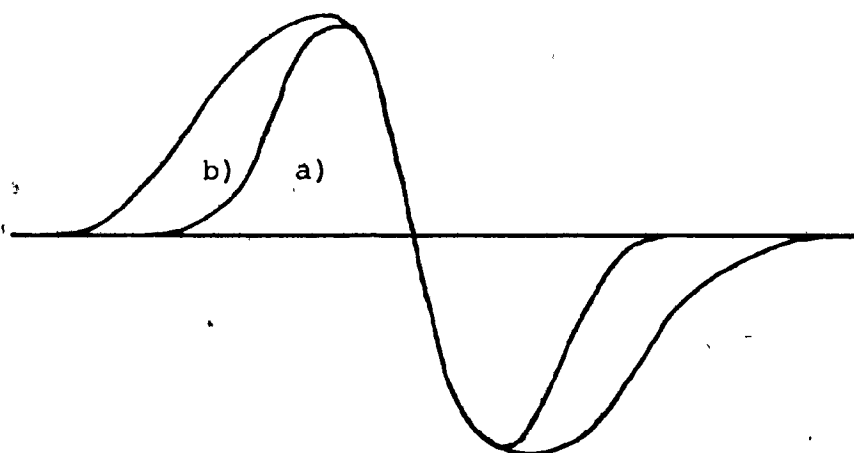


Fig. (III-16): Change of wide-line NMR lineshape with polymerization at 353 K - a) unirradiated sample, b) polymerizing sample.

These results prove that  $\gamma$  radiations used to initiate the polymerization of alkali acrylates do not

cause extensive changes in the monomer mobility; they do not however exclude that an enhanced molecular mobility could be produced by the irradiation near preexisting or radiation induced defects. The changes found in the spectra of K and Rb acrylates as the polymerization progresses are not clearly interpretable in terms of changes in the reaction matrix. The line broadening could be due either to a lower molecular mobility of the polymer formed or to a decreased mobility of the unreacted monomer or to both of these phenomena. Their effects on the lineshape are not separable so little direct information can be obtained by wide line NMR spectra on this particular point.

### III-3 DSC MEASUREMENTS

DSC measurements were performed on the acrylates to detect the possible occurrence of any phase transitions in the temperature range over which the polymerization was investigated. Both unirradiated and irradiated samples were studied to ascertain if the irradiation caused any change in their behaviour.

Li and Na acrylate did not show any phase transition between 273 K and 473 K while K and Rb acrylates showed one at 339 K and 333 K respectively. This transition occurs in both cases few degrees above the end of the motional transition detected by NMR.

Irradiated samples of Li and Na acrylate again did

not show any phase transition. An irradiated sample of K acrylate showed a transition at the same temperature of the unirradiated sample. No change in this behaviour was found after three days of polymerization at room temperature. During repetitive upwards and downwards scans the transition in K acrylate occurred always at the same temperature. This eliminates the possibility that the high temperature phase persists as a metastable phase below the transition.

#### III-4 ESR MEASUREMENTS

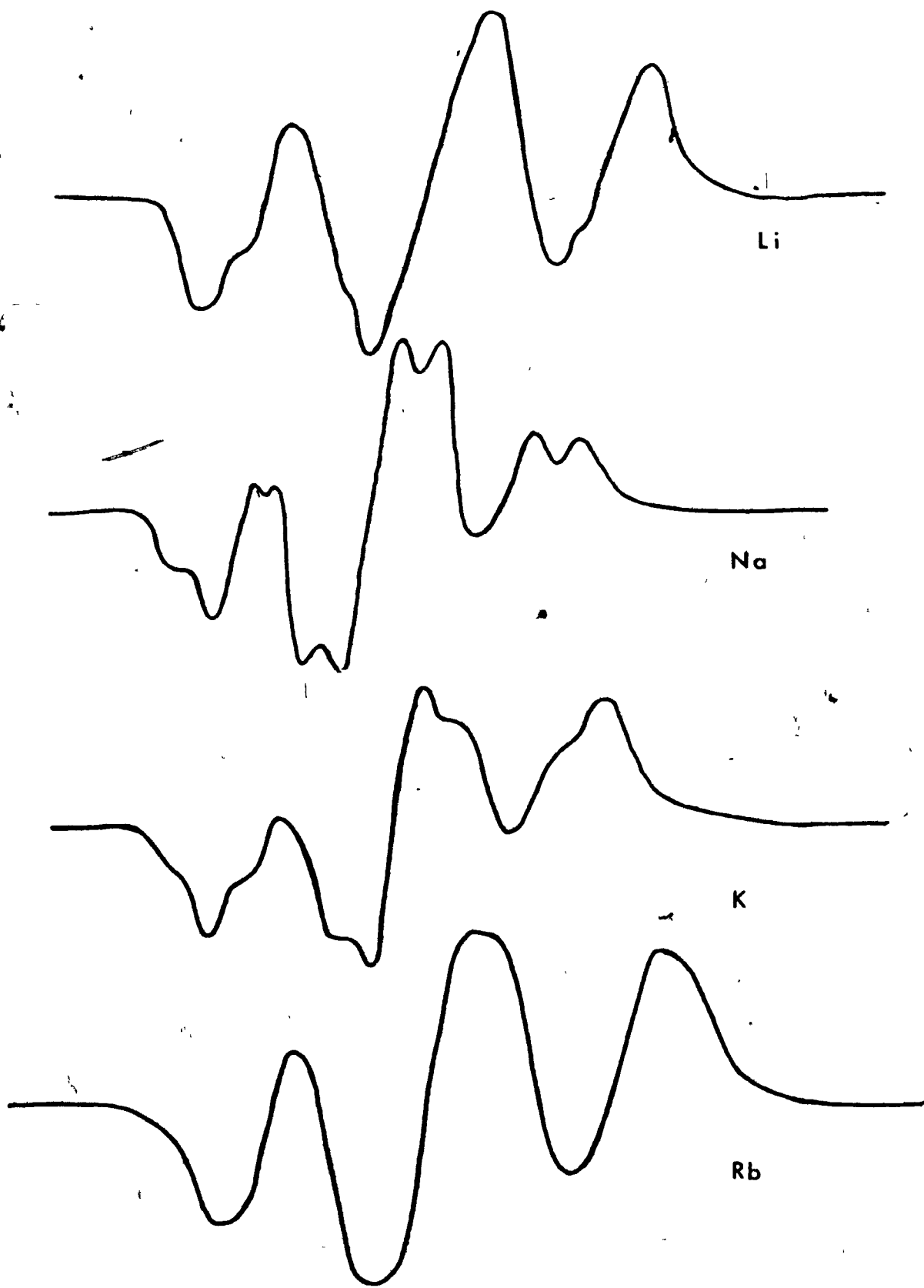
Esr spectra of the four acrylates were recorded as a function of time at temperatures varying between 303 K and 423 K. These measurements were performed with the aim of evaluating the relative importance of radical recombination and chain propagation in the polymerization reaction. The decay of acrylate radicals was followed below and above the temperature at which polymerization begins for Li and Na acrylates, below and above the phase transition for K and Rb acrylates.

The spectra of the four acrylate radicals are shown in Fig. (III-17). The dominant feature of all these spectra is the triplet found for most irradiated vinyl monomers (I-1). The spectrum of the acrylate radical in each salt is distinguishable by some secondary features: Li and K acrylates show some small shoulders superimposed on the main triplet, in Na acrylate each peak of the triplet shows an additional smaller

Fig. (III-17): ESR spectra of the alkali acrylate radicals recorded at low polymer yields or when no polymerization is occurring the spectra were recorded under the following conditions:

- magnetic field = 3205-3215 G;
- mod. ampl. = 4 G;
- sweep range = 200 G;
- sweep time = 200 s;
- time constant = 0.5 s;
- klystron power = 0.5-2.0 mw.

O



Li

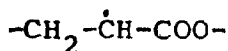
Na

K

Rb

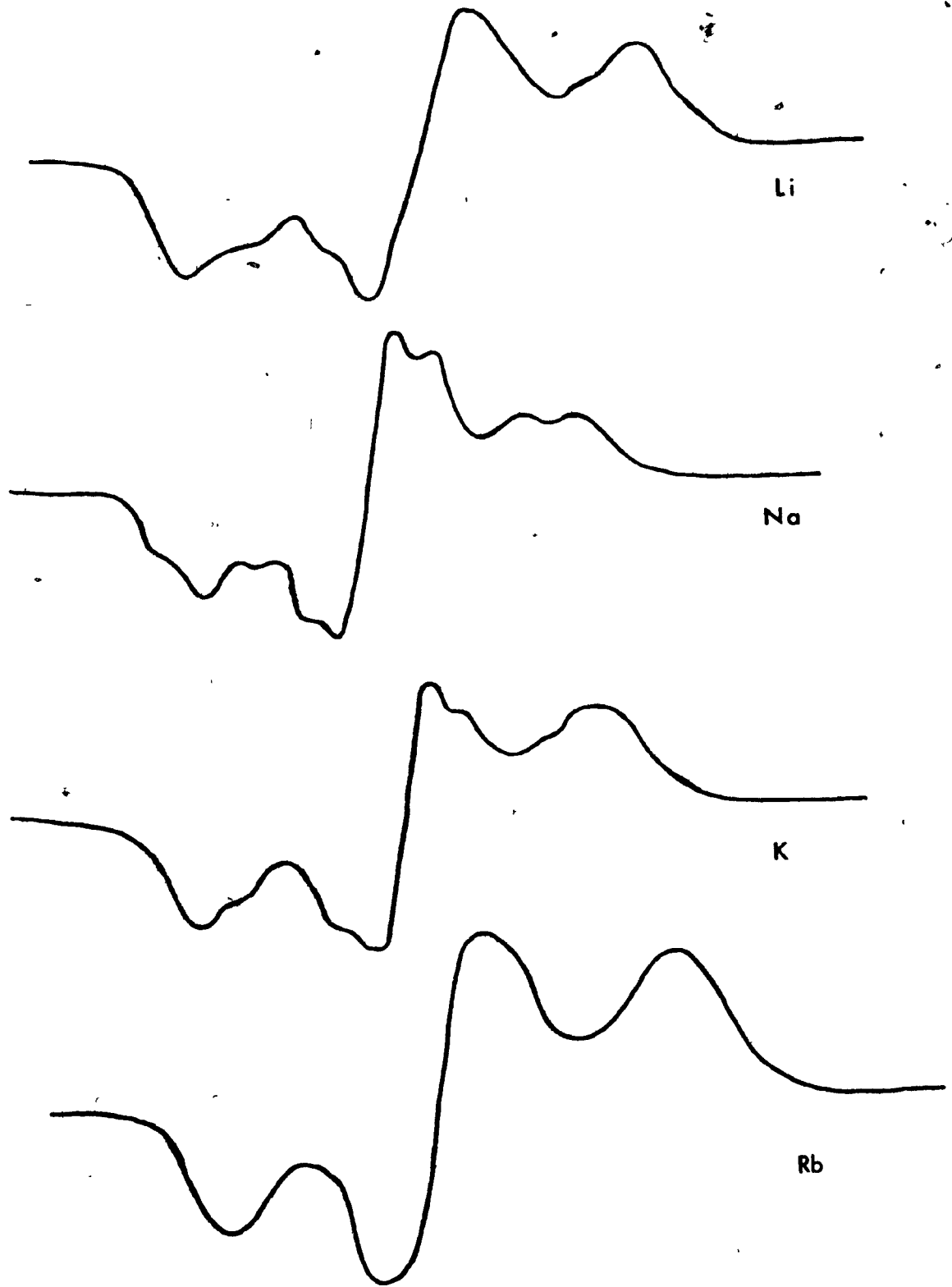
splitting and Rb acrylate shows an almost undeformed triplet. No difference was observed between spectra recorded at the irradiation temperature of 195 K and at temperatures at which polymerization to only very low conversions had occurred. With the progress of the polymerization there was no major change in the lineshape but each line broadened [Fig. (III-18)]. As the rate of broadening appeared comparable to the rate of polymerization a quantitative measurement of the broadening was obtained by means of the ratio of peak area, A, to peak height, h. Indeed A/h shows the same time dependence as the polymer yield: i.e. a plot of A/h versus logt is linear.

The acrylate radical must in all the cases be of the type:



Some oligomerization must already have occurred at the temperature of irradiation because the expected quintet spectrum of the monomer radical is never observed. The shoulders or splittings could be due either to the presence of more than one radical conformation or to an asymmetry of the spectrum of one radical conformation only. The broadening of the lines at high polymerization yields could be due to several causes: replacement of more mobile oligomer radicals by less mobile polymer radicals, decrease of mobility of the radicals due to changes in the reaction matrix caused by the

Fig: (III-18): ESR spectra of the alkali acrylate radicals  
at high polymer yields



Li

Na

K

Rb

polymerization, creation of a broader spectrum of local environments and consequently of local fields by means of the crystal damage caused by the polymerization, increase of molecular weight of the recombining radicals, presence of more radical conformations in the polymer radical than in the low oligomer radical. As the ESR line broadening occurs with a rate law analogous to the polymerization it is likely that an investigation of the causes of line broadening could help also to understand the polymerization mechanism. The decay of the radical concentration of the four acrylates [Figs. (III-19)-(III-24)] is second order when the correct radical concentration<sup>(\*)</sup> is plotted versus time except for Na acrylate at 423 K. In this case the rate of recombination seems to decrease with increasing reaction time. Second order plots for the decay of acrylate radicals are given in Figs. (III-25)-(III-29). Second order rate constants for radical recombination are shown in Table (III-3). Na acrylate has recombination constants considerably lower than the other acrylates which have recombination constants of the same order of magnitude. The recombination constant of K acrylate radicals shows a minimum at 323 K [Fig. (III-30)]. A minimum is shown too by the recombination constant of Rb acrylate around 313 K.

(\*) Difference between the actual radical concentration and the stable radical concentration  $[R\cdot]_{\infty}$ .

Fig. (III-19) Decay of Li acrylate radicals at 353 K

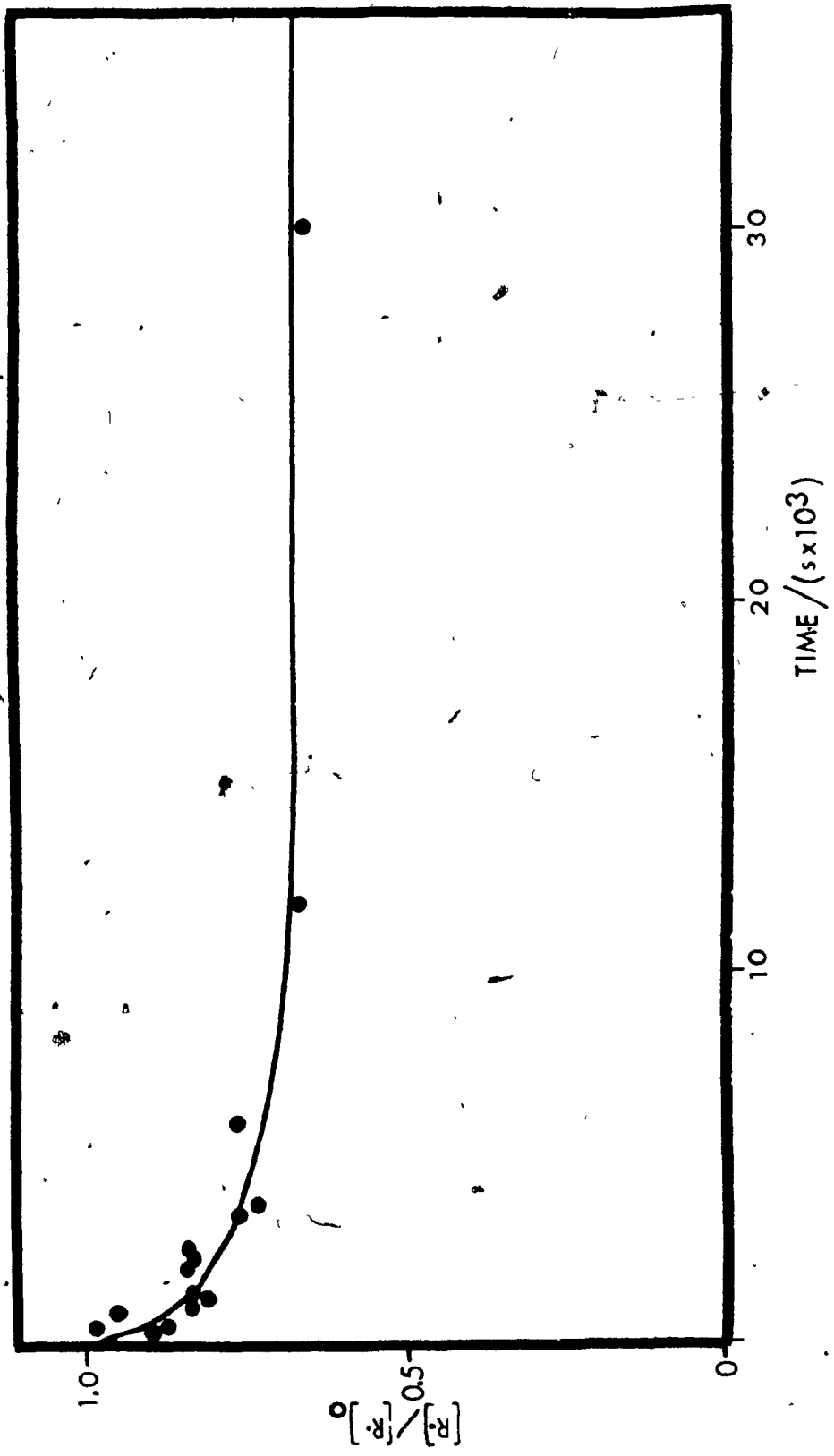


Fig. (III-20): Decay of Li acrylate radicals at 423 K

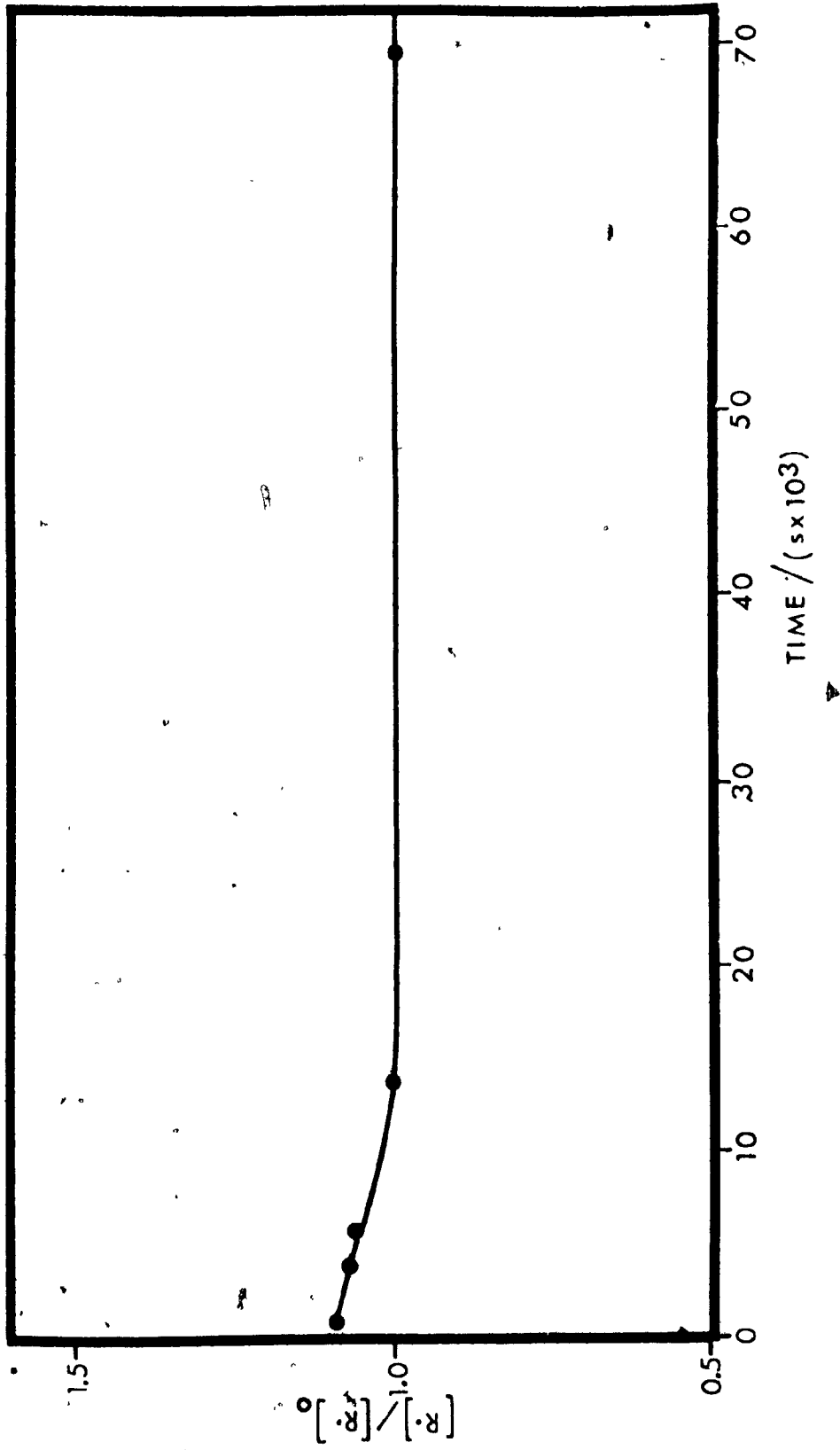


Fig. (III-21): Decay of Na acrylate radicals at 353 K

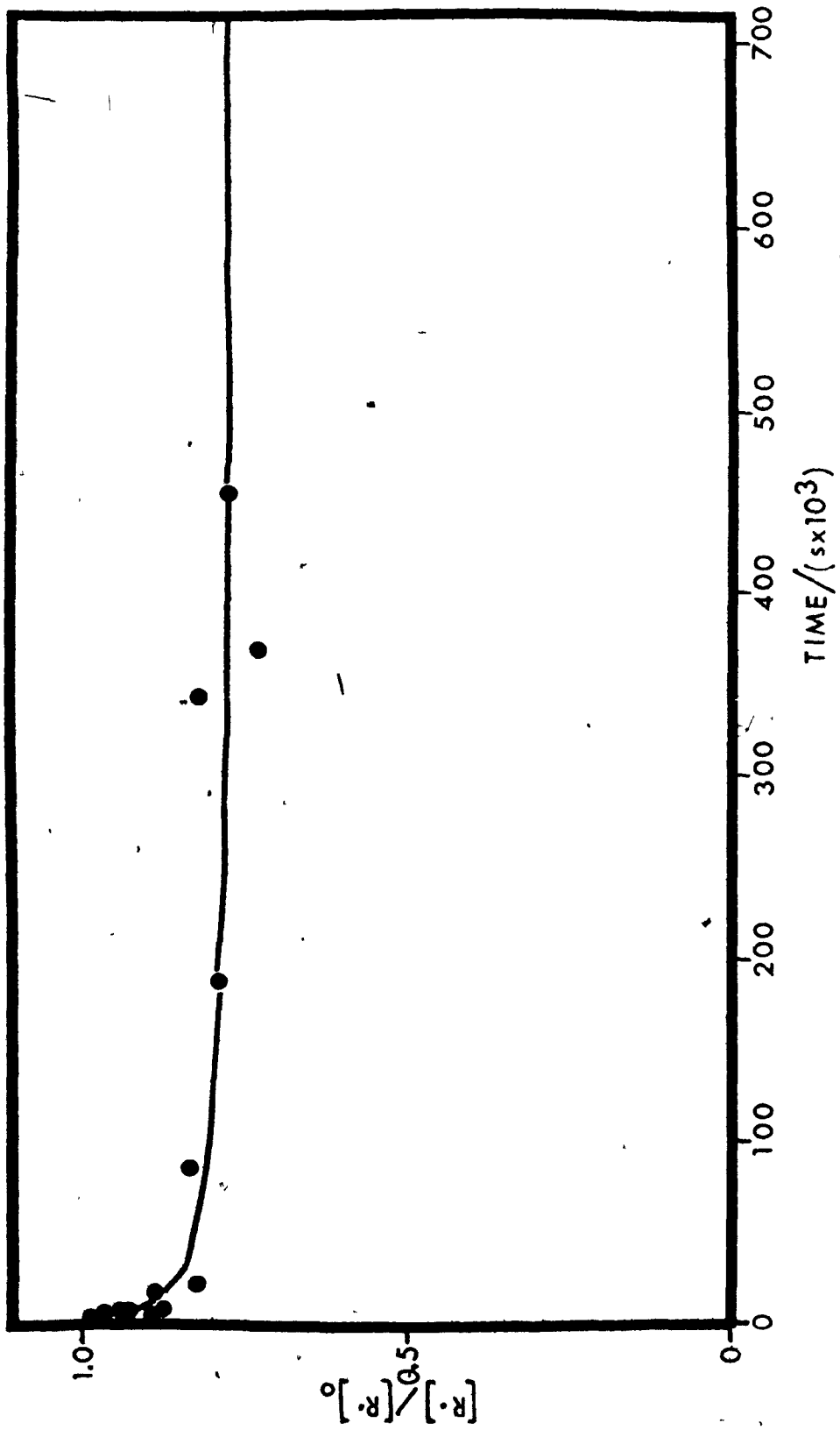


Fig. (III-22): Decay of Na acrylate radicals at 423 K

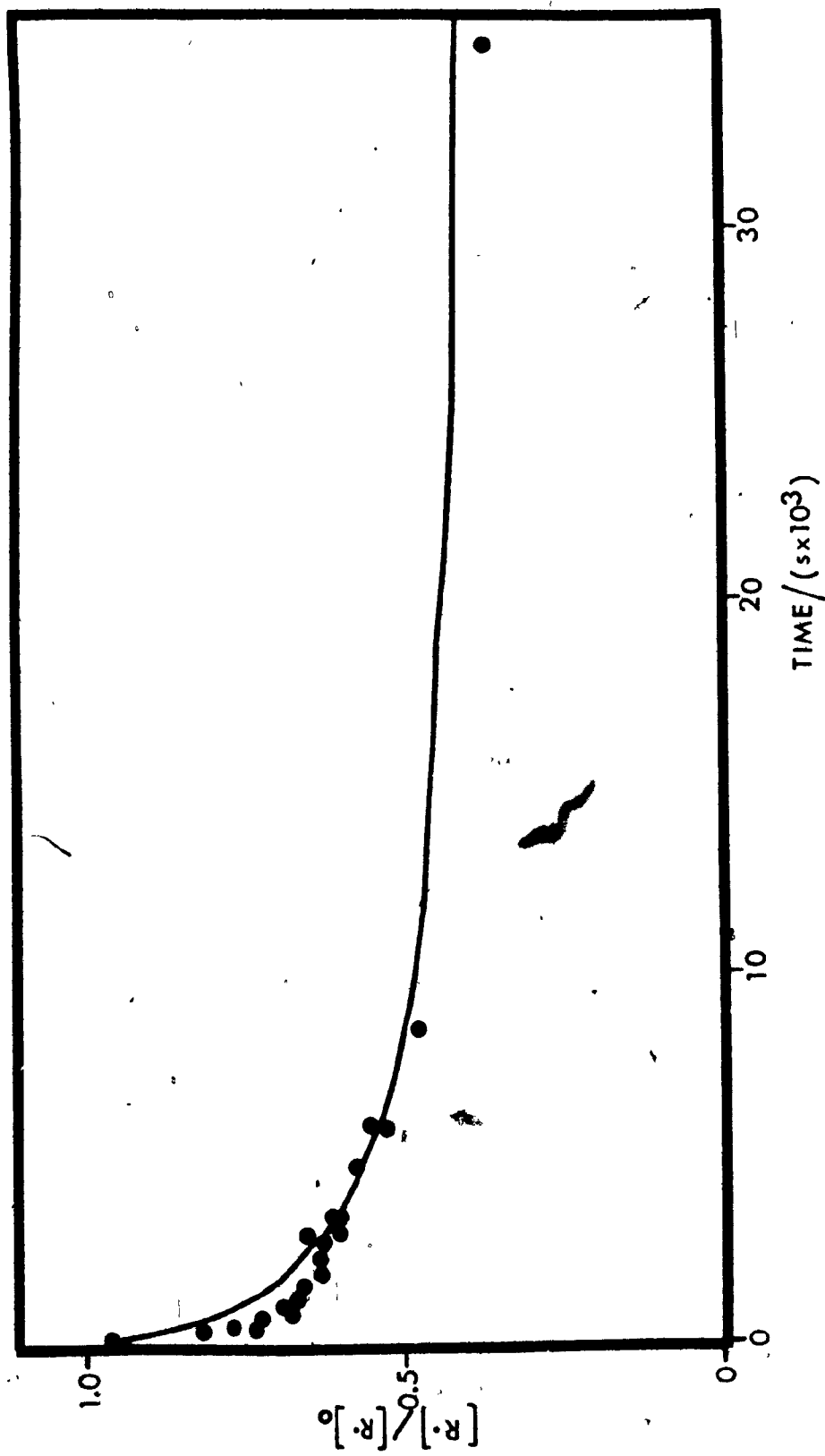


Fig. (III-23): Decay of K acrylate radicals at 313 K (●), 323 K (■), and 353 K (▲)

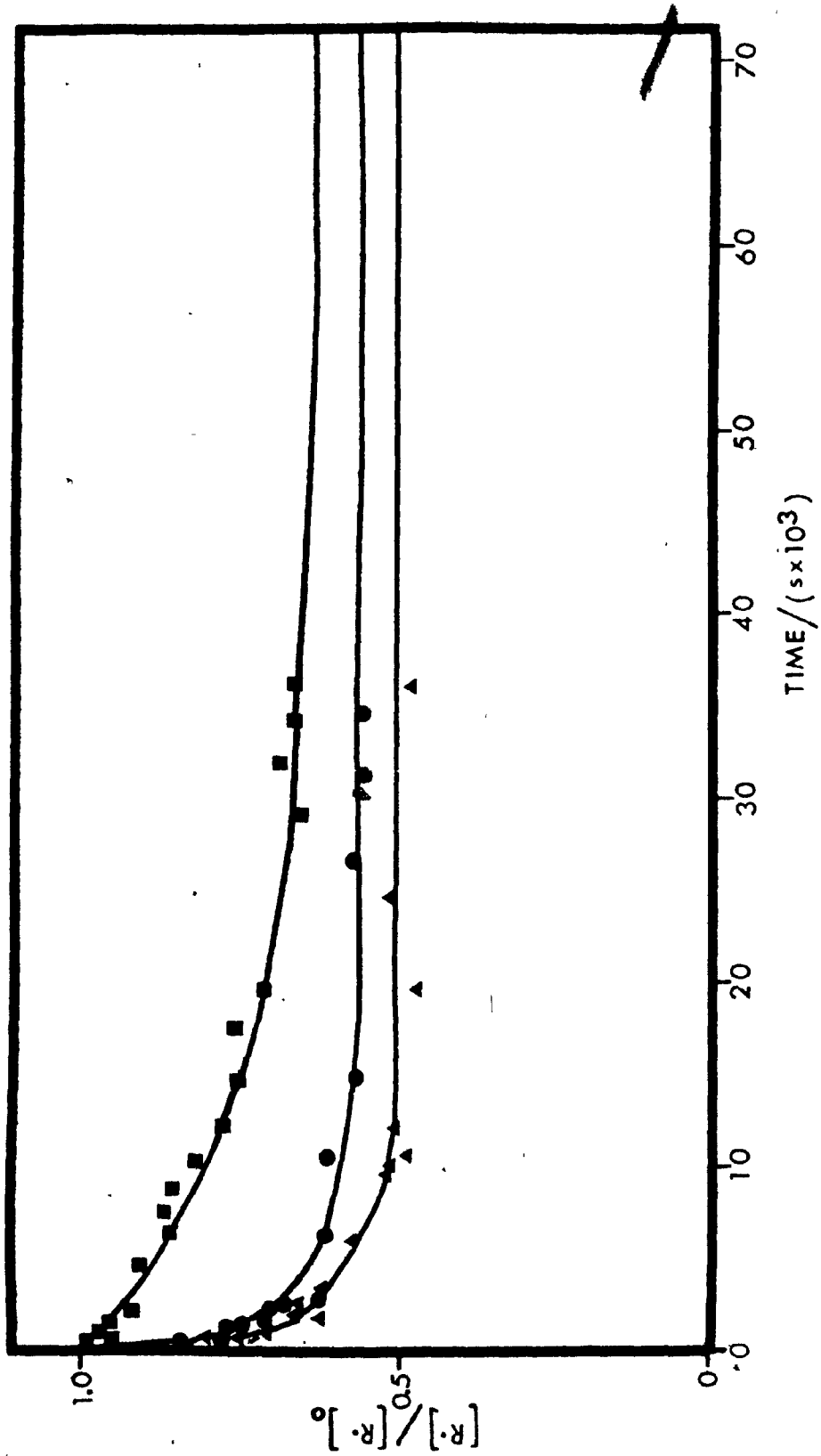


Fig. (III-24): Decay of Rb acrylate radicals at 303 K (■), 313 K (▲) and 353 K (●)

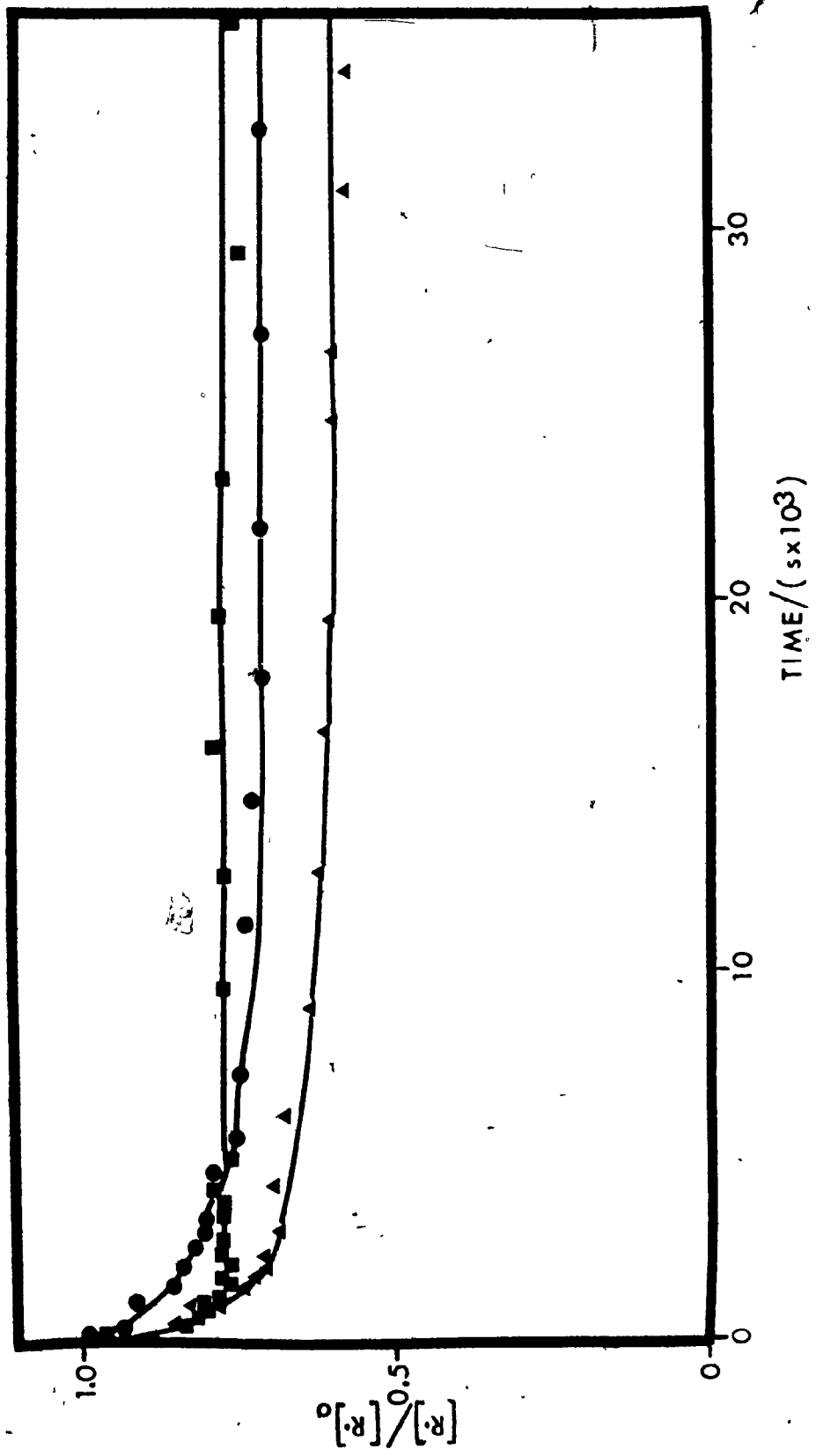
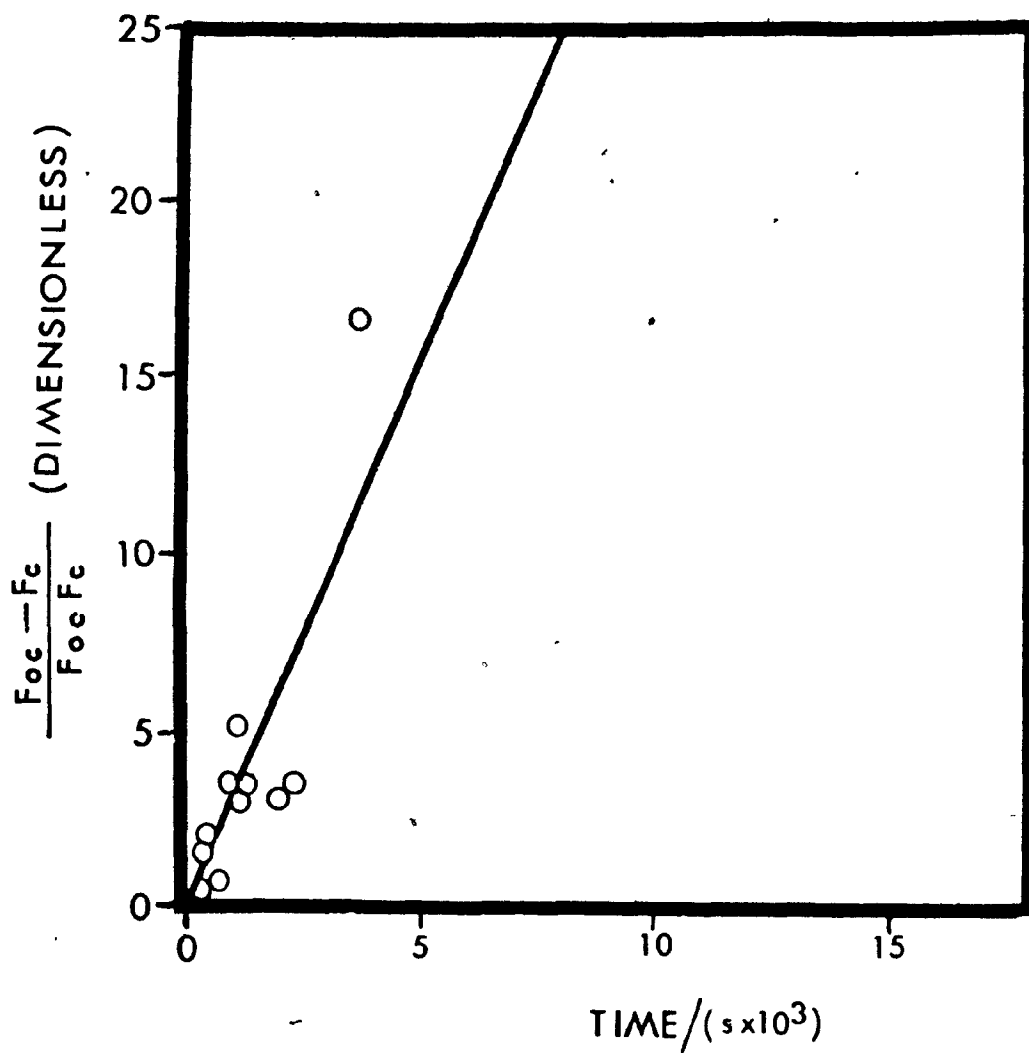


Fig. (III-25): Second order decay of Li acrylate radicals  
at 353 K.  $F_C = \frac{[R\cdot] - [R\cdot]_\infty}{[R\cdot]_0}$ ;  $F_{OC} = \frac{[R\cdot]_0 - [R\cdot]_\infty}{[R\cdot]_0}$



( )

Fig. (III-26): Second order decay of Na acrylate radicals  
at 353 K

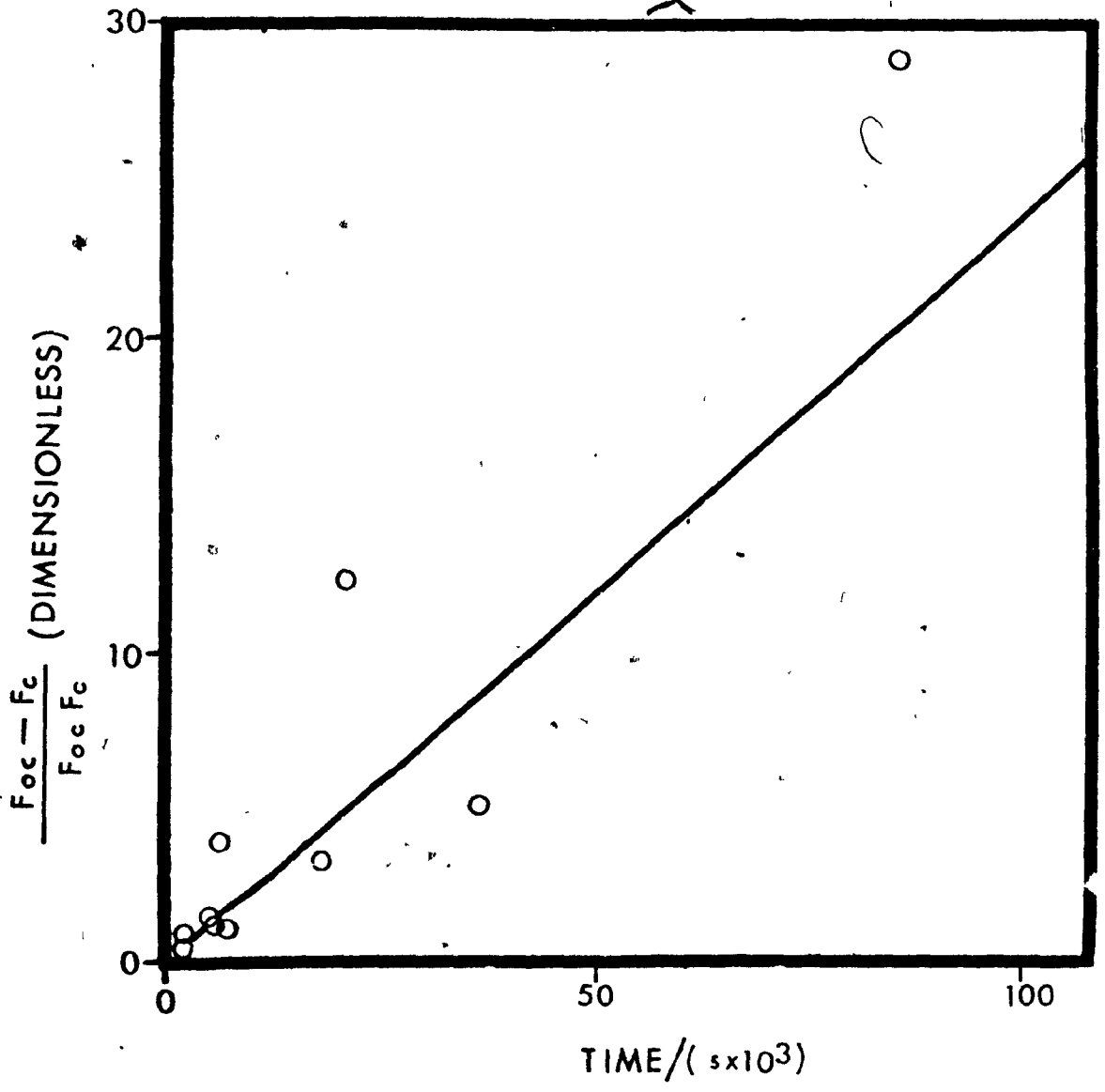
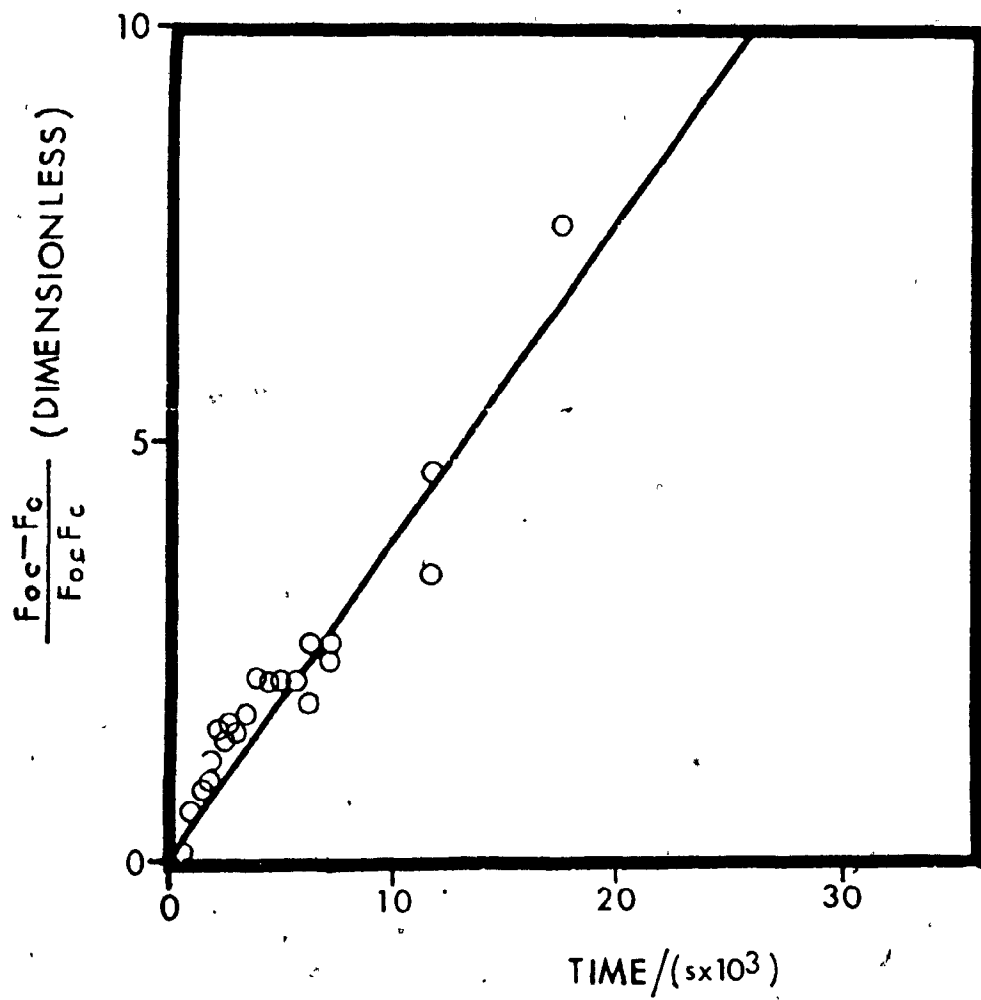


Fig. (III-27): Second order decay of Na acrylate radicals  
at 423 K



( )

Fig. (III-28): Second order decay of K acrylate radicals  
at 313 K ( $\Delta$ ), 323 K ( $\square$ ), 353 K (o) and  
373 K ( $\blacksquare$ )

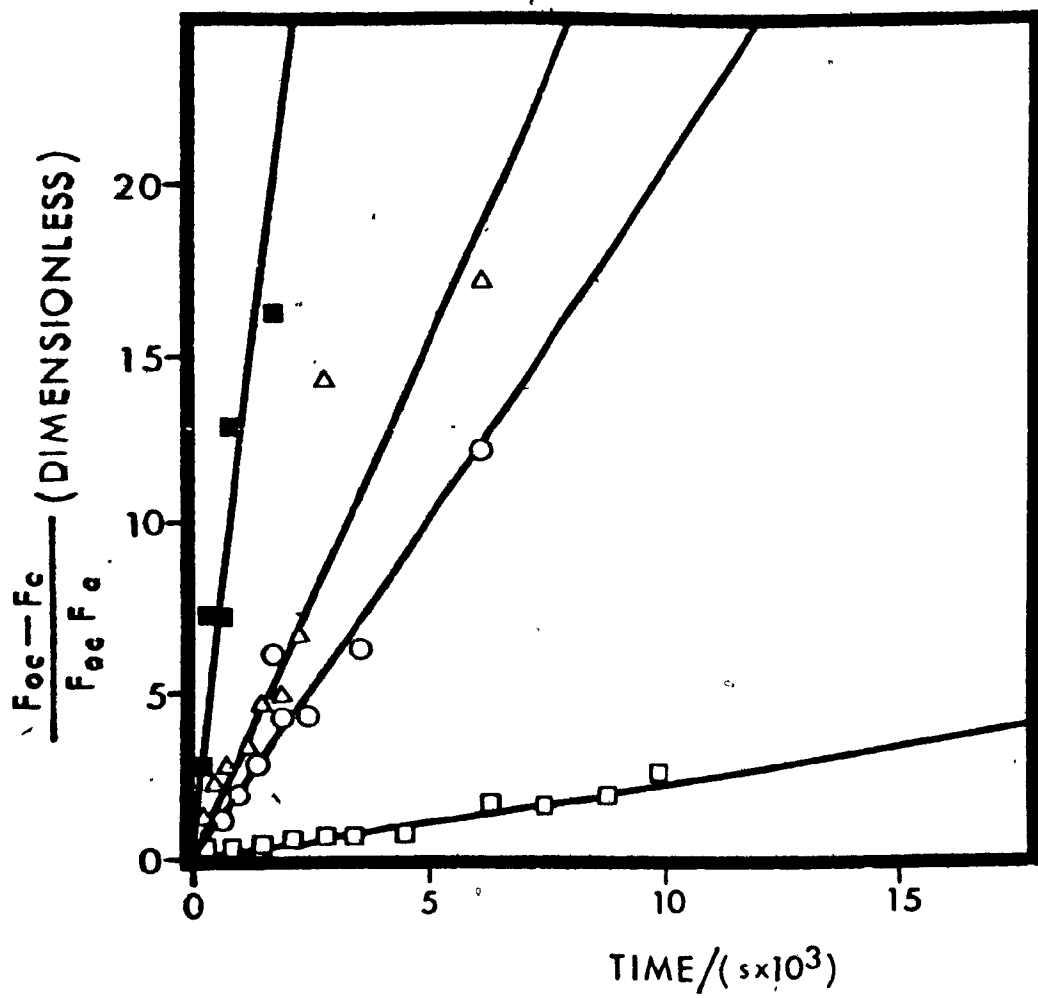


Fig. (III-29): Second order decay of Rb acrylate radicals  
at 303 K ( $\square$ ), 313 K ( $\Delta$ ) and 353 K ( $\circ$ )

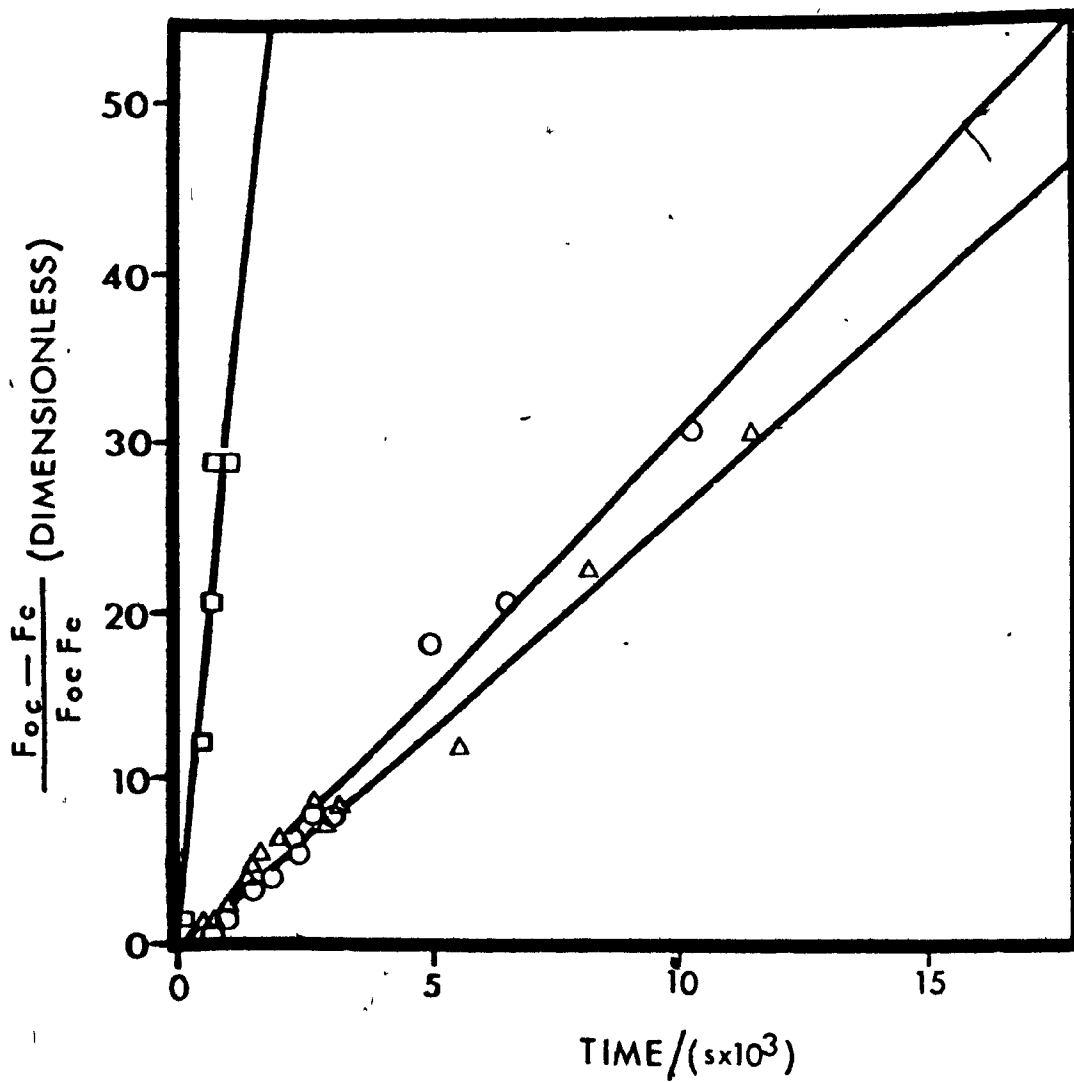
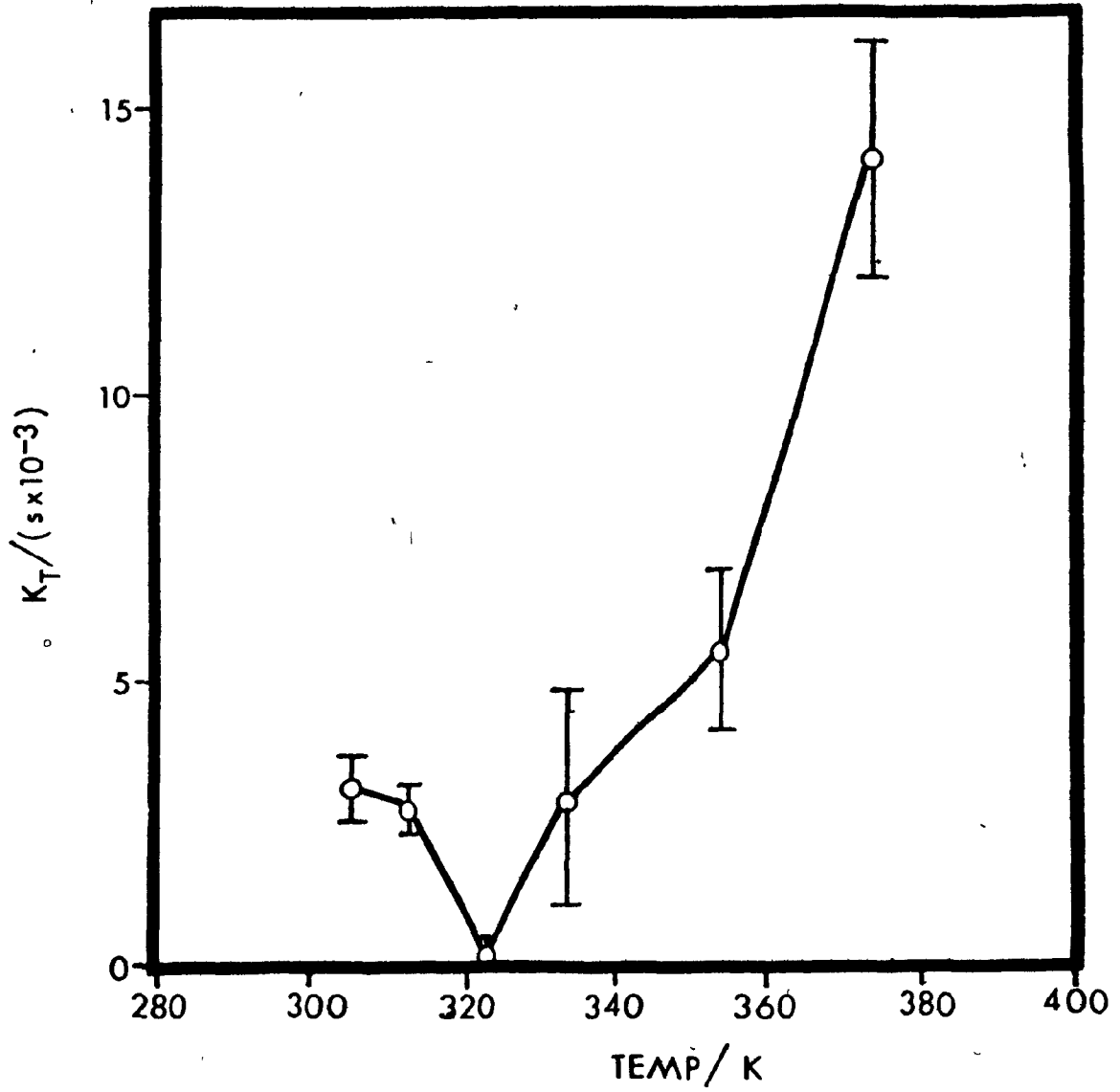


TABLE (III-3): Temperature dependence of the radical re-combination rate constants of the alkali acrylates radicals

<u>Cation</u>	<u>Temp/K</u>	<u><math>k_T / (s \times 10^{-3})</math></u>
Li	353	$3.06 \pm 0.58$
Li	423	extremely fast
Na	353	$(2.0 \pm 0.6) \times 10^{-1}$
Na	423	$(3.42 \pm 0.25) \times 10^{-1}$
K	305	$3.14 \pm 0.5$
K	313	$2.80 \pm 0.42$
K	323	$(2.25 \pm 0.19) \times 10^{-1}$
K	333	$2.92 \pm 1.89$
K	353	$5.55 \pm 1.42$
K	373	$14.11 \pm 2.28$
Rb	303	$29.81 \pm 4.56$
Rb	313	$2.28 \pm 0.14$
Rb	353	$2.94 \pm 0.17$

( )

Fig. (III-30): Temperature dependence of the second order radical recombination rate constants of K acrylate



III-5 DISCUSSION

The radical concentration of the alkali acrylates decays during the first hours of reaction to a value  $[R\cdot]_{\infty}$ , and then remains constant for the period over which the reaction was followed, up to several weeks [Figs. (III-20)-(III-25)]. The rate of polymerization is constant in reaction period B when the decay of the radical concentration is fastest. In the period C the rate of polymerization decays with the same rate law both before and after the limiting radical concentration  $[R\cdot]_{\infty}$  has been reached. Therefore the variation in radical concentration measured by ESR must be due to the recombination of radicals which do not contribute (in large amount) to the polymerization. The radical recombination seems to occur in the least reactive regions of the crystal, where the small oligomer radical cannot polymerize. Once the polymerization has started, however, radical chains quickly attain a length such that their probability of recombination becomes negligible. It is interesting to note that in Chachaty's kinetic scheme radical recombination is a second order process only in the regions of the crystal where there is negligible polymerization. The concentration of polymerizing radicals can thus be considered constant during the polymerization. The polymerizability of a certain region of the crystal could be determined by the rate of nucleation of the polymer phase. A similar behaviour was reported by Chachaty for acrylic acid and acrylamide [Chachaty (1972a), (1972b)].

ESR measurements of radical concentration for a polymerizing system are thus more useful measures of radical mobility. In fact, if recombining radicals do not polymerize then the measured rate constant for radical recombination  $k_T$  will be determined as for irradiated non-polymerizing crystals, mainly from the rate constant for radical diffusion  $k_D$  [see I-3,b] and therefore  $k_T = k_D$ .

Polymerizing systems could instead be expected to show recombination with a time dependent rate constant. If the polymerization modifies the crystal a corresponding change in the measured recombination rate constant  $k_T$  should be expected. The second order recombination observed for the alkali acrylates (and for most other polymerizing monomers) is either a proof that no modification of the reaction matrix occurs or that the change takes place so rapidly that it cannot be followed by ESR. In the latter case  $k_T$  should reflect the properties of the modified matrix. Indeed a deviation from a second order decay was found for Na acrylate\* at 423 K [Fig. (III-22)]. The recombination rate constant varies, apparently decreasing with increasing reaction time. This does not necessarily imply a change of the matrix because the simultaneous presence of two radicals in the same reaction cage could cause the same deviation [Butjagin (1972)]. On the other hand the low recombination rate constant and the large variation of radical concentration of Na acrylate at 423 K are the simplest conditions under

which a deviation should be observable. Deviations from a second order decay could thus occur for other acrylates at such short times as not to be observable. Evidence for a modification of the matrix caused by the polymerization comes from the minimum observed in the recombination rate constant of K acrylate at 323 K and of Rb acrylate at about 313 K. Both theory and experiment for nonpolymerizing irradiated crystals [see (I-3,b)] show that the rate constant for radical recombination should increase continuously with increasing temperature, this increase being particularly fast near a phase transition. The minimum observed for K and Rb acrylate must be due either to a change of the chain length of the recombining radical or to a change in the "reaction matrix". In view of the previously discussed independence of radical recombination and polymerization it seems unlikely that at 323 K a radical should start polymerizing and then undergo recombination. The minimum in the recombination rate constant of K and Rb acrylate must therefore reflect a property of the modified matrix. ESR measurements of the rates of radical recombination in a polymerizing crystal are expected to give the diffusion constant of radicals in the reaction matrix modified by the polymerization.

Rate constants or at least parameters independent of monomer and radical concentrations would be needed in order to understand the influence of crystal structure, defects, and molecular motions on the mechanism of polymerization.

Such parameters are difficult to obtain due to the lack of a kinetic scheme that accurately describes the polymerization. The unsuitability of Morawetz's kinetic scheme is emphasized by the previous discussion of the independence of radical recombination and polymerization. Chachaty's kinetic scheme is based on more realistic assumptions and predicts the constant and  $\log t$  dependent rates of polymerization found respectively for the acrylates in periods B and C [eqtns (I-27) and (I-29)]. On the other hand it has not been sufficiently tested experimentally. The slopes of the  $(Y,t)$  and  $(Y,\log t)$  straight lines have been used as parameters to follow the polymerization of the acrylates.  $dY/dt$  and  $dY/d\log t$  are indeed reaction rate constants because they do not depend on concentration terms since both the concentration of the polymerizing radical and of the monomer at the reactant-product interphase are constant during the polymerization, at least below the limiting conversions reached for most vinyl monomers. It is interesting to note that these two slopes could be used as rate constants also in Chachaty's kinetic scheme because  $[R\cdot]_{\infty}/M_0$  shows only small variations in all the situations in which the SSP of the acrylates was studied.

A polymerization behaviour characterized by the two reaction periods B and C is shown also by acrylic acid and acrylamide [Chachaty (1972a), (1972b)]. Many other compounds show the same time dependence of the polymer yield

but their reaction period B has not been investigated. The comparison of experimental data is therefore difficult both for the lack of data and for the different experimental conditions used.  $dY/dt$  increases with temperature for Li, Na and K acrylate, for acrylic acid and for acrylamide and it increases with radiation dose for acrylic acid and acrylamide.  $dY/d\log t$  is constant with respect to temperature for acrylic acid, acrylamide, Li, Na acrylate and for K acrylate at all temperatures except at 323 K. The polymer yield after a fixed polymerization time in period C increases with increasing temperature for all the above mentioned compounds.  $dY/d\log t$  is constant with respect to radiation dose for K acrylate. Reaction period B ends at lower yields for higher values of  $dY/dt$ . Values of  $dY/dt$  and  $dY/d\log t$  are reported in Table (III-4).

For each monomer temperature has the largest influence in reaction period B while  $dY/d\log t$  seems to be a constant for a given compound over a relatively large range of temperature. Table (III-4) also shows that  $dY/dt$  for K acrylate is slightly lower than for acrylic acid and slightly higher than for acrylamide. Considering that these two compounds were studied just below their melting point it seems that very favourable conditions for polymerization exist in K acrylate. In fact Li and Na acrylate at higher temperatures have smaller values of  $dY/dt$ .

To understand the effect of monomer mobility on

TABLE (III-4):  $dY/dt$  and  $dY/d\log t$  for the polymerization of some vinyl monomers

<u>Compound</u>	<u>Temp/K</u>	<u>T/T<sub>m</sub></u>	<u><math>(dY/dt)/(s \times 10^{-5})</math></u>	<u><math>dY/d\log t</math> (s<sup>-1</sup>)</u>
Acrylic acid	265	0.93	$6.41 \times 10$	3.96
Acrylic acid	276	0.97	$4.24 \times 10^2$	3.96
Acrylamide	310	0.87	$1.33 \times 10$	16.8
Acrylamide	326	0.91	$5.55 \times 10$	16.8
Li acrylate	374	----	$8.94 \times 10^{-2}$	7.53
Na acrylate	393	----	$1.75 \times 10^{-1}$	4.8
K acrylate	313	----	$7.94 \times 10$	6.05
K acrylate	353	----	$1.43 \times 10^2$	6.14
Ca acrylate $\cdot 2H_2O$	298	----	----	4.82
Ca acrylate anhydrous	298	----	----	8.48
Ca acrylate $\cdot 0.5H_2O$	298	----	----	23.84

SSP both the crystal structure of the monomer and the type of molecular motion should be known. The crystal structures of the acrylates have not been reported and the type of molecular motion can only be determined approximatively. The actual frequency of the motion can rarely be determined by wide-line NMR. Therefore only a qualitative correlation of rate constants of polymerization with molecular motions can be made.

A comparison of molecular motions and rate constants of polymerization is more meaningful if done separately for the reaction periods B and C. Polymerization starts occurring at measurable rates at 374 K for Li acrylate, at 393 K for Na acrylate and 273 K for K acrylate. At these temperatures, at which the acrylates are undergoing only a limited rotational oscillation [Figs. (III-12)-(III-15)],  $dY/dt$  is higher for K acrylate than for both Li and Na acrylate [Table (III-5)].

An oscillation amplitude of about  $25^\circ$  is obtained for Li and K and of about  $20^\circ$  for Na acrylate at 374, 273 and 393 K respectively, assuming in all the cases an oscillation about an axis passing through the C-H1 bond [Fig. (III-10)] and the same reduction factor for the inter- and intra-molecular second moment.  $dY/dt$  increases with increasing temperature for these three acrylates. Polymerization then starts occurring at about the same degree of molecular mobility for the three acrylates but the rate constants of polymerization are

TABLE (III-5):  $dY/dt$  for Li, Na and K acrylates

<u>Cat</u>	<u>Temp/K</u>	<u><math>(dY/dt)/(sx10^{-5})</math></u>
Li	374	$8.94 \times 10^{-1}$
Li	405	4.25
Na	393	1.75
Na	403	2.27
K	273	2.92

different.  $dY/dt$  must therefore depend on other variables such as crystal structure, presence of defects etc. Between 273 K and 373 K,  $dY/dt$  for K acrylate increases continuously while in the same range of temperature there is a motional transition terminating at 350 K above which the monomer molecule undergoes reorientation rather than oscillation [Fig. (III-31)]. The increase in  $dY/dt$  is faster during than below and above the NMR transition. Above the transition the rate of increase of  $dY/dt$  seems to slow down. Not enough information on K acrylate is at the moment available to understand the nature of this phenomenon.

$dY/dlogt$  was seen to be independent of temperature except for K acrylate at 323 K. No relationship can therefore be found in general between monomer mobility and rate constant for polymerization in period C. For K acrylate at 323 K instead the minimum in  $dY/dlogt$  corresponds to a minimum in radical recombination rate constant and in degree of polymerization of poly K acrylate [Fig. (III-32)]. This means that the rate constant for radical diffusion in the modified matrix is, in period C, a more meaningful parameter than monomer mobility. The difference between reaction periods B and C is probably the absence of any reaction matrix modification in B. The polymerization rate constant shows a correlation with the properties of the initial crystal in B and with the properties of the modified matrix in C.

Li and Na acrylate are reported not to polymerize

Fig. (III-31): Temperature dependence of  $dY/dt$  (o) and of the second moment, (●) of K acrylate

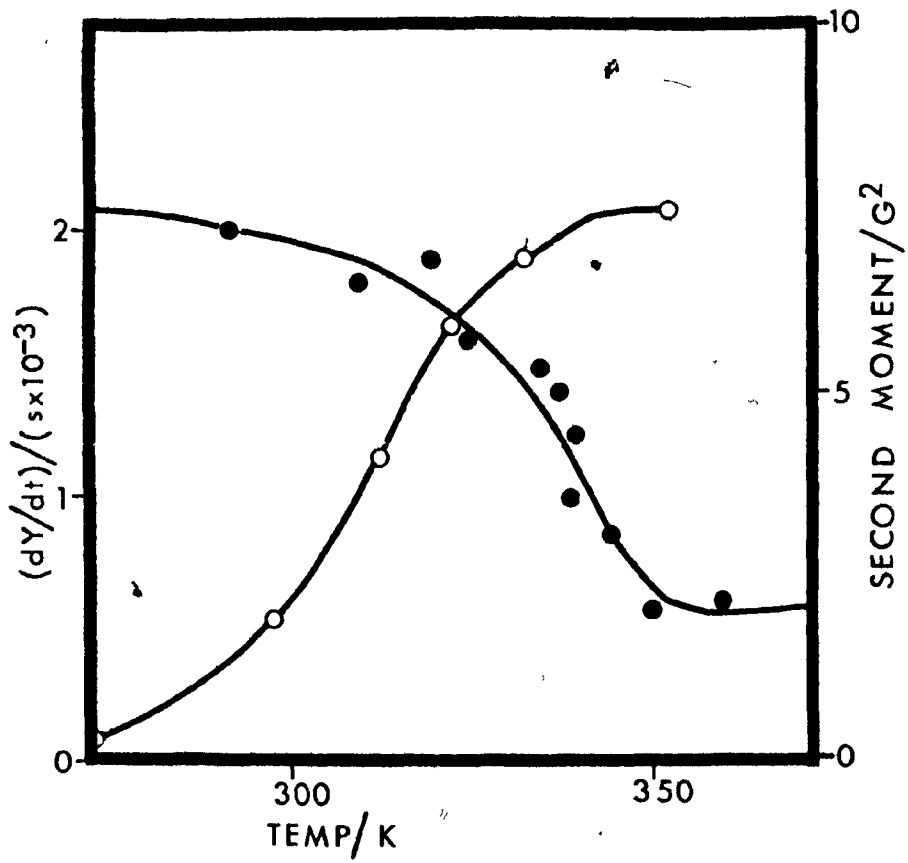
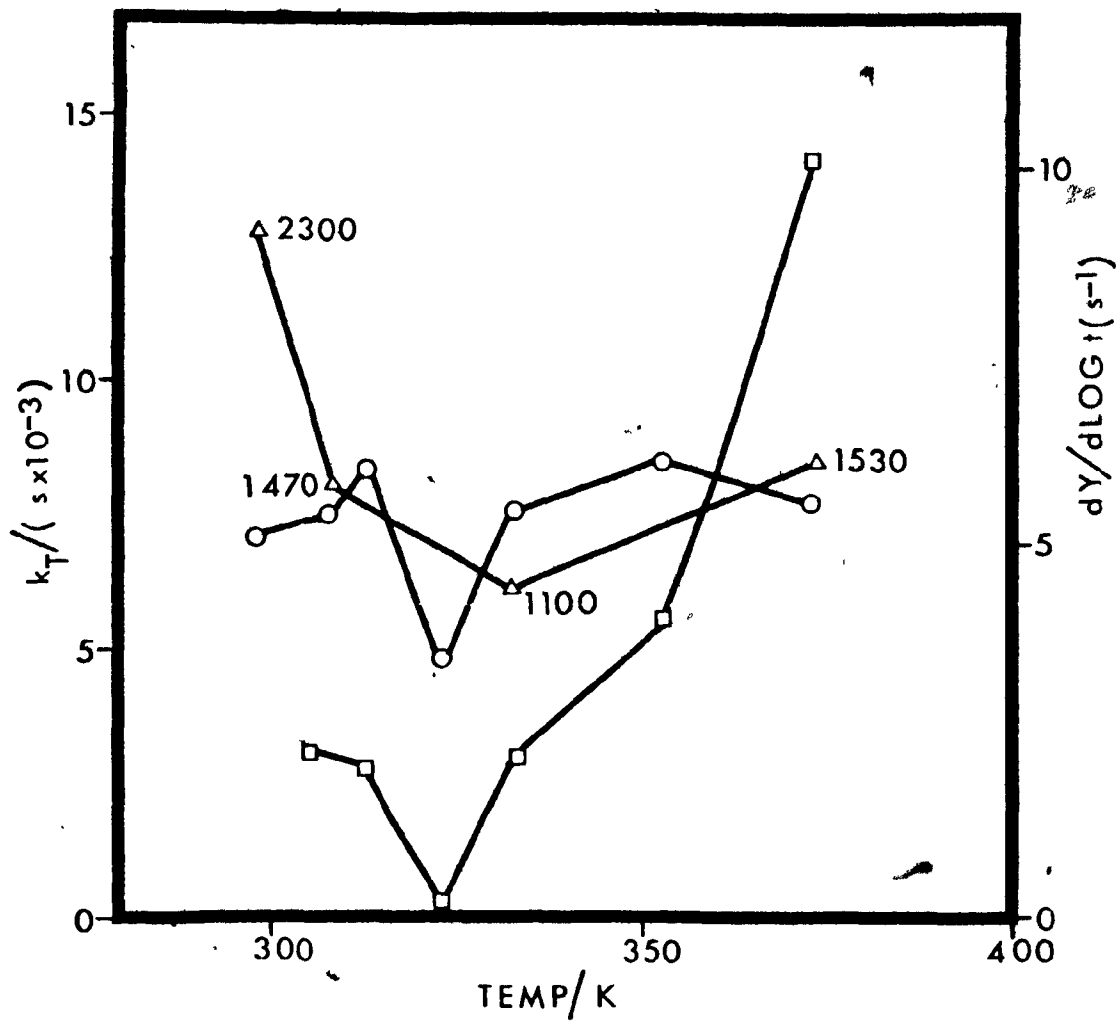


Fig. (III-32): Temperature dependence of the radical recombine rate constant ( $\square$ ),  $dY/d\log t$  (o) and of the average degree of polymerization ( $\Delta$ ) of K acrylate .



at 353 K [Morawetz (1962)]. At this temperature the monomer molecules can only undergo limited oscillations while the diffusion constant is considerably higher for Li than for Na acrylate radicals. The ESR spectrum of Li acrylate at 353 K broadens with time while that of Na acrylate remains unchanged. If the broadening of the ESR spectrum indicates the occurrence of polymerization then Li acrylate starts polymerizing but undergoes a sudden termination before either the molecular weight of the polymer or the polymer yield become measurable. Na acrylate instead fails to polymerize because the reaction cannot start at all.

A comparison of molecular mobilities with rate constants of polymerization of the alkali acrylates leads then to the following conclusions:

- a) A minimum molecular mobility seems to be a prerequisite for polymerization.
- b) It is not clear what role is played by molecular motions but it seems that they can play different roles in different reaction steps.
- c) In period B, monomer mobility is better correlated with the rate constant for polymerization  $dY/dt$ .
- d) During the polymerization a modification of the reaction matrix occurs after which the rate of polymerization correlates better with the motional properties of the modified matrix as measured by ESR.

The modification of the matrix probably plays a

quite important role in the SSP of the alkali acrylates and possibly for other systems as well. This point can be illustrated by a discussion of the mechanism of termination in SSP. All the possible causes for termination are of two types: either a decrease in the concentration of the reactants or a decrease in their reactivity. As radical recombination and polymerization are two distinct processes radical concentration cannot be the limiting factor. On the other hand it is also unlikely that monomer concentration is the limiting factor because in many solid state polymerizations a limiting conversion of less than 50% is achieved. It could be argued that although the monomer concentration left at the end of the reaction is still high the probability of collision between the macroradical and the polymer has become comparable with the probability of collision between the macroradical and the monomer. This cannot be true in general since there is a phase separation and the reaction occurs at the interphase between polymer and monomer. On one side of the boundary there is a constant concentration of monomer.

Termination could alternatively be caused by a decrease in the reactivity of the reactants. The reactivity of a species in the solid state is determined both by chemical and physical contributions. The chemical contributions should not vary with polymerization. A change in the physical contribution to reactivity is thus left as the most general cause for termination in SSP. In other words the parameters

that influence the polymerization (distance between reacting groups, defect concentration etc.) change during the reaction or equivalently the "reaction matrix" is modified.

The data obtained in this investigation do not allow an unequivocal identification of the mechanism of matrix modification. The following discussion is an attempt to clarify this mechanism. As the growing polymer cannot in general fit precisely into the crystal structure of the monomer there will undoubtedly be some build-up of strain in the monomer lattice. For example in a recent investigation of the SSP of trioxane [Voigt-Martin (1974)] it was impossible to find a reasonable value of interphase free energy without explicitly considering the elastic strain free-energy<sup>(\*)</sup>. However, the occurrence of dislocation multiplication and phase separation shows that the strain does not necessarily need to be elastic.

At a high enough temperature an annealing of the accumulated strains is likely to take place. The importance of annealing in the SSP of a solid solution of methacrylamide and isobutyramide has been demonstrated by Adler [Adler (1970)] who also suggested that insufficient annealing of the strain created by polymerization could be a cause for limiting conversion. The resultant strain accumulated in the lattice is then probably determined by the balance between creation and annealing of strain. Results obtained in this thesis and in other investigations can be explained by this mechanism

(\*) This represents a limit of the assumption that  $\Delta G_e \approx 0$ , see (I-2,d).

( ) of matrix modification. The "reanimation" at a temperature  $T_2 > T_1$  of a polymerization that had stopped at  $T_1$  [see page 20] can be explained by an annealing at  $T_2$  of the strains that at  $T_1$  had stopped the reaction. Both the rate of generation and the rate of annealing of strain are expected to increase with increasing temperature but not necessarily at the same rate. Both depend on molecular mobility, although in general not in the same way. Their rate of increase near a phase transition could be substantially different giving rise to a maximum or minimum in their balance. This is a possible explanation for the minimum found in rate of polymerization, rate constant of radical recombination and molecular weight of poly K acrylate at 323 K. If generation and annealing of strain increase at different rates with temperature then the strain accumulated in the monomer lattice should either decrease or increase with increasing temperature. The failure to polymerize at 313 K of the samples of K acrylate prepolymerized at 353 K shows that the strain built in the lattice is larger above the transition. The same matrix that would have continued to react at 353 K stops polymerizing at 313 K. The conservation of the high temperature phase of K acrylate as a metastable phase below the phase transition where it could not polymerize, is ruled out as an alternative explanation of this experiment, by the results of DSC measurements on irradiated K acrylate. Also a slight decrease of the stable radical concentration above the transition

( $[R\cdot]_{\infty}(353\text{ K}) = 0.7 [R\cdot]_{\infty}(313\text{ K})$ ) should at most cause a decrease in the polymerization rate and not its complete cessation. A negligible strain accumulation would leave almost unchanged the reaction matrix allowing the polymerization to occur at a constant rate (period B). When the strain accumulation becomes considerable and changes the properties of the reaction matrix the rate of polymerization decreases continuously (period C). The strain accumulation mechanism of matrix modification then provides an explanation of the data obtained in this thesis although not the only possible one.

It is not clear under what form the strain is accumulated in the lattice and why strain should decrease the reactivity. If dislocation multiplication occurs, as suggested by Thomas and Williams [Thomas (1967)] for the caramelization of sucrose, this could create a high enough dislocation concentration to "harden" the lattice (cf. work hardening of metals) and reduce its polymerizability. Again this is a possible mechanism by which the strain could be accommodated in the lattice. If this is the real mechanism of the modification of the matrix then monomer mobility can play another important role by helping to anneal the accumulated strains.

To summarize the previous discussion it could be said that a likely mechanism for the modification of the reaction matrix is the accumulation of strains in the reacting

( ) monomer lattice. The net accumulation is determined by the balance between generation and annealing of strain. A possible way in which the strains could be accommodated in the crystal lattice is by dislocation multiplication, which could cause a hardening of the lattice that stops the reaction. Molecular motions would be very important in such a mechanism by allowing the annealing of the accumulated strains. The existence of a matrix modification also suggests that a separate investigation should be conducted in reaction periods B and C. In this way information could be obtained respectively on the importance of physical parameters in the initial crystal and in the modified matrix. The present state of knowledge of the alkali acrylates and of SSP in general does not allow a test of this mechanism but in view of its importance for SSP it is certainly one area where further investigation should be conducted.

CHAPTER IV

CONTRIBUTIONS TO ORIGINAL KNOWLEDGE  
AND SUGGESTIONS FOR FURTHER WORK

IV-1

CONTRIBUTIONS TO ORIGINAL KNOWLEDGE

- 1) A motional transition at 315 K and a phase transition at 339 K were detected for K acrylate by wide-line NMR and by DSC respectively. Similar transitions were shown by Rb acrylate at 308 K and 333 K. Above the transitions molecular rotation about one axis occurred for both K and Rb acrylate. Li and Na acrylate showed no phase transition and only a smaller gradual variation of mobility in the range of temperature 273 K - 420 K.
- 2) Two different kinetic periods B and C were found in the SSP of the alkali acrylates, where the rate of polymerization is constant or continuously decreasing.
- 3) One hour of prepolymerization of K acrylate at 353 K results in the remaining monomer being totally unpolymerizable at 313 K.
- 4)  $dY/d\log t$ , the rate constant of radical recombination, and the average degree of polymerization of K acrylate show a minimum at about 323 K. This minimum, as well as the non-polymerizability at 313 K of the sample prepolymerized at 353 K are attributed to a modification of the reaction matrix caused by the polymerization. A minimum was found in the radical recombination rate constant of Rb acrylate at 313 K.
- 5) Li, Na and K acrylate were found to polymerize only above a temperature at which there is a minimum of molecular motion. The rate of polymerization of K acrylate in period

B is found to increase with increasing molecular mobility. Molecular mobility is then considered a prerequisite for solid state polymerization in these compounds.

6) The different causes for which Li and Na acrylate fail to produce a detectable amount of polymer show that the role of molecular motions can be different in each reaction step.

7) The effects of matrix modification are considered to become significant only in reaction period C. Separate consideration of reaction periods B and C can therefore show the importance respectively of the properties of the initial crystal and of the modified matrix.

#### IV-2      SUGGESTIONS FOR FURTHER WORK

1) An electron and optical microscopy study of the SSP of the alkali acrylates should be conducted to assess the importance of nucleation, to detect the simultaneous occurrence of more than one process and to study the structure of the monomer-polymer interphase.

2) If possible, crystal structures should be determined for the four acrylates, for K and Rb acrylates at least for the low temperature phase.

3) The effect of the motional and phase transitions on the polymerization of Rb acrylate should be studied and compared with that of K acrylate.

4) The nature of crystal lattice defects should be investi-

gated, for instance by etching methods, in the unirradiated and in the irradiated acrylates. In the last case the defects should be followed as a function of the conversion to polymer.

5) NMR relaxation times (and, if possible, other physical properties) of the monomer and polymer phase of the alkali acrylates should be followed as a function of the polymer yield to provide a quantitative basis for the interpretation of the modification of the matrix.

6) A calorimetric investigation of the phase transition of the monomer in K and Rb acrylate as a function of the conversion to polymer could possibly supply informations about the changes occurring in the monomer phase.

7) The same kind of information as in 5) and 6) could be obtained by studying the effect of prepolymerization on K acrylate samples at different temperatures of prepolymerization and reaction.

8) The tacticity of the alkali acrylate polymers should be studied as a function of temperature and conversion to polymer. A varying tacticity should be correlated with a modification of the matrix or of the monomer-polymer interphase.

9) The distribution of molecular weight of the alkali acrylates should be followed as a function of temperature and conversion to polymer.

10) Nondestructive methods should be found to follow the polymerization. In this regard wide-line NMR and ESR look promising because of the changes that the spectra show during the polymerization.

BIBLIOGRAPHY

- Adler (1960) - G. Adler, W. Reams, J. Chem. Phys., 32,  
1698-1700 (1960).
- Adler (1965) - G. Adler, J.H. Petropoulos, J. Phys. Chem.,  
69, 3712-18 (1965).
- Adler (1966) - G. Adler, J. Polym. Sci., A-1, 4, 2883-91 (1966).
- Adler (1969) - G. Adler, B. Baysal, Mol. Cryst. Liq. Cryst.,  
9, 361-82 (1969).
- Adler (1970) - A. Faucitano, G. Adler, J. Macromol. Sci.-Chem.,  
A4, (2), 261-75 (1970).
- Andrew (1950) - E.R. Andrew, J. Chem. Phys., 18, 607-18 (1950).
- Andrew (1953) - E.R. Andrew, R.E. Eades, Proc. Roy. Soc., A216,  
398-412 (1953).
- Andrew (1958) - E.R. Andrew, R.A. Newing, Proc. Phys. Soc.,  
B72, 959-72 (1958).
- Ayscough (1956) - P.B. Ayscough, J. Chem. Phys., 24, 944-46  
(1956).
- Bamford (1963) - C.H. Bamford, G.C. Eastmond, J.C. Ward, Proc.  
Roy. Soc., A271, 357-78 (1963).
- Bamford (1968) - C.H. Bamford, A. Bibby, G.C. Eastmond,  
Polymer, 9, 629-61 (1968).
- Bamford (1969) - C.H. Bamford, G.C. Eastmond, Quart. Rev.,  
23, 271-99 (1969).
- Baughman (1974) - R.H. Baughman, J. Polym. Sci., Polym. Phys.,  
12, 1511-35 (1974).

- Bensasson (1963) - R. Bensasson, M. Durup, A. Dworkin, M. Magat, R. Marx, H. Szwarc, *Farad. Soc. Disc.*, 36, 177-85 (1963).
- Butiagin (1972) - P. Ju. Butiagin, *Pure Appl. Chem.*, 30, 54-76 (1972).
- Carrington (1967) - Carrington, McLachlan, *Introduction to Magnetic Resonance*, Harper and Row (1967).
- Chachaty (1972a) - A. Forchioni, C. Chachaty, *J. Polym. Sci.*, A-1, 10, 1905-22 (1972).
- Chachaty (1972b) - A. Forchioni, C. Chachaty, *J. Polym. Sci.*, A-1, 10, 1923-43 (1972).
- Chachaty (1973) - B. Ban, C. Chachaty, *Can. J. Chem.*, 51, 3889-3900 (1973).
- Chachaty (1975) - C. Chachaty, M. Latimier, A. Forchioni, *J. Polym. Sci. Polym. Chem.*, 13, 189-99 (1975).
- Chapiro (1972) - A. Chapiro, *Israel J. Chem.*, 10, 129-41 (1972).
- Chatany (1963) - Y. Chatany, Y. Sakata, I. Nitta, *J. Polym. Sci.*, 1, 419-21, (1963).
- Claes (1973) - D. Mauer, B. Tilquin, P. Claes, *Bull. Soc. Chim. Belg.*, 82, 693-98 (1973).
- Costaschuck (1969) - Personal communication.
- Costaschuck (1970) - Ph.D. Thesis - McGill University.
- Dmitrieva (1964) - L.V. Dmitrieva, V.V. Moskalev, *Sov. Phys. Solid State*, 5, 1623-24 (1964).
- Eastmond (1970) - G.C. Eastmond, *Solid-State Polymerization, in Progress in Polymer Science*, Jenkins Ed., Vol. 2, pp. 1-46, Pergamon Press (1970).

- Eastmond (1971) - B. Arnold, G.C. Eastmond, Farad. Soc. Trans., 67, 772-85 (1971).
- Eastmond (1973) - G.C. Eastmond, Polym. J., 4, 392-400, (1973).
- Farad (1959) - Crystal Imperfections and Chemical Reactivity of Solids, Disc. Farad. Soc., 28 (1959).
- Fried (1973) - F. Fried, Mol. Cryst. Liq. Cryst., 20, 1-12 (1973).
- Galwey (1967) - A.K. Galwey, Chemistry of Solids, Chapman and Hall (1967).
- Garner (1955) - W.E. Garner, Chemistry of the Solid State, Butterworths (1955).
- Gol'danskii (1971a) - A.I. Bol'shakov, V.P. Mel'nikov, A.I. Mikhailov, I.M. Barkalov, V.I. Gol'danskii, High En. Chem., 5, 47-51 (1971).
- Gol'danskii (1971b) - A.M. Kaplan, A.I. Mikhailov, D.P. Kiryouchin, I.M. Barkalov, V.I. Gol'danskii, Proc. Tihany Symp. Radiat. Chem., 3rd Tihany, Hung. (1971), pp. 485-9
- Gol'danskii (1971c) - A.I. Mikhailov, A.I. Bol'shakov, I.M. Barkalov, V.I. Gol'danskii, Proc. Tihany<sup>\*</sup> Symp. Radiat. Chem., 3rd Tihany, Hung. (1971), pp. 493-501.
- Gol'danskii (1972) - A.I. Bol'shakov, A.I. Mikhailov, I.M. Barkalov, V.I. Gol'danskii, Doklady Phys. Chem., 205, 594-97 (1972).
- Grabar (1964) - C.S. Hsia, D.G. Grabar, J. Polym. Sci., C, 4, 849-68 (1964).
- Gutowsky (1950) - H.S. Gutowsky, G.E. Pake, J. Chem. Phys., 18, 162-70 (1950).

- Hannay (1967) - N.B. Hannay, Solid State Chemistry, Prentice Hall (1967).
- Hedvall (1966) - J.A. Hedvall, Solid State Chemistry, Elsevier (1966).
- Higgs (1963) - M.A. Higgs, R. Sass, Acta. Cryst., 16, 657-61, (1963).
- Kargin (1960) - V.A. Kargin, V.A. Kabanov, G.P. Andrianova, Polym. Sci. U.S.S.R., 1, 106-14 (1960).
- Kargin (1962) - V.A. Kargin, V.A. Kabanov, N. Ya. Rapaport-Molodtsova, Polym. Sci. U.S.S.R., 3, 657-64 (1962).
- Kargin (1965) - I.M. Papisov, V.A. Kabanov, V.A. Kargin, Doklady Phys. Chem., 162, 369-72 (1965).
- Kargin (1966) - V.A. Kabanov, I.M. Papisov, V.A. Kargin, Polym. Sci. U.S.S.R., 8, 1797-1805 (1966).
- Kargin (1967) - M. Azori, N.A. Plate, V.A. Kargin, Proc. Tihany Symp. Radiat. Chem., 2nd Tihany, Hung., (1967), pp. 547-53.
- Kittel (1966) - C. Kittel, Introduction to Solid State Physics, Wiley (1966).
- Komaki (1963) - A. Komaki, T. Matsuoto, J. Polym. Sci., B, 1, 671-73 (1963).
- Laing (1968) - M. Laing, E. Horsefield, Chem. Comm., 735 (1968).
- Lando (1972) - J.B. Lando, J. Semen, J. Polym. Sci. Polym. Chem., 10, 3003-16 (1972).
- Lebedev (1964) - A.I. Mikhailov, Ya. S. Lebedev, N.Ya. Buben, Kinet. and Catalysis, 5, 901-07 (1964).

- Lebedev (1967) - Ya. S. Lebedev, *Kinet. and Catalysis*, 8,  
2, 213-18 (1967).
- Martin (1972) - Strong materials, J. W. Martin, The Wykenham  
Science Press (1972).
- Marx (1963) - R. Bensasson, A. Bernas, M. Bodard, R. Marx,  
*J. Chim. Phys.*, 60, 950-56 (1963).
- Marx (1965) - R. Marx, D. Tchiboukdjian, *J. Chim. Phys.*, 62,  
1102-06 (1965).
- Marx (1966) - R. Marx, *J. Chim. Phys.*, 62, 128-36 (1966).
- McBrierty (1974) - V.J. McBrierty, *Polym.*, 15, 503-20 (1974).
- McCall (1960) - D.W. McCall, D.C. Douglas, *J. Chem. Phys.*, 33,  
777-78 (1960).
- Mesrobian (1954) - R.B. Mesrobian, R. Ander, D.S. Ballantine,  
G.J. Dienes, *J. Chem. Phys.*, 22, 565 (1954).
- Morawetz (1960) - T.A. Fadner, H. Morawetz, *J. Polym. Sci.*,  
15, 475-501 (1960).
- Morawetz (1962) - H. Morawetz, I.D. Rubin, *J. Polym. Sci.*,  
57, 669-86 (1962).
- Morawetz (1964) - S.Z. Jakabhazy, H. Morawetz, N. Morosoff,  
*J. Polym. Sci., C*, 4, 805-26 (1964).
- Morawetz (1965) - N. Morosoff, H. Morawetz, B. Post, *J. Amer.*  
*Chem. Soc.*, 87, 3035-40 (1965).
- Moriuchi (1970) - S. Moriuchi N. Nakamura, S. Shimada,  
H. Kashiwabara, J. Sohma, *Polym.*, 11, 630-39 (1970).
- Nakanishi (1972) - H. Nakanishi, M. Hasegawa, Y. Sasada,  
*J. Polym. Sci., A-2*, 10, 1537-53 (1972).

- Odajima (1961) - A. Odajima, A.E. Woodward, J.A. Sauer,  
J. Polym. Sci., 55, 181-96 (1961).
- O'Donnell (1964) - J.H. O'Donnell, B. McGarvey, H. Morawetz,  
J. Am. Chem. Soc., 86, 2322-25 (1964).
- O'Donnell (1970) - J.H. O'Donnell, D.F. Sangster, Principles  
of Radiation Chemistry, Elsevier (1970).
- Okamura (1960) - S. Okamura, K. Hayashi, Y. Nakamura,  
Isotopes and Radiation, 3, 416-509 (1960).
- Onishi (1963) - Y. Shioji, S. Onishi, I. Nitta, J. Polym.  
Sci., A, 1, 3373-84 (1963).
- Purcell (1948) - N. Bloembergen, E.M. Purcell, R.V. Pound,  
Phys. Rev., 73, 679-712 (1948).
- Reneker (1974) - D.H. Reneker, G.M. Martin, M.G. Broadhurst,  
J. Appl. Phys., 45, 4172-74 (1974).
- Schmidt (1964) - F.L. Hirschfeld, G.M.J. Schmidt, J. Polym.  
Sci., A, 2, 2181-90 (1964).
- Schwab (1965) - G.M. Schwab, Ed., Reactivity of Solids,  
Butterworths (1965).
- Sella (1961) - C. Sella, J.J. Trillat, Compt. Rend., 253,  
1511-13 (1961).
- Sella (1962) - C. Sella, R. Bensasson, J. Polym. Sci., 56,  
51-54 (1962).
- Shepp (1956) - A. Shepp, J. Chem. Phys., 24, 939-43 (1956).
- Smith (1965) - G.W. Smith, J. Chem. Phys., 42, 4229-43 (1965).
- Swallow (1973) - Radiation Chemistry, A.J. Swallow, Halsted  
Press, Wiley (1973).

- Szwarc (1962) - H. Szwarc, Thesis, Paris (1965).
- Thomas (1967) - J.M. Thomas, J.O. Williams, Trans. Faraday Soc., 63, 1922-28 (1967).
- Thomas (1969) - J.M. Thomas, J.O. Williams, Mol. Cryst. Liq. Cryst., 9, 59-79 (1969).
- Thomas (1971) - J.M. Thomas, J.O. Williams, in Progress in Solid State Chemistry, H. Reiss and J.O. McCaldin Eds., Pergamon Press, New York (1971) p. 119-54.
- Tolkachev (1970a) - V.A. Tolkachev, I.B. Sokolov, V.I. Kovalevskii, High En. Chem., 4, 407-08 (1970).
- Tolkachev (1970b) - V.A. Tolkachev, V.I. Kovalevskii, Russ. J. Phys. Chem., 44, 768 (1970).
- Tolkachev (1971) - V.A. Tolkachev, Proc. Tihany Symp. Radiat. Chem., 3rd Tihany, Hung., (1971) pp. 441-51.
- Ukaji (1959) - T. Ukaji, Bull. Chem. Soc. Japan., 32, 1266-70 (1959).
- Van Vleck (1948) - J.H. Van Vleck, Phys. Rev., 74, 1168-83 (1948).
- Voigt-Martin (1974) - I. Voigt-Martin, Makromol. Chem., 175, 2669-86 (1974).
- Waite (1957) - T.R. Waite, Phys. Rev., 107, 463-70 (1957).
- Waite (1958) - T.R. Waite, J. Chem. Phys., 28, 103-06 (1958).
- Waugh (1963) - J.S. Waugh, E.I. Fedin., Soviet Phys.-Solid State, 4, 1633-36 (1963).
- Wegner (1972) - J. Kaiser, G. Wegner, E.W. Fischer, Israel J. Chem., 10, 157-71 (1972).
- Wegner (1973a) - B. Keggenhoff, G. Wegner, J. Polym. Sci., B, 11, 759-68 (1973).

Wegner (1973b) - B. Keggenhoff, G. Wegner, J. Polym. Sci., B,  
( ) 11, 769-84 (1973).

Weiss (1956) - J. Weiss, E.O. Allen, H.A. Schwarz, Proc.  
Intern. Conf. Peaceful Uses Atomic Energy, United Nations,  
New York, 14, 179-81 (1956).

Wintle (1972) - H.J. Wintle, Radiat. Chem. Macromol., Vol. 1,  
93-107, M. Dole Ed., Academic Press (1972).

Young (1966) - D.A. Young, Decomposition of Solids, Pergamon  
Press (1966).

APPENDICES

## APPENDIX A - TABLES

TABLE (A-1): Polymerization of  
K acrylate at 313 K - Data for  
Fig. (III-1) -

<u>logt (s)</u>	<u>Y (%)</u>
2.99	10.28
3.57	14.90
4.09	18.45
4.51	21.58
5.01	27.80
5.50	29.08
6.02	34.12

TABLE (A-2): Polymerization of  
K acrylate at 323 K - Data for  
Fig. (III-1) -

<u>logt (s)</u>	<u>Y (%)</u>
3.08	20.22
3.58	21.77
4.04	23.60
4.57	23.83
5.00	26.95
5.48	27.74
6.19	30.84

TABLE (A-3): Polymerization of  
K acrylate at 333 K - Data for  
Fig. (III-2) -

<u>logt (s)</u>	<u>Y (%)</u>
3.02	13.62
3.60	20.50
4.01	22.38
4.53	26.24
5.00	26.38
5.50	30.06

TABLE (A-4): Polymerization of  
K acrylate at 353 K - Data for  
Fig. (III-2) -

<u>logt (s)</u>	<u>Y (%)</u>
3.07	20.12
3.60	22.32
4.08	24.46
4.52	26.79
5.00	30.90
5.48	32.31
6.04	39.04

TABLE (A-5): Temperature dependence of  $dY/d\log t$  for K. acrylate - Data for Fig. (III-3) -

<u>Temperature/K</u>	<u><math>dY/d\log t</math> (<math>s^{-1}</math>)</u>
273	$4.79 \pm 0.52$
298	$5.11 \pm 0.25$
308	$5.34 \pm 1.07$
313	$6.05 \pm 0.49$
323	$3.43 \pm 0.66$
333	$5.48 \pm 0.86$
353	$6.14 \pm 0.51$
373	$5.55 \pm 0.36$

TABLE (A-6): Polymerization of  
Li acrylate at 374 K - Data for  
Fig. (III-4) -

<u>Time/s</u>	<u>logt (s)</u>	<u>Y (%)</u>
$6.92 \times 10^3$	3.84	1.11
$1.55 \times 10^4$	4.19	1.66
$2.82 \times 10^4$	4.45	1.70
$9.33 \times 10^4$	4.97	1.97
$2.57 \times 10^5$	5.41	3.63

TABLE (A-7): Polymerization of  
Li acrylate at 405 K - Data for  
Fig. (III-4) -

<u>Time/s</u>	<u>logt (s)</u>	<u>Y (%)</u>
$4.47 \times 10^3$	3.65	1.85
$8.32 \times 10^3$	3.92	3.57
$1.70 \times 10^4$	4.23	3.69
$3.31 \times 10^4$	4.52	3.39

TABLE (A-8): Polymerization of  
Na acrylate at 393 K - Data for  
Fig. (III-5) -

<u>Time/s</u>	<u>logt (s)</u>	<u>Y (%)</u>
$3.95 \times 10^3$	3.60	0.77
$1.15 \times 10^4$	4.06	1.38
$3.09 \times 10^4$	4.49	1.69
$8.13 \times 10^4$	4.91	2.92
$1 \times 10^5$	5.00	3.23

TABLE (A-9): Polymerization of  
Na acrylate at 403 K - Data for  
Fig. (III-5) -

<u>Time/s</u>	<u>logt (s)</u>	<u>Y (%)</u>
$6.2 \times 10^3$	3.84	1.84
$1.15 \times 10^4$	4.06	2.00
$2.75 \times 10^4$	4.44	2.77
$8.51 \times 10^4$	4.93	3.69

TABLE (A-10): Polymerization of K acrylate at 273 K -  
Data for Fig. (III-6) -

<u>Time/s</u>	<u>logt (s)</u>	<u>Y (%)</u>
$7.09 \times 10^3$	3.85	2.20
$2.30 \times 10^4$	4.36	3.10
$9.78 \times 10^4$	4.99	5.30
$2.40 \times 10^5$	5.38	9.40

TABLE (A-11): Polymerization of K acrylate at 323 K -  
Data for Fig. (III-7) -

<u>Time/s</u>	<u>logt (s)</u>	<u>Y (%)</u>
$3 \times 10^2$	2.48	4.32
$6 \times 10^2$	2.78	5.43
$9 \times 10^2$	2.95	8.61
$1.5 \times 10^3$	3.18	10.91
$2.4 \times 10^3$	3.38	13.60
$1.26 \times 10^4$	4.10	15.49
$2.75 \times 10^5$	5.44	21.89

( )  
 TABLE (A-12): Temperature dependence of  $dY/dt$  for K  
 acrylate - Data for Fig. (III-8) -

<u>Temperature/K</u>	<u><math>(dY/dt)/(s \times 10^{-4})</math></u>
273	0.5 ± 0.02
298	3.69 ± 1.06
313	7.94 ± 1.53
323	11.47 ± 1.47
333	13.08 ± 2.67
353	14.31 ± 3.00

TABLE (A-13): Effect of one hour of prepolymerization  
 at 353 K on the polymerization of K acrylate at 313 K -  
 Data for Fig. (III-9) -

<u>logt (s)</u>	<u>Y (%)</u>	<u>Prepolymerization at 353 K</u>
4.03	7.55	No
4.57	11.04	No
4.92	11.40	No
5.53	14.18	No
4.57	15.40	Yes
4.94	15.14	Yes
5.53	15.26	Yes

TABLE (A-14): Temperature dependence of the linewidth and second moment of Li acrylate - Data for Fig. (III-11) -

<u>Temperature/K</u>	<u>Linewidth/G</u>	<u>Second moment/G<sup>2</sup></u>
77.0	10.5	9.7 ± 0.1
104.0	10.3	
151.2	10.2	
219.0	9.7	10.0 ± 0.2
235.7	9.7	10.6 ± 0.4
295.2	8.7	9.7 ± 0.5
353.2	8.6	8.0 ± 0.3
379.0	8.0	
409.0	7.6	
424.0	7.2	
439.0	7.9	6.3 ± 0.7

TABLE (A-15): Temperature dependence of the linewidth and second moment of Na acrylate - Data for Fig. (III-12) -

<u>Temperature/K</u>	<u>Linewidth/G</u>	<u>Second moment/G<sup>2</sup></u>
77.0	10.8	9.8 ± 0.6
144.0	9.8	
169.0	9.9	10.3 ± 0.1
221.0	10.0	
234.3	9.7	9.7 ± 1.0
297.5	8.9	9.1 ± 1.2
324.3		9.8 ± 0.9
346.2	8.2	8.7 ± 1.0
402.1		8.1 ± 0.6
426.3	8.1	8.1 ± 0.5

( ) TABLE (A-16): Temperature dependence of the linewidth and second moment of K acrylate - Data for Fig. (III-13) -

<u>Temperature/K</u>	<u>Linewidth/G</u>	<u>Second moment/G<sup>2</sup></u>
77.0	9.8	9.7 ± 1.2
119.5	9.5	9.6 ± 1.5
170.0	8.9	9.4 ± 0.4
193.0		9.4 ± 0.7
249.8	7.4	8.8 ± 2.2
266.5	7.6	7.6 ± 1.4
279.5	7.4	
292.0	7.6	7.2 ± 0.7
310.0	7.7	6.5 ± 0.3
314.5	7.9	
320.0		6.8 ± 0.6
325.0	7.2	5.7 ± 0.4
334.0	7.1	5.3 ± 0.6
337.0	5.0	5.0 ± 0.5
339.5	4.4	3.5 ± 0.4
340.0	4.4	4.4 ± 0.3
342.0	4.8	
343.0	5.3	
345.0	3.2	3.0 ± 1.0
347.0	3.9	
349.0	2.8	
351.0	2.8	2.0 ± 0.4

TABLE (A-16): (cont'd)

<u>Temperature/K</u>	<u>Linewidth/G</u>	<u>Second moment/G<sup>2</sup></u>
353.0	2.8	2.0 ± 0.7
355.0	2.9	2.2 ± 0.5
360.0	2.7	2.1 ± 0.3
371.0	2.9	
372.0	2.9	
378.0	2.7	1.8 ± 0.2
386.0	2.9	
396.0	2.8	1.8 ± 0.4
404.0	2.7	

TABLE (A-17): Temperature dependence of the linewidth  
and second moment of Rb acrylate - Data for Fig. (III-14) -

<u>Temperature/K</u>	<u>Linewidth/G</u>	<u>Second moment/G<sup>2</sup></u>
77.0	9.8	9.9 ± 0.7
113.5	9.5	
149.0	9.9	10.0 ± 0.4
223.0	10.2	
233.0	9.6	10.0 ± 1.5
284.0	8.7	9.3 ± 0.4
295.0	8.8	
309.0	8.7	9.0 ± 0.2
310.0	8.7	6.5 ± 0.3
313.0	8.9	
318.0	5.2	3.5 ± 0.4
318.0	9.0	9.0 ± 0.5
323.6	5.5	6.2 ± 0.8
324.8	5.2	
326.1		3.1 ± 0.5
342.5	5.2	3.8 ± 0.1
392.0	5.0	4.1 ± 0.5
433.0	4.7	3.8 ± 0.6
466.0	3.8	

TABLE (A-18): Decay of Li acrylate radicals at 353 K -  
Data for Fig. (III-19) -

Cation	$[R\cdot]_0/(\text{radicals} \times \text{kg} \times 10^{19})$	$[R\cdot]_\infty/(\text{radicals} \times \text{kg} \times 10^{19})$	$F_\infty = [R\cdot]_\infty/[R\cdot]_0$	Temperature/K
Li	1.86	1.29	0.67	353
Time/(s $\times 10^3$ )	$[R\cdot]/[R\cdot]_0 = F$	Time/(s $\times 10^3$ )	$[R\cdot]_\infty/[R\cdot]_0 = F$	
$2.52 \times 10^{-1}$	0.90	2.09	0.85	
$2.88 \times 10^{-1}$	0.99	2.34	0.84	
$3.60 \times 10^{-1}$	0.90	2.52	0.85	
$4.32 \times 10^{-1}$	0.98	3.42	0.77	
$4.68 \times 10^{-2}$	0.88	3.71	0.74	
$8.28 \times 10^{-1}$	0.77	11.84	0.67	
1.01	0.84	30.50	0.66	
1.15	0.81	80.39	0.66	
1.26	0.76	133.09	0.68	
1.33	0.84	361.30	0.68	
1.44	0.84	444.17	0.68	

TABLE (A-19): Decay of Li acrylate radicals at 423 K -  
 Data for Fig. (III-20) -

Cation	$[R\cdot]_0 / (\text{radicals} \times \text{kg} \times 10^{19})$	Temperature/K
Li	1.58	4.23
Time/(s $\times 10^3$ )	$[R\cdot] / [R\cdot]_\infty$	
5.76 $\times 10^{-1}$	1.09	
1.87	1.01	
3.67	1.07	
5.72	1.06	
13.97	1.00	
69.55	1.00	

TABLE (A-20): Decay of Na acrylate radicals at 353 K -  
Data for Fig. (III-21) -

Cation	$[R\cdot]_0 / (\text{radicals} \times \text{kg} \times 10^{19})$	$[R\cdot]_{\infty} / (\text{radicals} \times \text{kg} \times 10^{19})$	Temperature/K
Na	0.88	0.69	353
Time/(s $\times 10^3$ )	$[R\cdot] / [R\cdot]_0 = F$	Time/(s $\times 10^3$ )	$[R\cdot] / [R\cdot]_0 = F$
$4.32 \times 10^{-1}$	0.99	84.85	0.87
1.15	0.98	85.14	0.80
1.19	0.98	85.75	0.86
1.80	0.96	103.57	0.80
4.57	0.94	189.97	0.80
5.15	0.95	344.77	0.83
6.01	0.89	368.03	0.80
6.55	0.96	453.64	0.77
17.71	0.90	454.07	0.80
20.63	0.83		

TABLE (A-21): Decay of Na acrylate radicals at 423 K -

Data for Fig. (III-22) -

Cation	$[R\cdot]_0 / (\text{radicals} \times \text{kg} \times 10^{19})$	$[R\cdot]_\infty / (\text{radicals} \times \text{kg} \times 10^{19})$	$F_\infty = [R\cdot]_\infty / [R\cdot]_0$	Temperature/K
Na	3.36	1.21	0.36	423
Time/(s $\times 10^3$ )	$[R\cdot] / [R\cdot]_0 = F$	Time/(s $\times 10^3$ )	$[R\cdot] / [R\cdot]_0 = F$	
2.52 $\times 10^{-1}$	0.96	5.51	0.63	
6.12 $\times 10^{-1}$	0.82	5.83	0.65	
8.28 $\times 10^{-1}$	0.73	6.05	0.60	
1.01	0.77	6.55	0.61	
1.19	0.73	6.77	0.61	
1.37	0.76	6.95	0.63	
1.62	0.68	9.43	0.57	
1.98	0.69	11.34	0.56	
2.27	0.67	11.52	0.52	
2.88	0.68	17.1	0.47	
3.17	0.68	70.34	0.46	
3.67	0.63			
4.14	0.63			
4.68	0.63			

TABLE (A-22): Decay of K acrylate radicals at 313. K -  
 Data for Fig. (III-23) -

Cation	$[R\cdot]_0/(\text{radicals} \times \text{kg} \times 10^{19})$	$[R\cdot]_{\infty}/(\text{radicals} \times \text{kg} \times 10^{19})$	$F_{\infty} = [R\cdot]_{\infty}/[R\cdot]_0$	Temperature/K
K	1.90	1.08	0.57	313
Time/(s $\times 10^3$ )	$[R\cdot]/[R\cdot]_0 = F$	Time/(s $\times 10^3$ )	$[R\cdot]/[R\cdot]_0 = F$	
2.88 $\times 10^{-1}$	0.85	2.81	0.63	
4.68 $\times 10^{-1}$	0.78	6.23	0.62	
7.92 $\times 10^{-1}$	0.76	10.44	0.62	
1.26	0.75	14.76	0.57	
1.51	0.71	26.39	0.58	
1.87	0.71	31.20	0.56	
2.27	0.68	34.85	0.56	

TABLE (A-23): Decay of K acrylate radicals at 323 K -

Data for Fig. (III-23) -

Cation	$[R\cdot]_0 / (\text{radicals } \times \text{kg} \times 10^{19})$	$[R\cdot]_{\infty} / (\text{radicals } \times \text{kg} \times 10^{19})$	$F_{\infty} = [R\cdot]_{\infty} / [R\cdot]_0$	Temperature/K
K	2.42	1.54	0.64	323
Time/(s $\times 10^3$ )	$[R\cdot] / [R\cdot]_0 = F$	Time/(s $\times 10^3$ )	$[R\cdot] / [R\cdot]_0 = F$	
1.44 $\times 10^{-1}$	0.99	17.35	0.76	
3.60 $\times 10^{-1}$	0.95	19.51	0.71	
7.92 $\times 10^{-1}$	0.97	28.98	0.66	
1.44	0.96	31.93	0.69	
2.09	0.92	34.20	0.67	
4.39	0.91	36.18	0.67	
6.19	0.86			
7.38	0.87			
8.72	0.86			
10.19	0.82			
12.24	0.78			
14.47	0.76			

TABLE (A-24): Decay of K acrylate radicals at 353 K -  
Data for Fig. (III-23) -

Cation $[R\cdot]_0$ /(radicals $\times \text{kg} \times 10^{19}$ )	$[R\cdot]_\infty$ /(radicals $\times \text{kg} \times 10^{19}$ )	$F_\infty = [R\cdot]_\infty / [R\cdot]_0$	Temperature/K
K	1.72	0.87	353
Time/(s $\times 10^3$ )	$[R\cdot] / [R\cdot]_0 = F$	Time/(s $\times 10^3$ )	$[R\cdot] / [R\cdot]_0 = F$
6.12 $\times 10^{-1}$	0.81	9.43	0.52
9.72 $\times 10^{-1}$	0.78	9.97	0.51
1.26	0.71	10.51	0.49
1.73	0.63	12.13	0.50
1.87	0.67	19.66	0.47
2.45	0.67	24.73	0.52
3.49	0.63	37.08	0.48
5.94	0.58		

TABLE (A-25): Decay of Rb acrylate radicals at 303 K -  
Data for Fig. (III-24) -

Cation $[R\cdot]_0/(\text{radicals } [R\cdot]_0/(\text{radicals } F_\infty = [R\cdot]_\infty/[R\cdot]_0$ Temperature/K			
$x \text{ kg } x 10^{19}$	$x \text{ kg } x 10^{19}$		
Rb	3.34		
	2.60		
	0.78		
	303		
Time/(s $\times 10^3$ )	$[R\cdot]/[R\cdot]_0 = F$	Time/(s $\times 10^3$ )	$[R\cdot]/[R\cdot]_0 = F$
$1.44 \times 10^{-1}$	0.94	3.53	0.78
$4.32 \times 10^{-1}$	0.84	3.89	0.78
$6.48 \times 10^{-1}$	0.82	4.25	0.79
$8.64 \times 10^{-1}$	0.81	9.54	0.77
1.12	0.81	12.60	0.78
1.37	0.78	16.13	0.79
1.62	0.77	19.62	0.78
1.84	0.77	23.40	0.77
2.12	0.77	23.83	0.79
2.45	0.78	29.52	0.75
2.81	0.79	36.11	0.76
3.06	0.79		

TABLE (A-26): Decay of Rb acrylate radicals at 313 K - Data for Fig. (III-24) -

Cation	$[R\cdot]_0 / (\text{radicals} \times \text{kg} \times 10^{19})$	$[R\cdot]_{\infty} / (\text{radicals} \times \text{kg} \times 10^{19})$	$F_{\infty} = [R\cdot]_{\infty} / [R\cdot]_0$	Temperature/K	
RB	4.22	2.52	0.60	313	
Time/(s $\times 10^3$ )	$F = [R\cdot] / [R\cdot]_0$	Time/(s $\times 10^3$ )	$F = [R\cdot] / [R\cdot]_0$	Time/(5 $\times 10^3$ )	$F = [R\cdot] / [R\cdot]_0$
$5.40 \times 10^{-1}$	0.86	2.95	0.69	25.02	0.60
$8.28 \times 10^{-1}$	0.83	4.14	0.70	26.93	0.59
1.08	0.79	6.08	0.68	31.21	0.58
1.44	0.75	9.00	0.64	34.45	0.58
1.69	0.73	12.71	0.63		
1.87	0.72	16.56	0.62		
2.23	0.71	19.51	0.60		

TABLE (A-27): Decay of Rb acrylate radicals at 353 K -  
Data for Fig. (III-24) -

Cation $[R\cdot]_0$ / (radicals $[R\cdot]_\infty$ / (radicals $F_\infty = [R\cdot]_\infty / [R\cdot]_0$ . Temperature / K				
	$\times 10^{19}$ )	$\times 10^{19}$ )		
Rb	3.32	2.39	0.72	353
Time / (s $\times 10^3$ )	$F = [R\cdot] / [R\cdot]_0$	Time / (s $\times 10^3$ )	$F = [R\cdot] / [R\cdot]_0$	
$2.88 \times 10^{-1}$	0.99	7.2	0.76	
$6.48 \times 10^{-1}$	0.94	11.20	0.75	
1.08	0.91	14.65	0.74	
1.55	0.86	18.43	0.72	
2.09	0.85	21.96	0.72	
2.59	0.83	27.58	0.71	
2.95	0.81	32.83	0.71	
3.31	0.81			
4.57	0.80			
5.51	0.76			

TABLE (A-28): Second order decay of Li acrylate radicals  
at 353 K - Data for Fig. (III-25) -

Time/(sx10 <sup>3</sup> )	$\frac{Foc-Fc}{FocFc}$ (dimensionless)	Time/(sx10 <sup>3</sup> )	$\frac{Foc-Fc}{FocFc}$ (dimensionless)
2.52 x 10 <sup>-1</sup>	1.54	1.15	5.11
2.88 x 10 <sup>-1</sup>	0.11	1.26	3.02
3.60 x 10 <sup>-1</sup>	1.54	1.33	3.44
4.32 x 10 <sup>-1</sup>	0.22	1.44	3.44
4.68 x 10 <sup>-1</sup>	2.04	2.09	3.02
8.28 x 10 <sup>-1</sup>	0.62	2.34	3.44
1.01	3.44	2.52	3.02
		3.42	9.27
		3.71	16.77

TABLE (A-29): Second order decay of Na acrylate radicals  
at 353 K - Data for Fig. (III-26) -

Time/(sx10 <sup>3</sup> )	$\frac{Foc-Fc}{FocFc}$ (dimensionless)	Time/(sx10 <sup>3</sup> )	$\frac{Foc-Fc}{FocFc}$ (dimensionless)
4.32 x 10 <sup>-1</sup>	0.20	6.01	3.99
1.15	0.41	6.55	0.92
1.19	0.41	17.71	3.34
1.80	0.92	20.63	12.32
4.57	1.53	35.28	5.01
5.15	1.21	85.14	28.99

TABLE (A-30): Second order decay of Na acrylate radicals  
at 423 K - Data for Fig. (III-27) -

Time/(sx10 <sup>3</sup> )	$\frac{F_0 - F_c}{F_0 F_c}$ (dimensionless)	Time/(sx10 <sup>3</sup> )	$\frac{F_0 - F_c}{F_0 F_c}$ (dimensionless)
2.52 x 10 <sup>-1</sup>	0.10	4.14	2.14
6.12 x 10 <sup>-1</sup>	0.61	4.68	2.14
8.28 x 10 <sup>-1</sup>	1.14	5.51	2.14
1.01	0.88	5.83	1.89
1.19	1.14	6.05	2.60
1.37	0.94	6.55	2.44
1.62	1.56	6.95	2.64
1.98	1.47	11.34	3.43
2.27	1.66	11.52	4.69
3.17	1.77	17.10	7.53
3.67	2.14		

TABLE (A-31): Second order decay of K acrylate radicals  
at 313 K - Data for Fig. (III-28) -

Time/(sx10 <sup>3</sup> )	$\frac{Foc-Fc}{FocFc}$ (dimensionless)	Time/(sx10 <sup>3</sup> )	$\frac{Foc-Fc}{FocFc}$ (dimensionless)
2.88 x 10 <sup>-1</sup>	1.25	2.27	6.77
4.68 x 10 <sup>-1</sup>	2.44	2.81	14.34
1.01	2.67	6.23	17.67
1.26	3.25		
1.51	4.82		
1.87	4.82		

TABLE (A-32): Second order decay of K acrylate radicals  
at 323 K - Data for Fig. (III-28) -

Time/(sx10 <sup>3</sup> )	$\frac{Foc-Fc}{FocFc}$ (dimensionless)	Time/(sx10 <sup>3</sup> )	$\frac{Foc-Fc}{FocFc}$ (dimensionless)
1.44 x 10 <sup>-1</sup>	0.08	3.35	0.79
3.60 x 10 <sup>-1</sup>	0.45	4.39	0.93
7.92 x 10 <sup>-1</sup>	0.25	6.19	1.77
1.44	0.35	7.38	1.57
2.09	0.79	8.71	1.77
2.74	0.67	10.19	2.78

TABLE (A-33): Second order decay of K acrylate radicals  
at 353 K - Data for Fig. (III-28) -

Time/(sx10 <sup>3</sup> )	$\frac{Foc-Fc}{FocFc}$ (dimensionless)	Time/(sx10 <sup>3</sup> )	$\frac{Foc-Fc}{FocFc}$ (dimensionless)
6.12 x 10 <sup>-1</sup>	1.30	1.87	4.21
8.64 x 10 <sup>-1</sup>	1.96	2.45	4.21
1.26	2.96	3.49	6.30
1.73	6.30	5.94	12.24

TABLE (A-34): Second order decay of K acrylate radicals  
at 373 K - Data for Fig. (III-28) -

Time/(sx10 <sup>3</sup> )	$\frac{Foc-Fc}{FocFc}$ (dimensionless)	Time/(sx10 <sup>3</sup> )	$\frac{Foc-Fc}{FocFc}$ (dimensionless)
1.44 x 10 <sup>-1</sup>	0.84	6.84 x 10 <sup>-1</sup>	7.41
3.24 x 10 <sup>-1</sup>	2.96	9.00 x 10 <sup>-1</sup>	12.96
5.04 x 10 <sup>-1</sup>	7.41	1.44	29.63

TABLE (A-35): Second order decay of Rb acrylate radicals  
at 303 K - Data for Fig. (III-29) -

Time/(sx10 <sup>3</sup> )	$\frac{Foc-Fc}{FocFc}$ (dimensionless)	Time/(sx10 <sup>3</sup> )	$\frac{Foc-Fc}{FocFc}$ (dimensionless)
1.44 x 10 <sup>-1</sup>	1.70	8.64 x 10 <sup>-1</sup>	28.79
4.32 x 10 <sup>-1</sup>	12.12	1.12	28.79
6.48 x 10 <sup>-1</sup>	20.45		

TABLE (A-36): Second order decay of Rb acrylate radicals  
at 313 K - Data for Fig. (III-29) -

Time/(sx10 <sup>3</sup> )	$\frac{Foc-Fc}{FocFc}$ (dimensionless)	Time/(sx10 <sup>3</sup> )	$\frac{Foc-Fc}{FocFc}$ (dimensionless)
5.4 x 10 <sup>-1</sup>	1.35	2.63	6.59
8.28 x 10 <sup>-1</sup>	1.85	2.95	8.61
1.08	2.76	3.24	7.50
1.44	4.17	3.49	8.61
1.69	5.19	6.08	10.00
1.87	5.83	6.12	11.79
2.23	6.59	9.00	22.50

TABLE (A-37): Second order decay of Rb acrylate radicals  
at 353 K - Data for Fig. (III-29) -

Time/(s $\times 10^3$ )	$\frac{F_0 - F_c}{F_0 F_c}$ (dimensionless)	Time/(s $\times 10^3$ )	$\frac{F_0 - F_c}{F_0 F_c}$ (dimensionless)
$2.88 \times 10^{-1}$	0.08	2.52	5.54
$6.48 \times 10^{-1}$	0.90	2.95	7.95
1.08	1.56	3.31	7.95
1.55	3.40	5.51	18.19
2.09	3.97	7.2	20.84
		11.20	30.94

APPENDIX B - A WIDE LINE NMR STUDY OF MOLECULAR MOTIONS  
IN SOLID SULFOLANE

For crystalline substances in general fusion consists in the simultaneous loss of the rotational and long range positional order [Ubbelohde (1957), (1965)]. Plastic and liquid crystals occur respectively when either the loss of rotational order or the loss of long range positional order occurs at a lower temperature [Timmermans (1961)]. Plastic crystals are characterized by isotropic rotation of the molecules about their centres of gravity. This leads in most cases to a cubic or hexagonal structure. The fusion of plastic crystals implies usually only the loss of the long range positional order and is characterized by a very low entropy change [Timmermans (1961), Staveley (1962)]. In the absence of a very rigid definition of a plastic crystal this low entropy change is the main criterion used to identify them.

A transition was detected in solid sulfolane at 288 K, 13 K below its melting point by a variety of experimental methods [Jannelli (1964), (1966), (1968a), (1968b)]. The large change in dielectric constant at this temperature was attributed to the onset of molecular rotation in the solid. An entropy of fusion of 1.1 e.u. suggested that sulfolane could be a plastic crystal above 288 K. A wide-line NMR study was undertaken to determine the nature of

the molecular motion responsible for the transition.

### EXPERIMENTAL

Sulfolane was distilled twice over  $P_2O_5$  under reduced pressure. All the operations were performed in a vacuum-line because the material is very hygroscopic. The melting point of 301.6 K agreed with the literature value. The wide-line NMR spectrometer, the temperature control system and the program used to determine experimental second moments have been described in Chapter II.

High resolution NMR measurements were performed with a Varian HR-60 spectrometer.

### RESULTS

The temperature dependence of the linewidth and second moment is shown in Figs. (B-1) and (B-2). The second moment decreases from  $16.3 \pm 0.6 \text{ G}^2$  at 77 K to  $7.4 \pm 1.1 \text{ G}^2$  between 250 and 288 K through a transition centred at 200 K. The linewidths below and above the transition centred at 200 K are respectively 13.8 G and 8.6 G. Starting from around 250 K a narrow component was observed superimposed on the broad component of the spectrum. At 288 K both the second moment and the linewidth show a transition. Above 288 K only the narrow component of the spectrum is left with a linewidth of 0.2 G and a second moment of  $0.2 \text{ G}^2$ . Between 288 K and 296 K the linewidth, expressed as the half peak height width

Fig. (B-1): Temperature dependence of the linewidth of solid sulfolane

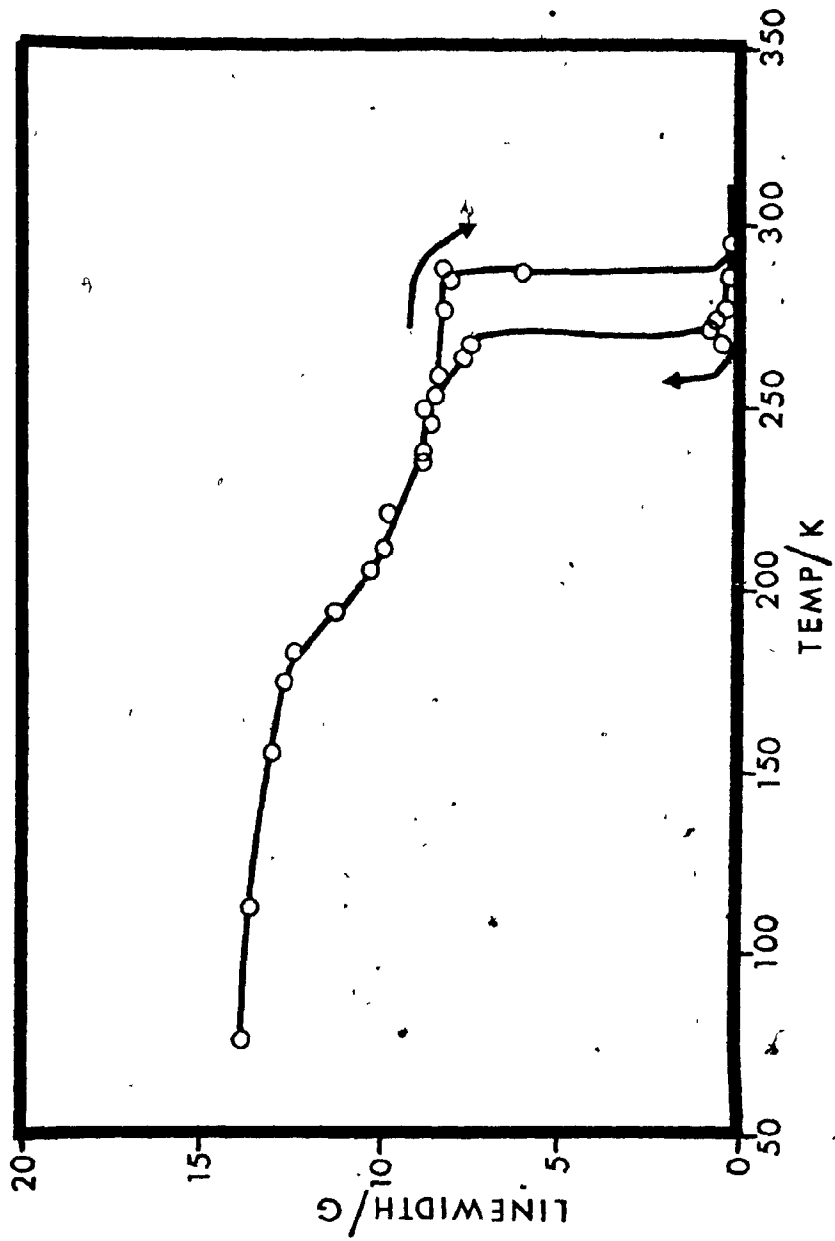
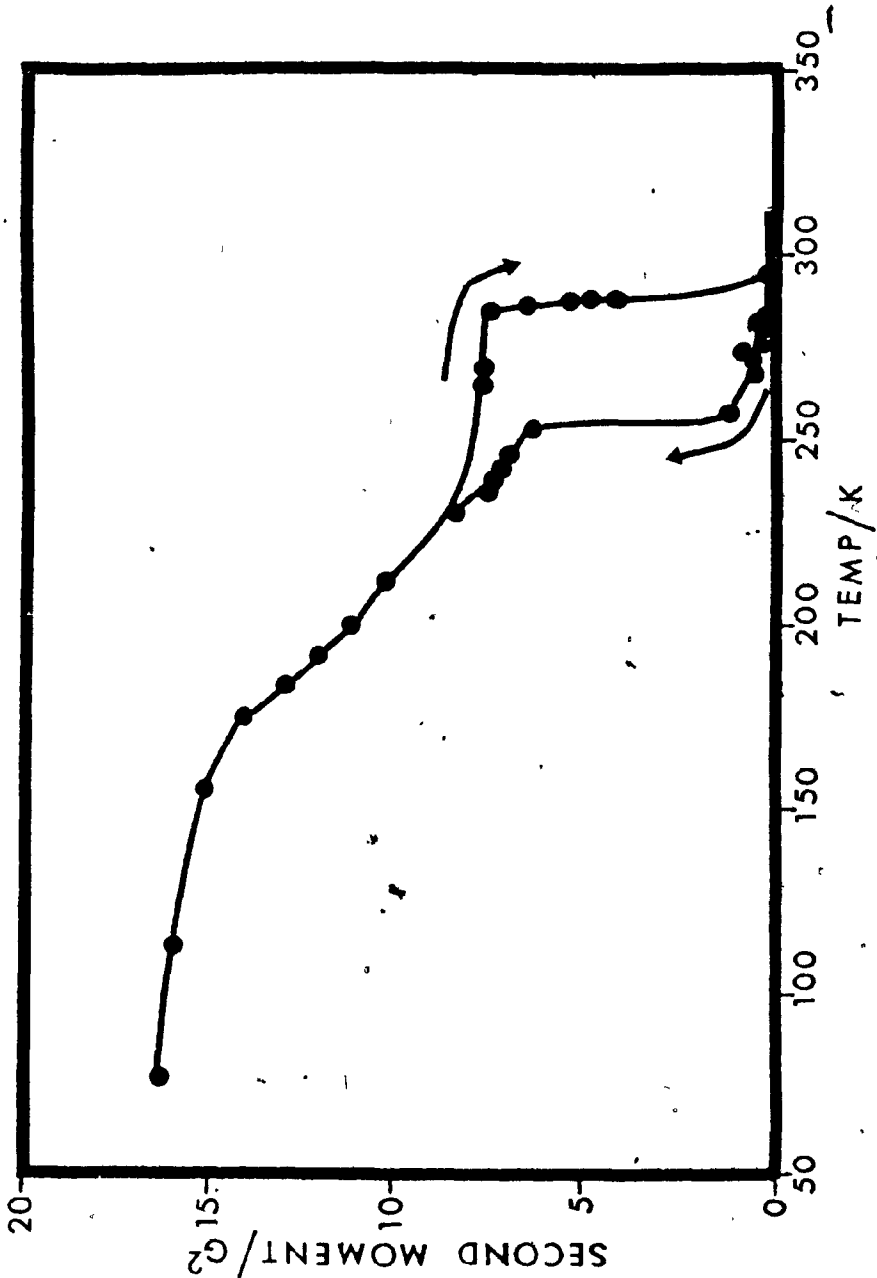


Fig. (B-2): Temperature dependence of the second moment of solid sulfblane



measured by high resolution NMR, remained at 0.2 G decreasing to 0.1 G immediately below the melting point. A hysteresis was found by measuring linewidths and second moments as a function of decreasing temperature: the line did not broaden at 288 K but remained narrow until 267 K. Only for very small samples it was possible to eliminate this hysteresis by cooling very slowly.

### DISCUSSION

The crystal structure of sulfolane is not known. Several measurements of molecular structure have instead been reported. Dipole moment calculations suggest a planar ring structure [Le Fevre (1963)] but infrared and Raman spectroscopic studies [Katon (1964), (1965)] and electron diffraction measurements [Naumov (1973)] indicate a puckered ring. It is however not possible to choose unequivocally between an envelope and a half-chair conformation although the half-chair seems more probable. The following bond lengths and angles, determined by electron diffraction for the half chair conformation, were used to calculate the second moment of sulfolane:

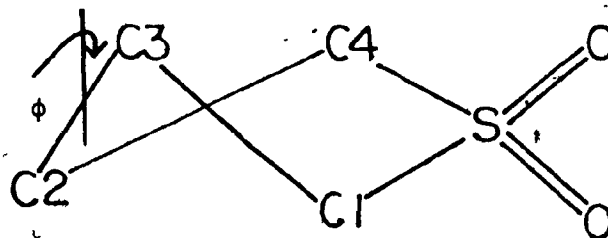
$$C1-C2 = 1.54 \text{ \AA}$$

$$C2-C3 = 1.53 \text{ \AA}$$

$$S=O = 1.45 \text{ \AA}$$

$$C=S = 1.80 \text{ \AA}$$

$$O=S=O = 114.5^\circ$$



$$\text{C-S-C} = 101.1^\circ$$

$$\text{C-C-S} = 104.3^\circ$$

$$\text{C-C-C} = 112.1^\circ$$

$$\phi = 14.3^\circ$$

$$\text{C-S=O} = 110^\circ$$

$$\text{C-H} = 1.10 \text{ \AA}$$

The intramolecular second moment calculated using this set of parameters is  $15.2 \text{ G}^2$ . A value of  $16.6 \text{ G}^2$  was instead obtained using a C-H bond length of  $1.08 \text{ \AA}$ . An approximate value of  $6.5 \pm 0.5 \text{ G}^2$  for the intermolecular second moment was obtained from those of the compounds cyclobutane [Rushworth (1964)], cyclopentane [Rushworth (1954)], cyclohexane [Andrew (1953)] and cyclohexene [Eades (1969)] which possess some structural similarity to sulfolane. A correction was applied where needed for the different proton density per molecule. The total calculated rigid lattice second moment is then  $22.4 \pm 1.2 \text{ G}^2$ . The experimental second moment at 77 K is thus less than the lower estimate of the rigid lattice value.

Three possible motions were considered in order to explain both the low second moment at 77 K and the line narrowing process at 190 K: (i) a ring puckering motion, (ii) re-orientation about the two-fold axis passing through the oxygen atom and the mid-point of the C(2)-C(3) bond, and (iii) re-orientation about the axis perpendicular to the ring. An intramolecular second moment of  $14.9 \pm 0.6 \text{ G}^2$  is obtained in the case of ring puckering by the reduction factor derived

by Andrew and Brookeman [Andrew (1970), (1973)]. The range of values for the intermolecular second moment can be estimated by the maximum and minimum reduction factor of 0.25 and 0.8 given by Smith [Smith (1965)]. A total second moment of  $18.3 \pm 2.4 \text{ G}^2$  is obtained. Therefore ring puckering could be responsible for the low second moment at 77 K. Reduced intramolecular second moments of 3.8 and  $9.4 \text{ G}^2$  respectively were calculated for motions (ii) and (iii) using the modified Van Vleck equation [Gutowsky (1950), Smith (1965)]. Total second moments are then  $7.2 \pm 2.0 \text{ G}^2$  and  $12.8 \pm 2.2 \text{ G}^2$  for motions (ii) and (iii). Motion (ii) thus seems from NMR data to be responsible for the motional transition at 190 K.

A study of the temperature dependence of the dielectric constant of sulfolane in the region of the first transition showed that the molecular dipoles are still aligned [Jannelli (1966)]. This rules out the rotation about an axis perpendicular to the plane of the ring. A rotation about the axis passing through the  $\text{SO}_2$  group and the mid-point of the C(2)-C(3) bond is then the motion most likely responsible for the line narrowing process at 190 K. An activation energy of  $22.6 \pm 1.7 \text{ kJ mol}^{-1}$  and a pre-exponential factor of  $1.0 \times 10^9 \text{ s}^{-1}$  were calculated using the modified BPP equation [Gutowsky (1950)].

The NMR transition at 288 K coincides with large increases in dielectric constant [Jannelli (1966)] and in

molar volume [Jannelli (1968a)]. Isotropic rotation of the molecules about their centres of gravity was considered as a possible cause of this line-narrowing process. In this case the second moment would be given only by an intermolecular contribution since the intramolecular interactions would be reduced to zero. The total second moment can be calculated as a function of the lattice constant and the number of protons per molecule [Smith (1965)]. The plastic phase is usually body-centred or face-centred cubic. Values of the lattice constant can be estimated by the measured molar volume leading to calculated second moments of  $0.8 \text{ G}^2$  and  $0.9 \text{ G}^2$  for b.c.c. and f.c.c. structures respectively. Isotropic rotation alone cannot then explain the observed value of  $0.2 \text{ G}^2$ . Self-diffusion must occur simultaneously.

The activation energy for the 288 K transition cannot be calculated by the modified BPP equation because the change in linewidth is too sharp. However, a value of  $44.5 \text{ kJ mol}^{-1}$  can be obtained by the Waugh-Fedin expression [Waugh (1963)]. This value must represent both the isotropic rotation and self-diffusion processes.

The value of the activation energy measured by NMR for self-diffusion in plastic crystals gives an indication of the mechanism of this process. When a single vacancy mechanism is responsible for self-diffusion an activation enthalpy twice the enthalpy of sublimation  $L_S$  is determined by all the possible techniques [Sherwood (1966)]. However

the activation enthalpy determined by NMR for many plastic crystals is in the range  $(L_S - 2L_S)$  while tracer and mechanical methods give the usual value of  $2L_S$ . Bladon et al. [Bladon (1971)] explained this discrepancy by a "relaxed vacancy" mechanism. A "relaxed vacancy" is a vacant lattice site into which a number of the surrounding molecules, (8-20), have collapsed to yield a small disordered region. Its progress through the lattice will be associated not only with macroscopic diffusive motions, as in a mono-vacancy mechanism, but also with microscopic motions. Both types of motion will be detected by NMR measurements, occurring on a much smaller time-scale than other measurements. On the contrary tracer and mechanical methods, which will detect only the macroscopic motions, will give the activation enthalpy for the single vacancy mechanism.

The activation enthalpy for self-diffusion in sulfolane must be less than  $45 \text{ kJ mol}^{-1}$ . Since the enthalpy of sublimation is  $48 \text{ kJ mol}^{-1}$  (the sum of the enthalpies of fusion and vaporization) the relaxed vacancy mechanism is more probable.

The further decrease in linewidth for sulfolane occurring above 296 K indicates a motion occurring over even more lattice spacings.

Supercooling of the plastic phase below 288 K may be the cause of the hysteresis effect. A similar behaviour has been reported by Fried [Fried (1973)] for

## cycloheptanone and cyclononanone

REFERENCES

- Andrew (1953) - E.R. Andrew, R.G. Eades, Proc. Roy. Soc.,  
A, 216, 398-412 (1953).
- Andrew (1970) - E.R. Andrew, J.R. Brookeman, J. Magn. Res.,  
2, 259-66 (1970).
- Andrew (1973) - E.R. Andrew, J. Magn. Res., 9, 108-13  
(1973).
- Bladon (1971) - P. Bladon, H.C. Lockart, J.N. Sherwood,  
Mol. Phys., 20, 577-84 (1971).
- Eades (1969) - Z.M. El Safar, R.G. Eades, J.P. Llewellyn,  
J. Chem. Phys., 50, 3462-66 (1969).
- Fried (1973) - F. Fried, Mol. Cryst. Liq. Cryst., 20, 1-12  
(1973).
- Gutowsky (1950) - H.S. Gutowsky, G.E. Pake, J. Chem. Phys.,  
18, 162-70 (1950).
- Jannelli (1964) - L. Jannelli, M. Della Monica, A. Della  
Monica, Gazz. Chim. Ital., 94, 552-66 (1964).
- Jannelli (1966) - U. Lamanna, O. Sciacovelli, L. Jannelli,  
Gazz. Chim. Ital., 96, 114-24 (1966).
- Jannelli (1968a) - O. Sciacovelli, L. Jannelli, A. Della  
Monica, Gazz. Chim. Ital., 98 936-48 (1968).
- Jannelli (1968b) - M. Della Monica, L. Jannelli, U. Lamanna,  
J. Phys. Chem., 72, 1068-71 (1968).
- Katon (1964) - W.R. Fearheller, J.E. Katon, Spectrochim.  
Acta, 20, 1099-1108 (1964).

Katon (1965) - J.E. Katon, W.R. Fearheller, Spectrochim. Acta, 21, 199-201(1965).

Le Fevre (1963) - M.J. Atorey, L.R. Fisher, R.J.W. Le Fevre, J. Chem. Soc., 4450-54 (1963).

Naumov (1973) - V.A. Naumov, V.N. Semashko, S.A. Shaidulin, J. Struct. Chem., 14, 555-59 (1973).

Rushworth (1954) - F.A. Rushworth, Proc. Roy. Soc., A, 222, 526-41 (1954).

Rushworth (1964) - M.J.R. Hoch, F.A. Rushworth, Proc. Phys. Soc., 83, 949-58 (1964).

Sherwood (1966) - G.M. Hood, J.N. Sherwood, J. Chim. Phys., 63, 121-7 (1966).

Smith (1965) - G.W. Smith, J. Chem. Phys., 42, 4229-43, (1965).

Staveley (1962) - L.A.K. Staveley, Ann. Rev. Phys. Chem., 13, 351-68 (1962).

Timmermans (1961) - J. Timmermans, J. Phys. Chem. Solids, 18, 1-8 (1961).

Ubbelohde (1957) - A.R. Ubbelohde, Quart. Rev., 11, 246-72 (1957).

Ubbelohde (1965) - A.R. Ubbelohde, Angew. Chem. Intern. Edit., 4, 587-91 (1965).

Waugh (1963) - J.S. Waugh, E.I. Fedin, Soviet Phys.-Solid State, 4, 1633-36 (1963).

TABLE (B-1): Temperature dependence of the linewidth of solid sulfolane - Data for Fig. (B-1) -

<u>Temperature/K</u>	<u>Linewidth/G</u>
77	13.8
113	13.6
155	13.0
175	12.7
183	12.4
194	11.2
206	10.2
211	9.9
221	9.7
235	8.8
238	8.7
245	8.5
250	8.7
253	8.4
259	8.3
264	7.6
267	7.5
267	0.5
271	0.8
273	0.8
277	8.2
277	0.4

TABLE (B-1): (cont'd)

<u>Temperature/K</u>	<u>Linewidth/G</u>
286	0.3
286	8.0
287	6.0
288	8.2
295	0.2

TABLE (B-2): Temperature dependence of the second moment of solid sulfolane - Data for Fig. (B-2)

<u>Temperature/K</u>	<u>Second moment/G<sup>2</sup></u>
77	16.3
113	15.9
155	15.1
175	14.0
183	13.9
192	12.0
199	11.2
211	10.3
229	8.5
235	7.6
238	7.5
241	7.4
245	7.0

TABLE (B-2): (cont'd)

<u>Temperature/K</u>	<u>Second moment/G<sup>2</sup></u>
253	6.4
257	1.2
265	7.7
267	0.5
269	7.7
271	0.7
272	0.9
276	0.4
278	0.4
281	0.6
283	0.2
285	7.5
286	6.6
287	4.2
288	5.4
288	4.9
295	0.1